AD A046280

AFFDL-TR-77-31
VOLUME I

2=AD-A046179

CHARACTERIZATION OF FATIGUE CRACK GROWTH IN BONDED STRUCTURES

VOLUME I: Crack Growth Prediction in Bonded Structures

NORTHROP CORPORATION, AIRCRAFT DIVISION
HAWTHORNE, CALIFORNIA 90250

JUNE 1977

FINAL REPORT JULY 1975 - FEBRUARY 1977

Approved for public release; distribution unlimited.

AD No. DDC FILE COPY

DDC
RECEIVED
NOV 9 1977
D

AIR FORCE FLIGHT DYNAMICS LABORATORY
AIR FORCE WRIGHT AERONAUTICAL LABORATORIES
AIR FORCE SYSTEMS COMMAND
WRIGHT-PATTERSON AIR FORCE BASE, OHIO 45433

NOTICE

When Government drawings, specifications, or other data are used for any purpose other than in connection with a definitely related Government procurement operation, the United States Government thereby incurs no responsibility nor any obligation whatsoever; and the fact that the Government may have formulated, furnished, or in any way supplied the said drawings, specifications, or other data, is not to be regarded by implication or otherwise as in any manner licensing the holder or any other person or corporation, or conveying any rights or permission to manufacture, use, or sell any patented invention that may in any way be related thereto.

This report has been reviewed by the Office of Information (OI) and is releasable to the National Technical Information Serivce (NTIS). At NTIS, it will be available to the general public, including foreign nations.

This technical report has been reviewed and is approved for publication.

JOSEPH P. GALLAGHER,
Project Engineer

ROBERT M. BADER, Chief
Structural Integrity Br

FOR THE COMMANDER

HOWARD L. FARMER, Col, USAF
Chief, Structural Mechanics Division

Copies of this report should not be returned unless return is required by security considerations, contractual obligations, or notice on a specific document.

AIR FORCE/56780/25 October 1977 — 500

UNCLASSIFIED

SECURITY CLASSIFICATION OF THIS PAGE (When Data Entered)

REPORT DOCUMENTATION PAGE	READ INSTRUCTIONS BEFORE COMPLETING FORM
1. REPORT NUMBER: AFFDL-TR-77-31-Vol I	2. GOVT ACCESSION NO.
3. RECIPIENT'S CATALOG NUMBER	
4. TITLE (and Subtitle): CHARACTERIZATION OF FATIGUE CRACK GROWTH IN BONDED STRUCTURES. VOLUME I. CRACK GROWTH PREDICTION IN BONDED STRUCTURES.	5. TYPE OF REPORT & PERIOD COVERED: Final rept. Jul 75 - Feb 77
	6. PERFORMING ORG. REPORT NUMBER: NOR-77-41-Vol-I
7. AUTHOR(s): M. M. Ratwani	8. CONTRACT OR GRANT NUMBER(s): F33615-75-C-3127
9. PERFORMING ORGANIZATION NAME AND ADDRESS: Northrop Corporation, Aircraft Division, 3901 West Broadway, Hawthorne, CA 90250	10. PROGRAM ELEMENT, PROJECT, TASK AREA & WORK UNIT NUMBERS: 486U 6321 1F 17 02
11. CONTROLLING OFFICE NAME AND ADDRESS: Air Force Flight Dynamics Laboratory, Wright Patterson Air Force Base, Ohio 45433	12. REPORT DATE: June 77
	13. NUMBER OF PAGES: 78, Appendices - 42 (121 p.)
14. MONITORING AGENCY NAME & ADDRESS (if different from Controlling Office)	15. SECURITY CLASS. (of this report): Unclassified
	15a. DECLASSIFICATION/DOWNGRADING SCHEDULE

16. DISTRIBUTION STATEMENT (of this Report)

Approved for public release, distribution unlimited.

17. DISTRIBUTION STATEMENT (of the abstract entered in Block 20, if different from Report)

18. SUPPLEMENTARY NOTES

19. KEY WORDS (Continue on reverse side if necessary and identify by block number)

Adhesive Bonding
Fracture Mechanics Analysis
Stress Intensity Factors
Finite Element Modeling
Cracked Element
Integral Equations
Complex Variables
Logarithmic Singularities
Numerical Analysis
Debond in Adhesive
Cracking of Sound Layer
Weldbonding

20. ABSTRACT (Continue on reverse side if necessary and identify by block number)

This is the first of two volumes that present methods for solving crack problems in the metallic elements of adhesively bonded structures. There are six major sections in the report that cover the following topics:

1. Methods of analysis, namely the finite element method and the integral equation method. Assumptions in the analysis and the influence of various parameters on the analytical results.

DD FORM 1 JAN 73 1473 EDITION OF 1 NOV 65 IS OBSOLETE

UNCLASSIFIED

SECURITY CLASSIFICATION OF THIS PAGE (When Data Entered)

110526

2. Criterion for the propagation of a debond.
3. Criterion for the crack transfer to a sound layer.
4. Verification test program.
5. Sensitivity of analysis to various parameters.
6. Limitations of the analysis.

The stress intensity factors have been obtained for the geometries of (1) a cracked sheet with an adhesively bonded stringer, and (2) a two-layer, bonded structure with a center crack, an edge crack, and a crack at a hole. The influence of finite boundaries, adhesive methods, debond size, and bending on stress intensity factors has been studied. Comparison has been made of actual crack growth life and that based on analytical stress intensity factors. The crack growth life has been predicted analytically within ten percent of actual life. The influence of adhesive and adherend materials and thicknesses on crack growth life has been studied. The predicted debond sizes have been compared with those observed experimentally. A criterion for the cracking of a sound layer, based on load transfer to a sound layer, has been developed.

FOREWORD

This report was prepared by Northrop Corporation, Aircraft Division, Hawthorne, California, under Air Force Contract F33615-75-C-3127. The project was initiated under Project Number 486U, "Advanced Metallic Structures," Advanced Development Program. The work reported herein was administered under the direction of the Air Force Flight Dynamics Laboratory, Air Force Systems Command, Wright-Patterson Air Force Base, Ohio, by Dr. Joseph P. Gallagher (FBEC), Project Engineer.

This report is Volume I of two volumes covering the research conducted between July 1975 and February 1977. The research was conducted by D. P. Wilhem and by the author, Dr. M. M. Ratwani. This report was submitted by the author in March 1977.

The author wishes to acknowledge the help of P. A. Hill, in graphic work and data reduction, and the help and constructive suggestions of Dr. J. P. Gallagher (FBEC) in crack growth life predictions. The support of Mr. D. Clark in testing program and the secretarial assistance of P. E. Barnes is also acknowledged. The aforementioned program was under the technical supervision of L. Jeans, Manager of the Structural Life Assurance Research Department.

DDC
RECEIVED
NOV 9 1977
D

ACCESSION for
NTIS White Section
DDC Buff Section
UNANNOUNCED
JUSTIFICATION
BY
DISTRIBUTION/AVAILABILITY CODES
Dist. Avail. and/or SPECIAL
A

CONTENTS

PRECEDING PAGE NOT FILMED BLANK

CONTENTS (continued)

CONTENTS (continued)

ILLUSTRATIONS

ILLUSTRATIONS (continued)

ILLUSTRATIONS (continued)

ILLUSTRATIONS (continued)

TABLES

SECTION 1

INTRODUCTION

The use of adhesive bonding in structural application has attracted considerable attention in recent years. Metal laminates have features that make them attractive from the point-of-view of fracture control. Kaufman (Reference 1) showed that the fracture toughness of multilayered, adhesively bonded panels is greater than that of a sheet or plate of the same total thickness as the multilayered panel. Similar effects have been observed by Alic and Anchang in Reference 2. The concept of bonding has been used to produce dual-hardness steel armor for increased fracture toughness (Reference 3). The increased fatigue crack growth life of adhesively bonded structures has been demonstrated in References 4 through 6. In these references, crack growth studies were done experimentally, and no analytical techniques were developed. In Reference 7, the finite element analysis method was used to analyze bonded structures. In this reference, an attempt was made without success, to correlate analytical debond propagation in the adhesive with that observed in the experiments. The problem of debond propagation in a metal-to-composite bonded structure has been investigated in Reference 8.

The use of brazing in multilayered structures to improve structural efficiency and damage tolerance has been demonstrated in Reference 9.

Several investigators have attempted to analyze cracked, adhesively bonded structures (References 7, 10, 11, 12, 13, 14). In References 10 through 12, a complex variable approach has been used to analyze the problem. In Reference 13, the problem is solved using the Fourier Transform Technique and reducing it to the solution of an integral equation. A finite element approach has been used to study the problem in References 7 and 14. However, in these studies, no attempt was made to correlate the experimental crack growth data with the analytical results. Hence, these methods

had to be investigated, and if necessary, new analytical techniques developed to analyze cracked, adhesively bonded structures.

The object of this research effort was to develop basic structural criteria and analysis methods that can be utilized to predict the slow crack growth of flawed metal elements in adhesively bonded structures. The analytical techniques should predict the crack growth in adherends, debond propagation in the adhesive, and the subsequent crack initiation of the initially sound layer. Through-flaw geometries, typical of those that could exist in single-ply metallic elements of two ply bonded structures, were assumed for the methodology development and for experimental verification. The analytical development focused on the methods of finite element analysis and mathematical (closed form) techniques. Experimental verification tests included center-cracked, 12-inch wide, 6-inch wide, and flawed hole, adhesively bonded panels.

It is shown that by using properly computed analytical stress intensity factors, crack growth prediction of an adhesively bonded structure can be within 10 percent of the empirically determined life of the structure. A comparison of predicted and observed debond shapes and sizes have shown very good agreement. A criterion for the cracking of a sound layer has also been developed.

The investigation conducted under this contract has been reported in two volumes. This volume consists of a discussion of analysis methods, experimental results, and the correlation of analytical and experimental results. The details of the analytical techniques developed, the comparison of various analysis methods, the application of each technique to different problems, as well as multi-ply bonded structures, and the associated computer programs are given in Volume II.

Section 2 of this volume, contains a brief discussion of the finite element and mathematical methods of analysis, as well as assumptions made in each method. The influence of various factors, such as debond size, adhesive properties, bending, and cracking of a sound layer, on the analytical results, is also discussed. The stress intensity factors obtained by finite element analysis for two-ply, adhesively bonded panels (7075-T73

aluminum to 7075-T73 aluminum) with a center crack, an edge crack, a crack emanating from an eccentric hole, and for a three-ply (aluminum-titanium-aluminum) bonded panel are given.

Section 3 introduces a new concept for the propagation of debonding in an adhesive. Using this concept, debond shape is predicted for a variety of structural and crack geometries.

Section 4 describes the details of the verification test program. Tests were conducted to determine the influence of adhesive type and thickness, the uncracked layer material and thickness, and the finite boundary effects on crack growth life of a structure. A comparison of analytical and experimental stress intensity factors and life predictions for various crack geometries is given.

In Section 5, the details of a sensitivity analytical study carried out to investigate the influence of adhesive properties and thickness, cracked layer properties, and sound layer properties and thicknesses on stress intensity factors are given. The influence of these parameters on stress intensity factors for various crack lengths has been studied for the cases of a cracked plate with an adhesively bonded stringer, a cracked plate with two bonded stringers, and a two-layer, adhesively bonded structure with a center crack.

In Section 6, the limitations of the analysis techniques used are discussed. The influence of debond size and adhesive properties on crack growth life is outlined.

Finally, in Section 7, the conclusions based on the results of this study are discussed. The typical flaws occurring in adhesively bonded structures are discussed in Appendix A. The purpose of this study and testing philosophy are discussed in the following paragraphs.

1.1 PURPOSE

A recent Air Force Specification, MIL-A-83444, "Airplane Damage Tolerance Design Requirement," requires that all primary structures be designed

and qualified to be damage tolerant, i.e., to maintain structural integrity in the presence of undetected cracks for specified periods of time. The specification defines these periods of time on the basis of frequency and sensitivity of inspection and flaw sizes, and can range from the entire service life for noninspectable structures, to a few flights, for those structures with extensive damage that can easily be detected at the completion of each flight.

Bonded aircraft structure has long been efficiently used in secondary structural applications. The potentials of primary, adhesively bonded metal aircraft structure, for cost reduction and improved structural efficiency, are becoming more evident from the in-depth evaluation of other programs. Rational flaw requirements and analysis methods for bonded structures must be available to the analyst during design development in order to satisfy the damage tolerance requirements and to establish an allowable design stress for limiting the amount of slow crack growth. The growth patterns of these initial flaws, in complex, built-up structures, must be determined where no other information exists. In particular, methods must be developed to predict the sequence of events where subcritical growth causes failure of one or more individual elements prior to complete loss of the structure.

The linear elastic fracture mechanics approach has been successfully used to predict crack growth in single-layer metallic structures, and is also applicable to bonded structures if proper analytical techniques are available that are unique to adhesively bonded structures. The main factors to be considered in developing such techniques are, an appropriate model that accounts for the load transfer occurring between the cracked and uncracked layers, and the criterion associated with crack formulation in the initially sound layers. The primary purpose of this program has been to identify these critical factors and use them as a basis for developing and verifying methods of analysis for flaws in the metallic elements (hereinafter referred to as metallic flaws) of bonded structures.

1.2 TESTING PHILOSOPHY

Various crack and panel geometries were tested to verify the analytical results. A sufficient number of variations of these geometries were tested to verify the applicability of the analysis techniques to most through-crack

situations one could reasonably expect to encounter in adhesively bonded structures. A maximum amount of information was obtained from each test panel by putting in multiple cracks. The cracks in each panel were spaced so that the interference between them was negligible. Basic data for a single layer were also obtained so that experimental stress intensity factors could be obtained from crack growth data on adhesively bonded structures. These experimental stress intensity factors have been compared with the analytical stress intensity factors in Section 4.

SECTION 2

ANALYSIS OF ADHESIVELY BONDED STRUCTURES

The analytical tool of linear elastic fracture mechanics has long been successfully used to predict the fatigue crack growth behavior in metallic structures. The use of this tool requires the determination of a single parameter correlating the crack growth with crack tip environment. This parameter is known as a stress intensity factor, and is defined as the coefficient of singularity ahead of a crack tip. The analytical techniques to obtain stress intensity factors for cracks in isotropic materials consisting of a single (two-dimensional) layer are well established. The basic analytical techniques commonly used are the finite element method, or various mathematical methods. Special elements have been developed to account for the singular stresses ahead of a crack tip in the finite element analysis, making it possible to obtain stress intensity factors for a variety of crack and structure geometries. These stress intensity factors are available in numerous papers and handbooks (References 15, 16). The two-dimensional structural geometries for which stress intensity factors are not available in literature, can be easily analyzed using finite element techniques.

The successful use of fracture mechanics techniques to predict fatigue crack growth in single-layer, metallic structures, suggests that these same techniques can be used to predict fatigue crack growth in adhesively bonded, metallic structures having flaws in the adherend, provided the stress intensity factors ahead of a crack tip are properly computed. The computation of these stress intensity factors must consider the load transfer from a cracked layer to an uncracked layer. This load transfer will, in turn, depend on the properties and thickness of the adherends and adhesive, the crack length, and the debond size in the adhesive.

PRECEDING PAGE NOT FILMED
BLANK

A rigorous analysis of a cracked, adhesively bonded structure, represents several additional degrees of complexity as the structure-crack interaction is three-dimensional. Hence, an analysis of such a problem suggests the need for a good, three-dimensional cracked element, in order to do a finite element analysis. Unfortunately, this type of three-dimensional element is not generally available. In addition, closed form mathematical techniques required to analyze this as a three-dimensional problem appear to be beyond the present state of knowledge. Therefore, certain simplifying assumptions have to be made in the finite element, as well as the mathematical methods, to analyze the bonded structure problem. The particular methods, analysis assumptions, and factors influencing the analytical results are discussed in the following paragraphs.

2.1 METHODS AND ASSUMPTIONS IN ANALYSIS

The two methods of analysis used in this program are discussed in considerable detail in Volume II of this report. Assumptions and limitations of each method of analysis are discussed in the following paragraphs.

2.1.1 Finite Element Method of Analysis

A rigorous analysis of cracked, adhesively bonded structures would require analysis of a layered, three-dimensional, cracked body, and is beyond the scope of the available state of knowledge. Hence, a modified finite element approach, considering each layer as a two-dimensional structure has been developed for use in this program. The following assumptions are made in the analysis:

1. Each layer is considered as a two-dimensional structure under a state of plane stress.
2. The adhesive layer is treated as a shear spring, rather than as an elastic continuum (Reference 17). In the finite element analysis, the continuous shear spring is replaced by shear elements (Reference 14).
3. The layers are connected by shear elements, representing the adhesive.

4. The thickness of the adhesive is small compared to the thickness of the plates.

5. The bending stiffness of the cracked and sound layers is negligible.

With these assumptions, it is possible to model the adhesively bonded structure as a two-dimensional structure. In the finite element model, each layer is modeled as a two-dimensional structure with triangular or rectangular elements, and a cracked element is provided ahead of each crack tip to account for the singular behavior of stresses. The x and y coordinates of the grid points in the bonded regions of the two layers are kept the same. In the debonded region, the finite element model of the two layers need not be the same. In the bonded region, two layers are connected by shear elements provided at grid points. Around the periphery of the debond in the bonded region, the adhesive is subjected to high shear stresses, hence closely spaced grid points are provided to reduce the length of shear elements. The closely spaced shear elements give an accurate estimate of shear stresses and load transfer between the cracked and uncracked layers and therefore, the stress intensity factors can be more accurately computed.

The finite element analysis has been used for the following types of panel geometries (Figure 1):

1. Two-Ply, adhesively bonded panel with a center-crack in one layer (12 inches wide and 6 inches wide).

2. A cracked panel with a bonded stringer.

3. Two-ply, adhesively bonded panel with an edge crack.

4. Two-ply, adhesively bonded panel with a crack in one layer emanating from a central hole (12 inches wide and 6 inches wide).

5. Two-ply, adhesievly bonded panel with a crack in one layer emanating from an eccentric hole

6. Three-ply, aluminum-titanium-aluminum panel with a center-crack in the outer ply.

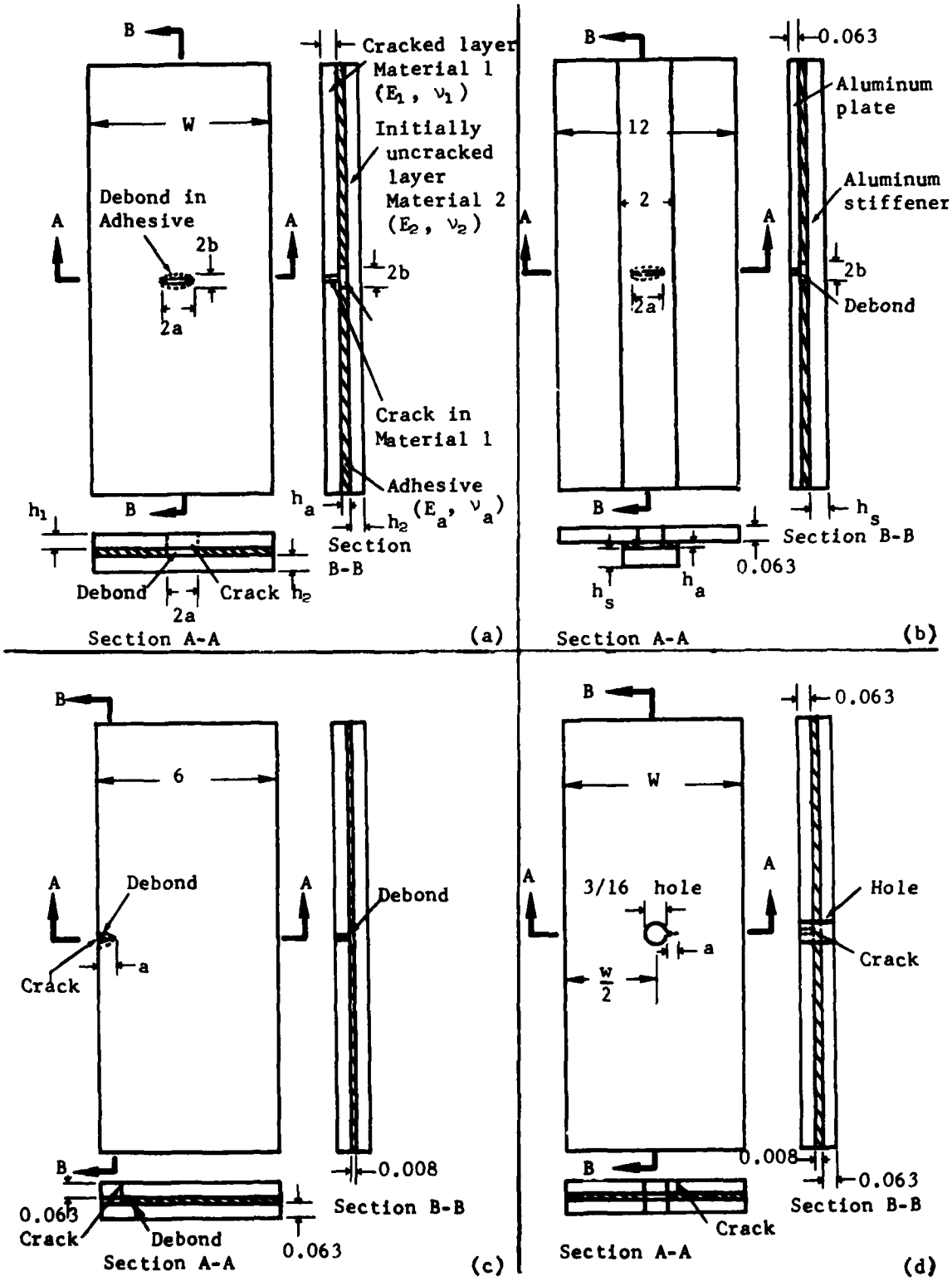

Figure 1. Panel and Crack Geometries Investigated (all dimensions in inches)

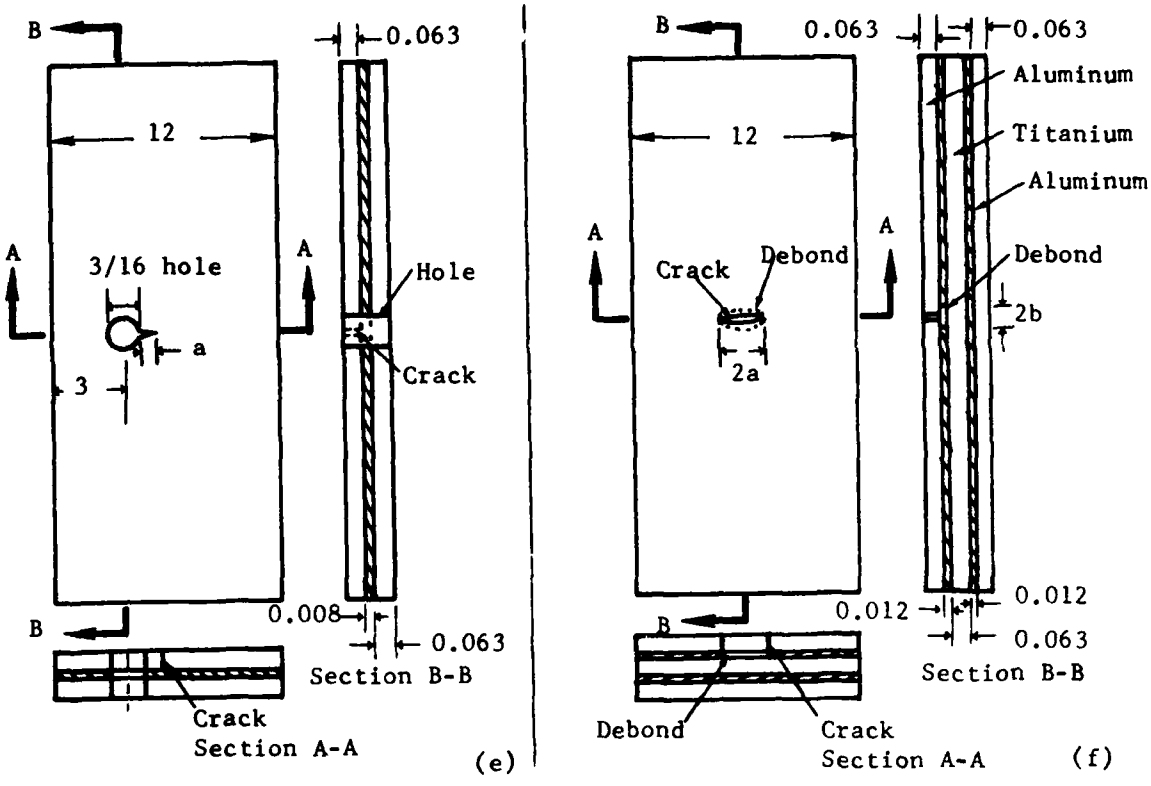

(a) Two-ply, adhesively bonded structure with a center-crack in one ply.

(b) A cracked plate with an adhesively bonded stringer.

(c) Two-ply, adhesively bonded structure with an edge crack in one ply.

(d) Two-ply, adhesively bonded structure with a crack emanating from a hole.

(e) Two-ply, adhesively bonded structure with a crack emanating from an eccentric hole.

(f) Three-ply (aluminum-titanium-aluminum), adhesively bonded structure with a center-crack in one aluminum ply.

Figure 1. Panel and Crack Geometries Investigated (all dimensions in inches) (continued)

For the finite element analysis the NASTRAN program with a two-dimensional, cracked element, developed by Professor Pian of MIT (Reference 18), was used. The comparison of analytical and experimental results are discussed in Section 4.

The present analysis was carried out assuming the adhesive to behave as an elastic material. The nonlinear behavior of the adhesive can be indirectly incorporated in the finite element analysis by using the reduced shear modulus for the shear elements in the regions where the adhesive is subjected to high shear stresses.

2.1.2 Mathematical Methods of Analysis

Mathematical methods provide a very useful tool to analyze crack problems in adhesively bonded structures. The use of such methods may be more expedient than finite element analysis, where the problem parameters (displacements, geometry, material properties, etc.) can be expressed as mathematical functions, solvable by closed form or numerical techniques. This is particularly so where the boundaries are regular and the crack lengths are small compared to the dimensions of the structure. The complex variable approach, using Kolosov-Muskhellishvili functions to reduce the problem of cracked structures to the solution of integral equations, is considered for the present investigations. Certain simplifying assumptions have to be made in the mathematical modeling of these bonded structures. These assumptions are:

1. The thickness of the plates or stiffeners is small compared to the in-plane dimensions so that the structure may be considered to be under a generalized plane stress loading.
2. The adherends and adhesive are homogeneous and linearly elastic.
3. Variation of stresses through the thickness in the layers is neglected.
4. The thickness of the adhesive is small compared to the thickness of the adherends, hence the adhesive may be treated as a shear spring rather than as an elastic continuum.

5. The surface shear transmitted through the adhesive acts as a body force.

6. The bending stiffness of adherends is negligible.

7. For the case of a plate with an adhesively bonded stringer, it is assumed that the stringer area is concentrated at one point at the centerline of the stringer.

The crack problems in an adhesively bonded structure can be analyzed as a two-dimensional structure if the above mentioned assumptions are satisfied. The problem is reduced to the solution of integral equations that have logarithmic singularities. These integral equations are solved numerically for the shear stresses in the adhesive and stress intensity factors. This approach has been used for three classes of problems:

1. A cracked plate stiffened by a partially debonded stringer.

2. A cracked plate stiffened by two partially debonded stringers symmetrically located about the centerline.

3. A two-layer, adhesively bonded structure with a debond in the adhesive and a crack in one adherend.

The details of the formulation of these problems are given in Volume II of this report. The computer programs for the numerical solution of the problems are also listed in Volume II. These computer programs have the following inputs:

1. For a cracked sheet with adhesively bonded stringers

   a. Modulus, Poisson's ratio, and thickness of a cracked sheet
   b. Modulus, Poisson's ratio, width and thickness of the stiffener
   c. Shear modulus and thickness of the adhesive layer
   d. Half-crack length
   e. Length of the debond
   f. Location of the stringer

2. Adhesively bonded plates with a debonding crack

   a. Modulus, Poisson's ratio, and thickness of the cracked layer

   b. Modulus, Poisson's ratio and thickness of the sound layer

   c. Shear modulus and thickness of the adhesive layer

   d. Ratio of minor-to-major axis of debond (in the computer programs, the debond is assumed to be elliptical with a minor-to-major axis ratio equal to 0.0, 0.1, 0.2, or 0.3)

   e. Half-crack length a

These computer programs give shear stresses in the adhesive and stress intensity factors as outputs. For a two-layer, adhesively bonded structure with a crack in one layer, two different programs are written due to a convergence problem. The first program gives converging results up to a half-crack length of 0.4 inch, and the second program gives converging results between half-crack lengths of 0.5 inch and 1.0 inch. The details of convergence of the programs are discussed in Volume II. The computer program is written for an elliptically shaped debond, however the program can easily be modified to incorporate a debond of any shape.

2.2 FACTORS INFLUENCING THE ANALYTICAL RESULTS

The analytical stress intensity factors obtained by finite element or mathematical methods are affected by several factors, such as adhesive properties, debond size, etc. The influence of these factors on the analytical stress intensity factors are discussed in the following paragraphs.

2.2.1 Influence of Debond Size

In a cracked, adhesively bonded multilayered structure, the stress intensity factors are lower than those for a crack in a single layer having the same remote boundary conditions as the multilayered, bonded structure. This results from the load transfer that takes place from the cracked layer to the uncracked layer. This load transfer to the uncracked layer depends on the properties of the adhesive and adherends, the crack length, and debond size. With the increased debond size, there will be less load

transfer to the uncracked layer, hence increased values of the cracked layer stress intensity factors.

Consider the two-ply, adhesively bonded structure shown in Figure 1a, where a through-crack exists in the plate of Material 1, and a debond exists in the adhesive around the crack in Material 1. There is no crack in Material 2. For such a structure, finite element analysis is carried out assuming no debond in the adhesive, as well as an elliptical debond, with a minor-to-major axis ratio (b/a) of 0.1 (debond size observed in experiments). The stress intensity factors as a function of half-crack length a, are shown in Figure 2 for two adhesively bonded plates (W = 6 inches) of the same material.

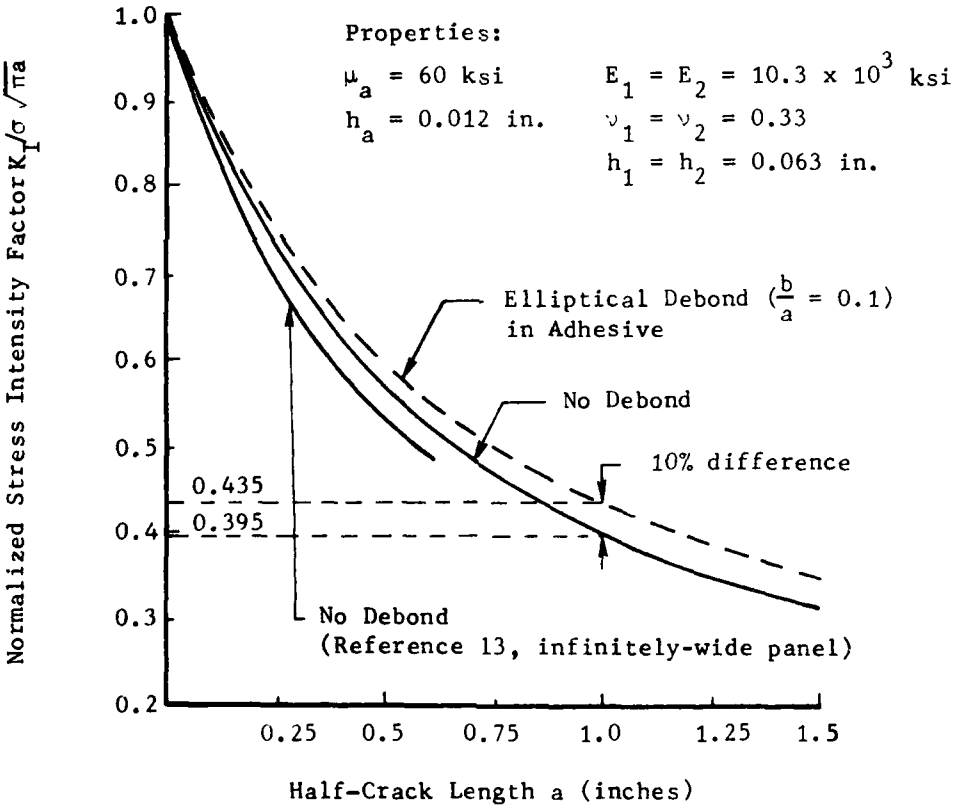

Figure 2. Influence of Debond Size on Stress Intensity Factors in a Center-cracked Panel (W = 6 inches)

It is seen that for a fixed crack length, the stress intensity factors increase due to the presence of a debond, the percentage increase being dependent on the crack length. In this example, neglecting the effect of the debond would result in computed stress intensity factors that are lower than the actual value by about 10 percent at half-crack lengths of one inch or greater. The use of these lower factors in crack growth analysis could result in a life prediction that exceeds the test life by 50 to 60 percent.

Figure 2 also shows the stress intensity factors obtained in Reference 13 for a two-ply, infinitely wide, bonded structure. It is seen that the stress intensity factors obtained in this reference are slightly lower than those obtained by finite element analysis for a six-inch wide panel. At a half-crack length of 0.5 inch, the stress intensity factors of Reference 13 are about six percent lower than the finite element results.

The stress intensity factors to be used in crack growth analysis or residual strength prediction, should be computed for the associated debond size in the adhesive, thus the debond size corresponding to each crack length has to be known. The influence of different debond sizes on elastic stress intensity factors is discussed in the sensitivity studies in Section 5.

2.2.2 Influence of Adhesive Properties

The analytical stress intensity factors obtained by finite element or mathematical methods, depend on the adhesive and adherend elastic properties and thicknesses used in the analysis. An accurate estimate of the elastic modulus is necessary for the analysis, since the result will be lower stress intensity factors if modulus values larger than the actual value are used. This is due to the fact that with a larger value of the elastic modulus, the adhesive around the crack will not undergo large shear deformation as the crack opens under the load. Hence, there will be more load transfer to the uncracked layer, resulting in lower stress intensity factors. If a shear modulus lower than the actual value is used, the result will be higher stress intensity factors.

The influence of adhesive thickness on the stress intensity factors will be the opposite of the elastic modulus. A reduced adhesive thickness

will give lower stress intensity factors, as a smaller thickness gives rise to larger shear stresses in the adhesive, hence a larger load transfer to the sound layer. Conversely, an increase in the adhesive thickness, will increase the stress intensity factors. It may be noted that an increase in adhesive thickness will give a smaller debond size (discussed in Section 3), which will result in higher stress intensity factors. Thus, an increase in adhesive thickness gives an increase in stress intensity factors because of the more flexible adhesive, but a reduction in stress intensity factors, due to the smaller debond size produced. The net influence of adhesive thickness on stress intensity factors will depend on the type of structure. The integral equation formulation of the cracked, adhesively bonded structures discussed in Paragraph 2.1.2 (details of the analysis are discussed in Section 2 of Volume II), shows that the influence of adhesive thickness and shear modulus on the stress intensity factors can be studied by a single parameter, the ratio of adhesive thickness to adhesive modulus (h_a/μ_a).

For a two-ply, bonded structure six inches wide, the plot of stress intensity factors as a function of half-crack length a, is shown in Figure 3, for two different values of h_a/μ_a. It is seen that for the same crack length, the higher the value of h_a/μ_a, the higher the value of the stress intensity factors. Figure 3 shows that doubling the adhesive thickness and reducing the shear modulus at the same time by about a factor of three, can increase the adherend stress intensity factor by about 15 percent for a half-crack length of one inch, and reduce the crack growth life by a factor of about 3.

The elastic properties of metal adherends are well established, and are easily obtained from handbooks or in the laboratory. The procedure for obtaining adhesive properties has not yet been well established, and considerable variation in the elastic modulus (corresponding to the initial slope) may be obtained from different specimens.

2.2.3 Influence of Bending

The finite element and mathematical methods for the analysis of cracked, adhesively bonded structures discussed earlier in this section are for the

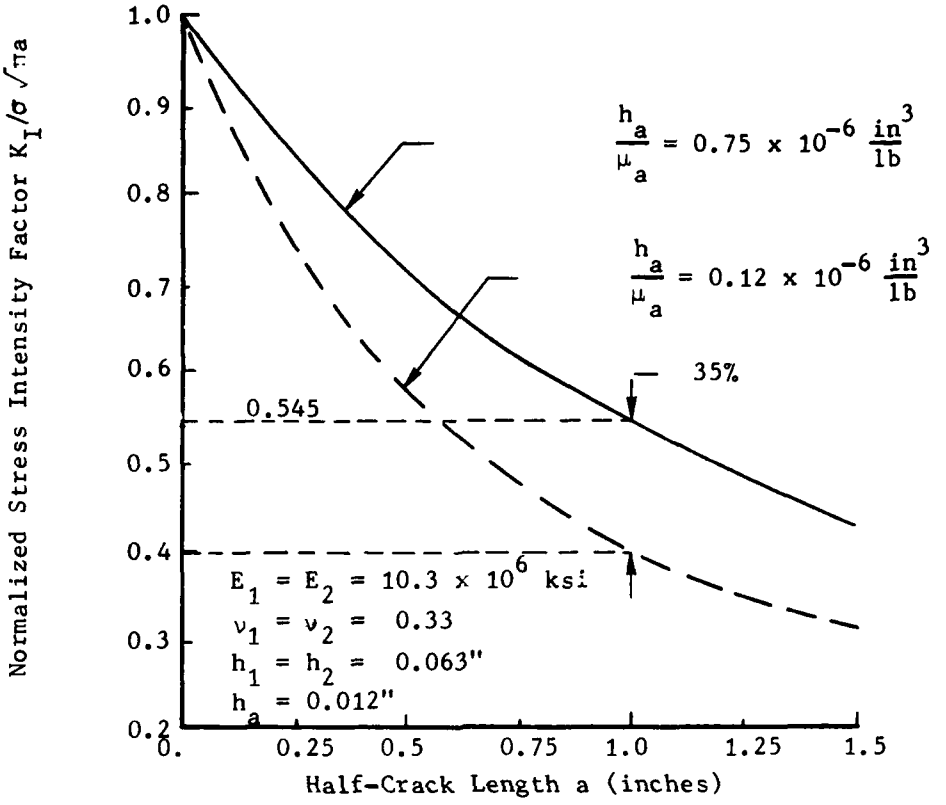

Figure 3. Influence of Adhesive Thickness to Modulus Ratio on Stress Intensity Factors (elliptical debond in adhesive, $\frac{b}{a} = 0.1$)

extensional type of loading and it was assumed that both the cracked and sound layer had no bending stiffness. The presence of a crack in one layer of a bonded structure will give rise to out-of-plane bending due to lack of symmetry caused by the presence of a crack. This out-of-plane bending will produce tensile stresses in the cracked layer, hence increase the stress intensity factors. This influence of bending (increase in stress intensity factors) in a structure, will increase as the crack length increases. This increase in stress intensity factors will affect the crack propagation rates and should be accounted for in the analysis. A rigorous analysis of adhesively bonded structures to account for all boundary conditions, out-of-plane bending, etc., will require a three-dimensional analysis, which is not presently feasible. Thus, the two-dimensional finite element and the mathematical analysis discussed earlier, must be modified to account for the influence of

bending. A method based on the load transferred to the sound layer has been developed to account for the out-of-plane bending, and from this, the stress intensity correction factors are determined. The method of bending correction calculates the load transferred to the sound layer from the stress intensity factors obtained by the two-dimensional analysis of a cracked, adhesively bonded structure, and the bending effects are calculated from the load transferred to the sound layer. The details of the bending correction are given in Section 3 of Volume II of this report.

The two-ply, adhesively bonded structure shown in Figure 1a was analyzed by the finite element method. The bonded panel has a width of six inches, and the thickness of each layer is 0.063 inch. The stress intensity factors obtained for the elliptical debond case (b/a = 0.1) using the finite element method are shown in Figure 4. The figure also shows the stress intensity factors obtained experimentally. It is seen that the stress intensity factors obtained by finite element analysis are considerably lower than the experimental stress intensity factors. The stress intensity factors obtained by finite element analysis and corrected for the influence of bending (for details, see Volume II, Section 4) are also shown. It is seen that these stress intensity factors agree well with the experimental results. It is seen that the increase in stress intensity factors due to bending is a function of crack length, and this increase may be as much as 30 percent for a half-crack length of one inch.

2.2.4 Influence of the Cracking of a Sound Layer

In a cracked, multilayered, adhesively bonded structure, the presence of a crack in one layer causes a high stress concentration in the adjacent uncracked layers due to the load transfer taking place to these layers. The load transferred to the sound layer from the initially cracked layer will depend on the relative elastic properties and thickness of the layers, properties of the bonding medium, crack length, and stress concentration due to the presence of holes, etc. A crack in a sound layer might initiate at these stress concentrations during subsequent fatigue loads. The cracking of the initially sound layer will depend on the load transferred to the

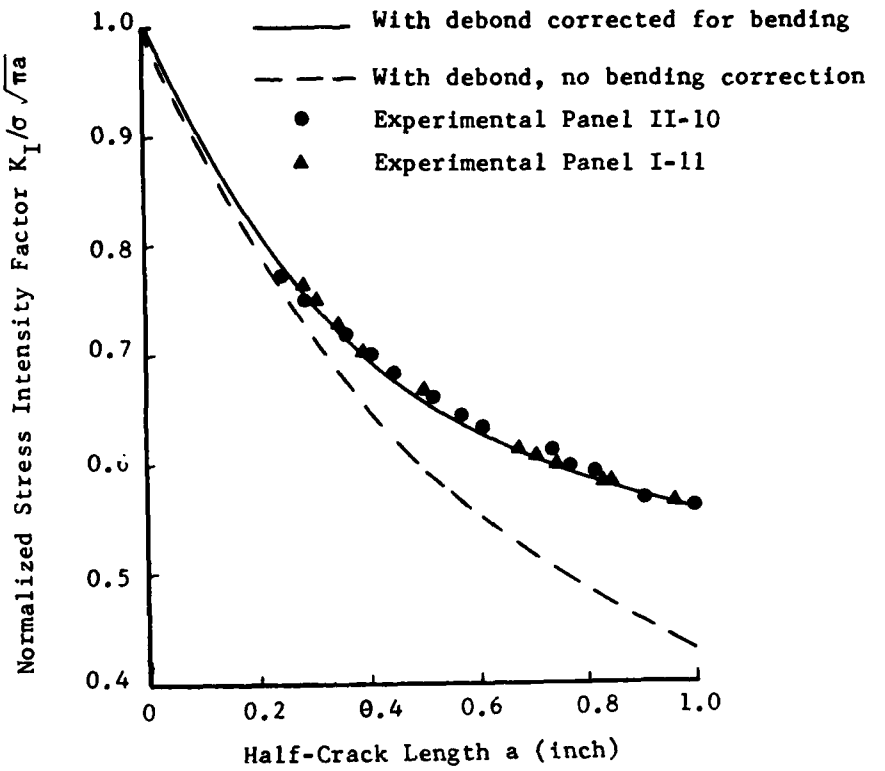

Figure 4. Comparison of Analytical and Experimental Stress Intensity Factors for a Two-Ply, Cracked, Adhesively Bonded Panel (6 inches wide)

layer and the number of fatigue cycles applied. The number of cycles required will depend on the material of the sound layer. A criterion has been developed for the cracking of a sound layer, based on the load transferred to the sound layer. In this development it is assumed that the initially cracked layer has a small flaw that will propagate under fatigue loads. During the subsequent crack propagation, the sound layer is subjected to increasing fatigue loads in the load transfer region, as the load transfer is a function of crack length. When the load transferred to the sound layer reaches a critical value, a crack will initiate in the sound layer.

The computation of shear stresses in the adhesive have shown that the maximum load transfer will be at the centerline of the crack for center-crack geometries, and the point of maximum stress concentration for cracks

emanating from stress concentrations. Hence, the load transferred to the uncracked layer is computed at the point of maximum stress concentration. The load transferred to the sound layer is computed from the stress intensity factors for the adhesively bonded structure and the single cracked layer.

It may be noted that with the above assumption, the criterion for the cracking of a sound layer depends indirectly on the number of fatigue cycles required to initiate the crack. The application of this criterion to the cracking of the sound layer for various structural geometries and the details of the development are discussed in Section 5 of Volume II.

The initiation of a crack in the sound layer will give rise to stress concentrations in the layer, hence there will be less load transfer to this layer from the initially cracked layer. This will result in higher stress intensity factors and crack propagation rates in the initially cracked layer. The crack propagation rates in the initiated crack are higher than those in the initially cracked layer for the same crack length due to the load transfer effects. Eventually, new and old cracks join tips and propagate together.

The initiation of a crack in a sound layer should be taken into consideration in the life prediction analysis. When the initiated crack has become a through-crack, it can easily be modeled in the finite element analysis by providing a cracked element ahead of each crack. The mathematical solutions can also be obtained for such cases. However, the kernels of the integral equations will have to be changed (Paragraph 2.2.3 of Volume II) to account for the presence of a crack in a second layer.

2.3 COMPARISON OF RESULTS OBTAINED BY FINITE ELEMENT AND MATHEMATICAL METHODS OF ANALYSIS

In the finite element and mathematical methods of analysis, certain simplifying assumptions were made. In the finite element analysis, the adhesive was represented by shear elements and the influence of shear stresses in the x direction was neglected. In the mathematical analysis, stresses in both x and y directions were taken into consideration. Certain other assumptions outlined earlier were also made. The results obtained by the two methods of analysis (for the same problem) are detailed in Paragraph 2.3 of Volume II.

The computer run times (IBM 370 computer) for the finite element analsis are between four to six minutes (CPU time between two to four minutes) depending on the type of structure, whereas the mathematical analysis computer program run time for a cracked plate with an adhesively bonded stringer, is 16 seconds (CPU time, 8 seconds) and about one minute for a two-ply, adhesively bonded system (CPU time, 48 seconds). Thus, it is seen that a considerable saving in computer run time is achieved by using the mathematical methods. Also, with the mathematical approach, a number of cases can be run simultaneously, varying the adhesive or adherend thickness and properties, as well as the crack lengths, etc. Similar analysis by the finite element approach will require a change in finite element modeling (grid point locations) if the thickness of the adhesive is varied, and a change in shear elements if the debond size is varied, hence increasing the preparation time requirements. While mathematical methods are well suited for parametric studies, their application has to be carefully reviewed for finite and irregular boundaries, and in such cases, the finite element methods may be more suitable.

The comparison of the results of the two methods for a two-ply, adhesively bonded structure with a crack in one ply (Figure 1a) showed excellent agreement. The stress intensity factors obtained by these analyses were within four percent.

The comparison of the results obtained by the two methods of analysis for a cracked plate with a bonded stiffener (Figure 1b) is shown in Figure 5. The results of the two methods are close for small crack lengths only ($a \leq 0.1$ inch). For larger crack lengths, the stress intensity results obtained by the complex variable technique are much larger than those obtained using the finite element analysis. This is due to the fact that in the complex variable formulation, it is assumed that the entire stringer area is concentrated at the centerline of the stringer, hence the load shedding from the cracked plate to the stringer is not fully effective. In the finite element analysis the entire width of the strap is modeled, therefore load transfer is permitted over the entire width, resulting in lower stress intensity factors.

To obtain better solutions using the complex variable approach, it was assumed that the area of the strap is concentrated at two points that are

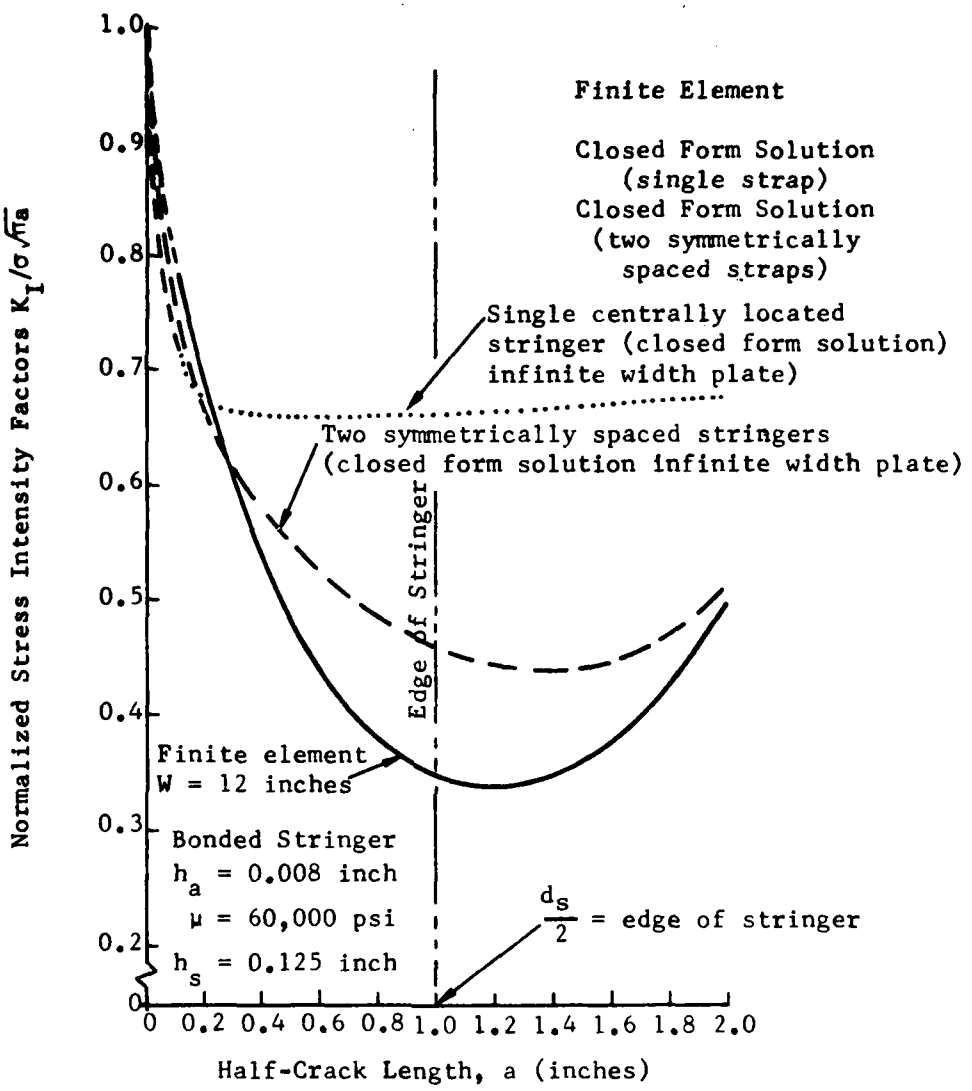

Figure 5. Comparison of Finite Element Determined Stress Intensities with Integral Equation Solutions (Cracked Plate with Bonded Stringer)

symmetrically located about the centerline of the plate. These areas were assumed to be concentrated at the crack tip if $2a > B$ (B = width of the strap), and at the edge of the strap if $2a > B$. The problem was formulated using a complex variable approach. The plot of $K_I/\sigma\sqrt{\pi a}$ versus the half-crack length a for the two symmetrically placed straps is also shown in Figure 5. It is seen that up to a half-crack length of about 0.3 inch, the results given by the two methods are very close. Beyond this point, the integral equation approach gives higher values of the stress intensity factor.

The finite elemtnt results corrected for the influence of bending agree well with the experimental results (Section 4). This indicates that either the finite element method or the two-stringer formulation should be used for the analysis. The complex variable approach assuming a stringer area at one point may be used for very small crack lengths ($a \leq 0.1$ inch).

2.4 ANALYTICAL STRESS INTENSITY FACTORS

Analytical stress intensity factors were obtained by the finite element method for the various crack geometries shown in Figure 1. These stress intensity factors were used for theoretical life predictions, which were then verified experimentally. In the analysis, Poisson's ratio for all metallic materials was assumed as 0.33, and the shear modulus of the adhesive was assumed as 60,000 psi. The analytical stress intensity factors obtained are given in Appendix B.

SECTION 3

CRITERION FOR PROPAGATION OF DEBOND

In a cracked, adhesively bonded structure subjected to cyclic loading, debonding develops in the adhesive layer around the crack. The debond propagates as the crack in the metallic layer propagates. The leading edge of the debond almost coincides with the leading edge of the crack. The experimental results in the present program and also in References (7, 19) indicate that the debond is elliptical in shape, with $\frac{b}{a} \cong 0.1$ (Figure 1a) for center crack geometries. In References 7 and 10 the debond size was predicted analytically based on the rupture criterion for the adhesive. However, the predicted debond size was much larger than that observed in the experiments.

Adhesives exhibit nonlinear behavior at relatively small stresses, hence for such materials a simple failure criterion could be critical strain.

It may be assumed that the adhesive has failed if the strain in the adhesive reaches a critical value. This critical value of strain may be taken as the strain at failure in a static tension test. Based on these assumptions, a criterion for the propagation of a debond was developed in this program. The details of this criterion are discussed in Section 6 of Volume II. From the criterion developed for debond propagation, the following points are observed:

1. The size of the debond is dependent on the adhesive thickness. If the thickness of the adhesive is large, the strain in the adhesive will be small, hence the size of the debond will be small. If the adhesive thickness is very large, the size of the debond may be zero.

2. The debond size will be small if the failure strain of the adhesive is larger and vice-versa.

3. The size of the debond will depend on the applied loads (σ_{max} for fatigue loads). The large applied loads will cause large crack openings, hence large shear strain in the adhesive and larger debond size.

4. The size of the debond will depend on the relative elastic properties of the sound and cracked layer, and the elastic modulus of the adhesive as these will influence the relative displacements between the adherends.

3.1 PREDICTED DEBOND SHAPES

Predicted debond shapes for various crack geometries are shown in Figure 6. These predictions are based on critical failure strain (ϵ_R) equal to 0.04 for the FM-73 adhesive.

For the two-ply, 12-inch wide, adhesively bonded structure of Figure 1a, the predicted debond size at a half-crack length of one inch is shown in Figure 6a. The debond is elliptical in shape with $\frac{b}{a} \approx 0.1$. For the cracked plate with a bonded stiffener (Figure 1b), the predicted debond shape for a = 0.75 (crack within the stiffener) is shown in Figure 6b, and for a = 2.0 (crack outside the stiffener) is shown in Figure 6c. It is seen that the debond transitions from elliptical to the shape shown.

The predicted debond shape for a crack-at-a-hole geometry (Figure 1d) in a 12-inch wide plate is shown in Figure 6d.

It may be noted that the predicted debond sizes are based on the critical strain in the adhesive. The critical failure strain will depend on the temperature, moisture content and the strain rate in the adhesive. The critical failure strain has to be carefully selected in predicting debond size.

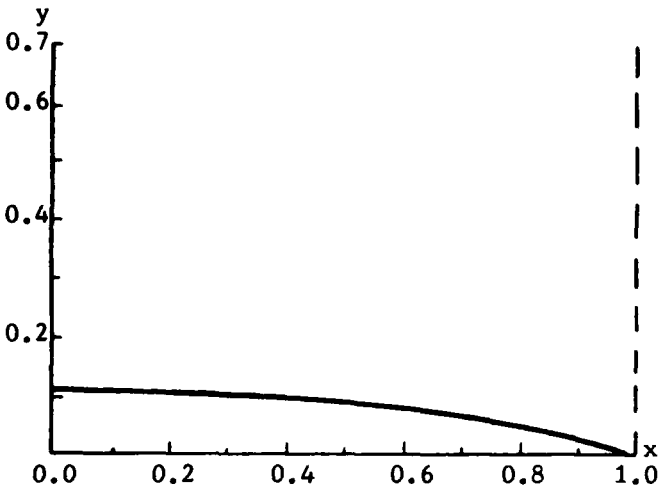

(a) Two-ply bonded panel with a center crack in one ply (one-quarter of debond shown, a = 1.0 inch)

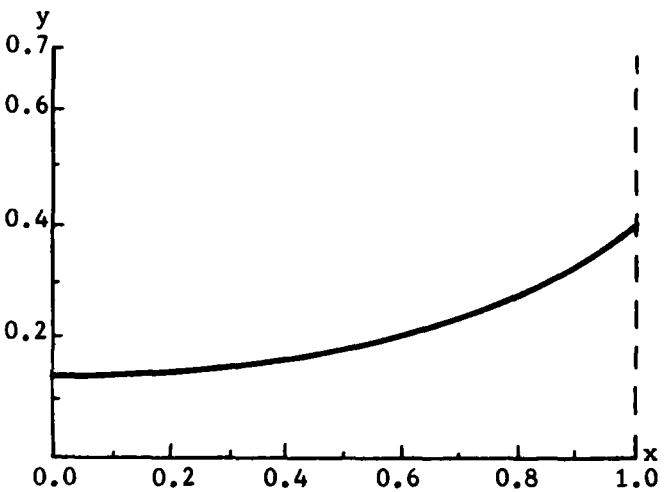

(c) Cracked plate with a bonded stiffener (one-quarter of debond shown, a = 2.0 inches)

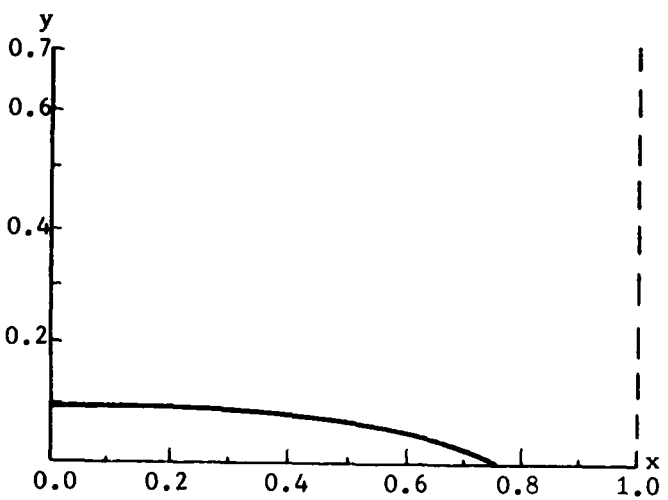

(b) Cracked plate with a bonded stiffener (one-quarter of debond shown, a = 0.75 inch)

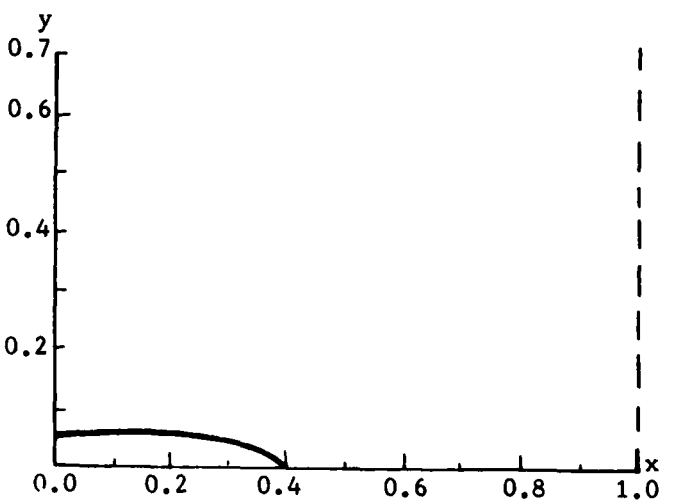

(d) Panel with a crack at a hole (one-half of debond shown, a = 0.406 inch)

Figure 6. Predicted Debond Shape at Applied Stress of 15.5 ksi for Various Panels

SECTION 4

VERIFICATION TEST PROGRAM

In Section 2, the analysis of adhesively bonded structures with various crack geometries was discussed. The crack and panel geometries for which analytical stress intensity factors were obtained (Paragraph 2.4) have been tested to verify the analysis. The details of this test verification program and the correlation of the analytical and experimental results are discussed in the following paragraphs.

4.1 DETAILS OF BONDED PANELS TESTED

All the testing was conducted at a constant amplitude, sinusoidal loading with a frequency of 10 Hz. In all tests (except one), maximum stress was kept at 15,500 psi. All but two tests were conducted at R = 0.1. Two tests were conducted at R = -1.0 to observe the effect of compression loads on debond size. Table 1 summarizes the details of the panels tested. The cracked layer in all panels was 7075-T73 aluminum with a thickness of 0.063 inch. A typical geometry of a 12-inch wide, center-cracked panel is shown in Figure 7a, with three crack locations (A, B, and C). The geometry of the six-inch wide panel is shown in Figure 7b, where the width at the grips was kept at 12 inches, and the specimen was tapered to 6 inches. The geometry of the bonded strap panel is shown in Figure 7c. The hole pattern at the grips was the same as for the 12-inch and 6-inch wide panels. The 12-inch wide panels with a crack at a central hole, had a geometry similar to the panel in Figure 7a, except central holes with a diameter of 3/16-inch were located at A, B, and C, with a crack in one layer emanating from each hole. The 6-inch wide panel with a crack at a hole, was similar to the panel in Figure 7b.

PRECEDING PAGE NOT FILMED
BLANK

TABLE 1. SUMMARY OF TEST PANEL GEOMETRIES

PANEL NUMBER	WIDTH INCHES		CRACK GEOMETRY	ADHESIVE THICKNESS	THICKNESS INCHES		NUMBER OF CRACKS	TYPE OF ADHESIVE	REMARKS
	CRACKED LAYER	SOUND LAYER			CRACKED LAYER	SOUND LAYER			
1	12	12	Center crack	-	0.063	-	3	-	Basic data
I-1	12	12	Center crack	0.015	0.063	0.063	3	FM-73	Infinite width panel
II-2	12	12	Center crack	0.012	0.063	0.063	3	FM-73	Infinite width panel
II-16	12	12	Center crack	0.008	0.063	0.063	3	FM-73	Infinite width panel (thin bondline) max. stress = 19,950 psi
II-10	6	6	Center crack	0.015	0.063	0.063	3	FM-73	Finite width panel
I-11	6	6	Center crack	0.015	0.063	0.063	3	FM-73	Finite width panel
I-19	12	2	Center crack	0.006	0.063	0.125	3	FM-73	Bonded 7075-T6 strap
II-8	12	2	Center crack	0.011	0.063	0.250	3	FM-73	Thick 7075-T6 bonded strap
I-21	12	2	Center crack	0.006	0.063	0.125	3	FM-73	2024-T3 bonded strap
I-7	12	2	Center crack	0.003	0.063	0.125	3	FM-73	Thin bondline
II-6	12	2	Center crack	0.023	0.063	0.125	3	FM-73	Thick bondline
II-20	12	2	Center crack	0.010	0.063	0.125	3	FM-400	Different adhesive
I-23	12	2	Center crack	0.010	0.063	0.125	3	FM-400	Different adhesive
II-24	6	6	Edge crack	0.010	0.063	0.063	1	FM-73	Edge crack specimen
I-13	6	6	Edge crack	0.010	0.063	0.063	1	FM-73	Edge crack specimen
II-4	12	12	Center crack	0.009	0.063	0.063	3	FM-73	3-ply panel (two outer layers 7075-T6 aluminum and inner layer titanium) Ti-6Al-4V-2Sn
I-5	12	12	Crack at a central hole	0.007	0.063	0.063	3	FM-73	Crack at a central hole, infinite width
II-22	12	12	Crack at a central hole	0.007	0.063	0.063	3	FM-73	Crack at a central hole, infinite width
I-24	6	6	Crack at a central hole	0.010	0.063	0.063	3	FM-73	Crack at a central hole, finite width
I-15	12	12	Eccentric hole	0.006	0.063	0.063	3	FM-73	Crack at an eccentric hole
II-12	12	12	Eccentric hole	0.009	0.063	0.063	3	FM-73	Crack at an eccentric hole
II-25	4	4	Center crack	0.008	0.063	0.063	2	FM-73	R = -1.0
II-26	4	4	Center crack	0.008	0.063	0.063	2	FM-73	R = -1.0

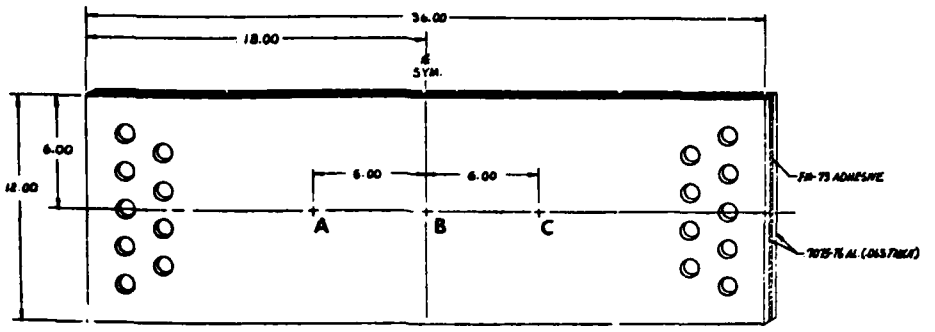

(a) Geometry of a 12-inch wide, center-cracked tension specimen

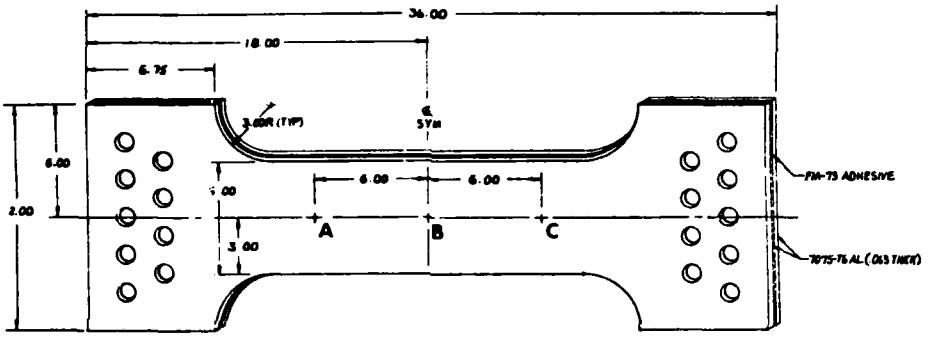

(b) Geometry of a finite width, center-cracked tension specimen

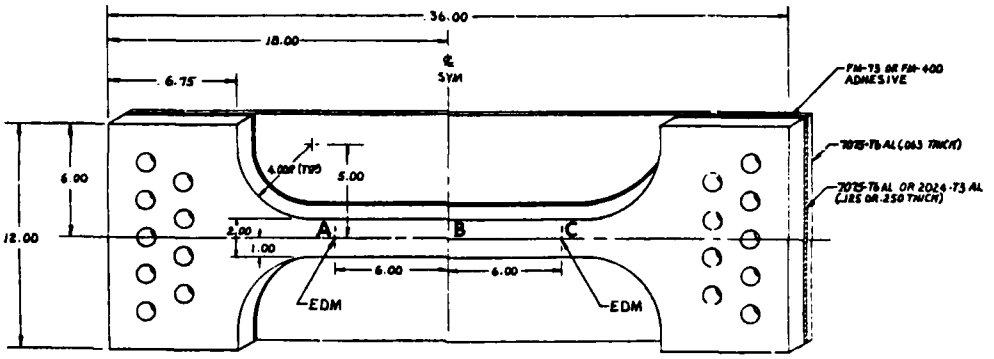

(c) Bonded strap specimen

Figure 7. Geometries of Test Specimens

The test program was carried out to experimentally study the following effects on fatigue crack propagation and debond size:

1. Influence of Finite Width

   Panels I-1 and II-2 were 12 inches wide, and Panels II-10 and I-11 were 6 inches wide.

2. Influence of Stiffener Thickness

   Panel I-19 had a stiffener thickness of 0.125 inch, and Panel II-8 had a stiffener thickness of 0.25 inch.

3. Influence of Sound Layer Ductility

   Panel I-19 had a 7075-T6 bonded strap, and Panel I-21 had a 2024-T3 bonded strap.

4. Influence of Bondline Thickness

   Panel I-7 had a bond thickness of 0.003 inch, and Panel II-6 had a bond thickness of 0.023 inch.

5. Influence of Adhesive Type

   The relatively brittle adhesive, FM-400 was used in Panels II-20 and I-23, whereas all other panels had the more ductile, FM-73 adhesive.

6. Influence of Edge Crack

   Panels II-24 and I-13 had an edge crack.

7. Influence of a Sound Layer (Other Than Aluminum) Adjacent to a Flawed Aluminum Layer

   Panel II-5 had a flaw in one of two outer 7075-T6 aluminum layers, with a central titanium Ti-6Al-4V-2Sn layer.

8. Influence of a Crack at a Central Hole

   Panels I-5 and II-22 were 12 inches wide and had a crack emanating from a central hole. Panel I-24 was six inches wide, with a crack emanating from a central hole.

9. Influence of a Crack at an Eccentric Hole

   Panel I-15 and II-12 had cracks emanating from eccentric holes.

10. Influence of Compression Loads

Panels II-25 and II-26 were tested under R = -1.0.

In each case, the panels were tested after the analysis was completed and the analytical stress intensity factors obtained.

4.2 COMPARISON OF ANALYTICAL AND EXPERIMENTAL STRESS INTENSITY FACTORS

The experimental stress intensity factors for the two-ply, cracked, adhesively bonded structure were obtained from the fatigue crack growth data using the Anderson-James approach (Reference 20). Essentially, the procedure determines the percentage correction required to reduce the bonded fatigue crack growth data to coincide with the basic material (single-ply) data. The constants in Equation (1) were obtained for the single layer at R = 0.1.

$$\frac{da}{dN} = 0.0169 \times 10^{-6} \, (K_{max})^{2.731} \qquad (1)$$

Using these constants and crack growth rate $\frac{da}{dN}$ for the adhesively bonded structure, the values of K_{max}, hence the stress intensity factors, are obtained for various crack lengths.

The experimentally computed stress intensity factors for a two-ply, center-cracked, adhesively bonded panel, with a six-inch width (Figure 7a) are shown in Figure 4. The agreement between the experimental stress intensity factors and the analytical stress intensity factors, assuming an elliptical debond in the adhesive with $\frac{b}{a} = 0.1$ and corrected for the influence of bending is very good. Figure 8, shows the comparison of experimental and analytical stress intensity factors corrected for the influence of bending for a cracked plate with a bonded stiffener (Figure 1b), a two-ply, bonded structure with an edge crack (Figure 1c), and a two-ply, bonded structure with a radial crack emanating from a hole (Figure 1d). The analytical stress intensity factors are obtained by assuming an elliptical debond in the adhesive with $\frac{b}{a} = 0.1$ for the bonded stiffener panel and the panel with an edge crack. Do debond was assumed for a panel with a crack at a hole since the debond for this case is a very narrow strip, and its influence on stress intensity factors is negligible. It is seen that the correlation of analytical

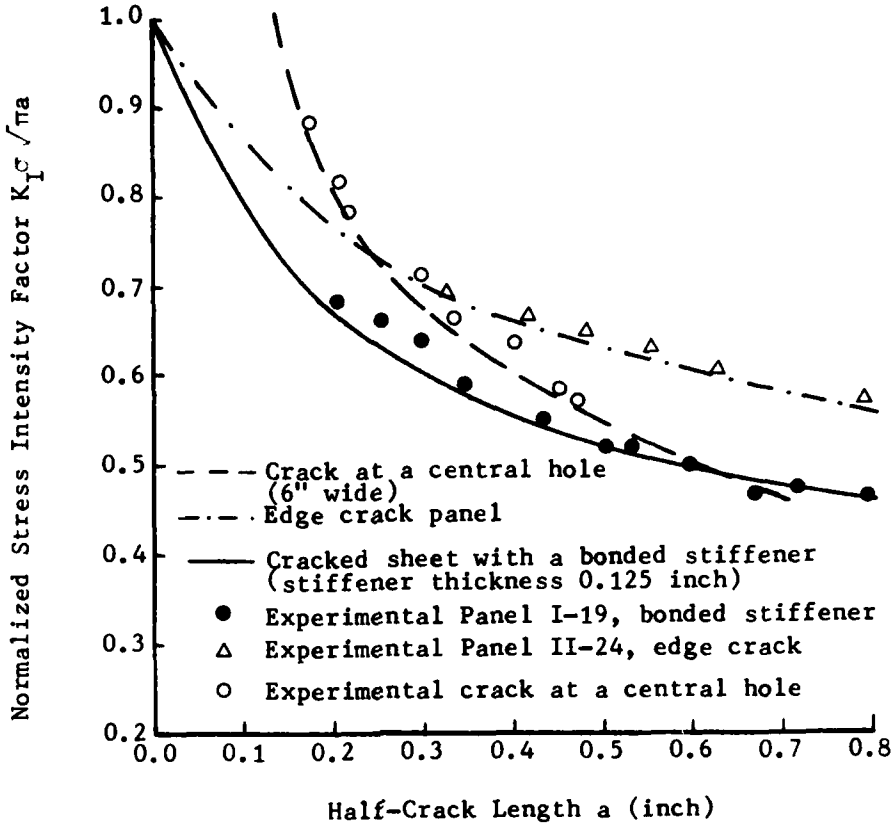

Figure 8. Comparison of Analytical and Experimental Stress Intensity Factors for Various Crack Geometries

It is seen that the correlation of analytical stress intensity factors corrected for bending, and the experimental results is very good.

4.3 COMPARISON OF ANALYTICAL AND EXPERIMENTAL CRACK GROWTH LIFE

In Paragraph 4.2, the comparison of analytical and experimental stress intensity factors was discussed. A more useful method of comparing the experimental and analytical results is to look at the crack growth life of the structure. Using the analytical stress intensity factors and the crack growth data from a single layer, the crack growth life of the various panels tested (Table 1), was predicted and compared to actual crack growth

life. Figure 9 shows the plot of half-crack length a versus the actual and predicted number of constant amplitude fatigue cycles for a center-cracked, two-ply, six-inch wide, adhesively bonded panel. It is seen that the correlation of predicted and actual life, is very good, with the predicted life three percent greater than actual life at a half-crack length of 1.0 inch. Life predictions for a six-inch wide, two-ply, adhesively bonded panel with an edge crack, are also shown in this figure. In this case, the actual number of cycles required to propagate the crack from 0.25 inch to 1.0 inch, are within about one percent of the predicted cycles.

The measured cycles and predicted cycles as a function of crack growth for a two-ply, bonded panel with a crack emanating from a central hole, and a crack emanating from an eccentric hole, are shown in Figure 10. In this case, the correlation of predicted life and actual life is also considered good. These life predictions are shown for a crack length of 0.15 inch to 0.45 inch, due to the fact that at a crack length of about 0.45 inch, a secondary crack develops in the sound layer. This gives rise to high stress intensity factors in an initially cracked layer and higher propagation rates.

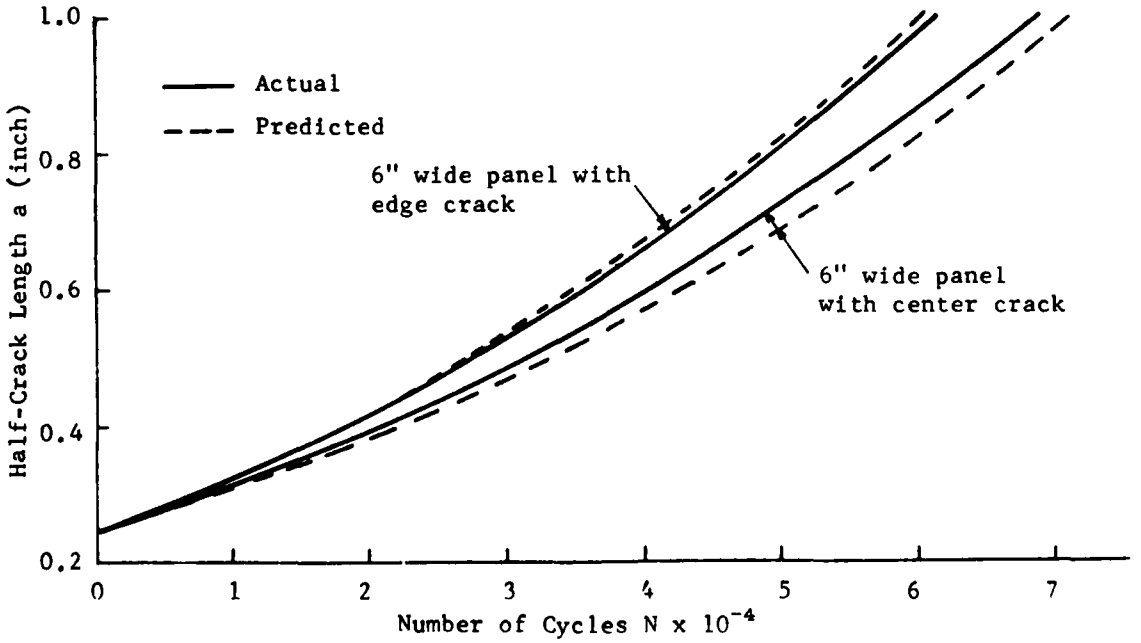

Figure 9. Comparison of Actual Life and Predicted Life for a 6-Inch Wide Panel

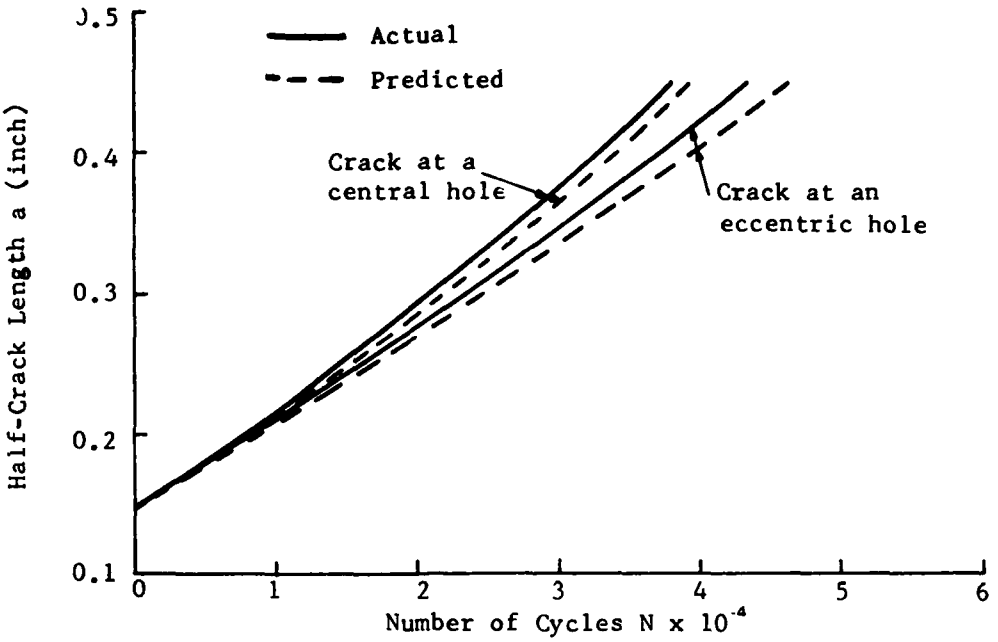

Figure 10. Comparison of Actual Life and Predicted Life for a 12-Inch Wide Panel with a Crack at a Hole

While the analysis technique is applicable to the structure after the cracking of the sound layer, in the present program, stress intensity factors were computed for a crack in one layer only.

A summary of the number of experimental and predicted cycles to propagate the crack from an initial crack length of a_o, to a final crack length of a_f, are shown in Table 2 for all the comparisons made in this program. These life predictions are shown for all the initial cracks in each panel. The table also shows the ratio of predicted life cycles to actual cycles, and it is seen that the predictions are within ten percent, with the exception of the 12-inch wide, center-cracked panels (I-1, II-2, andI-16). The overestimated life for these panels is expected, as the entire width (12 inches) was considered effective in the application of bending correction. In practice, the entire panel width will probably not be effective in resisting bending, and the effect of bending may be localized in the small width extending beyond either crack tip. In this case, the bending correction

TABLE 2. COMPARISON OF ACTUAL AND PREDICTED LIFE CYCLES

PANEL	CRACK GEOMETRY	CRACK	a_o (inches)	a_f (inches)	ACTUAL CYCLES N_A	PREDICTED CYCLES N_P	N_P/N_A
I	12" wide single layer	A	0.248	1.00	30,220	--	-
		B	0.270	1.02	31,170	--	-
		C	0.254	1.01	27,050	--	-
I-1	12" wide center crack	A	0.250	1.00	61,780	77,422[1]	1.250
		B	0.250	1.00	66,278	79,651[1]	1.202
		C	0.250	1.00	62,605	77,052[1]	1.240
II-2	12" wide center crack	B	0.250	1.00	71,800	83,165[1]	1.158
		C	0.250	1.00	65,854	80,753[1]	1.226
II-16	12" wide center crack	A	0.250	1.00	32,052	39,244[1]	1.224
		B	0.250	1.00	34,526	39,969[1]	1.158
		C	0.250	1.00	30,563	38,454[1]	1.258
II-10	6" wide center crack	A	0.250	1.00	73,048	74,551	1.020
		B	0.250	1.00	73,242	79,642	1.087
		C	0.250	1.00	78,962	78,331	0.992
I-11	6" wide center crack	A	0.250	1.00	68,927	71,063	1.031
		B	0.250	1.00	74,480	75,372	1.012
		C	0.250	1.00	70,402	72,566	1.031
I-19	12" wide center crack with 7075-T6 bonded strap thickness 0.125"	A	0.250	0.80	83,080	85,824	1.033
		B	0.250	0.80	79,824	84,885	1.063
		C	0.250	0.71	72,595	74,275	1.022
II-8	12" wide center crack with 7075-T6 bonded strap thickness 0.25"	A	0.250	0.80	170,768	147,909	0.866
		B	0.250	0.80	154,864	147,765	0.952
		C	0.250	0.80	157,130	146,457	0.932

[1] 12-inch width assumed effective in resisting bending.

TABLE 2. COMPARISON OF ACTUAL AND PREDICTED LIFE CYCLES (continued)

PANEL	CRACK GEOMETRY	CRACK	a_o (inches)	a_f (inches)	ACTUAL CYCLES N_A	PREDICTED CYCLES N_P	N_P/N_A
I-21	12" wide center crack with 2024-T3 bonded strap thickness 0.125"	A	0.250	0.80	75,347	84,149[1]	1.116
		B	0.250	0.80	97,099	87,183[1]	0.898
		C	0.250	0.80	75,660	84,437[1]	1.116
I-7	12" wide center crack with 7075-T6 bonded strap	A	0.250	0.80	79,412	84,912[1]	1.069
		B	0.250	0.80	83,585	86,922[1]	1.040
		C	0.250	0.80	78,598	84,665[1]	1.077
II-6	12" wide center crack with 7075-T6 bonded strap. Thick bondline	A	0.250	0.65	42,560	39,980[1]	0.939
		B	0.250	0.65	42,120	40,095[1]	0.952
		C	0.250	0.32	8,050	8,823[1]	1.096
II-24	Edge crack	A	0.250	1.00	61,403	60,685	0.988
I-13	Edge crack	A	0.250	1.00	55,272	58,171	1.052
II-4	3-ply (Al-Ti-Al) center crack	A	0.250	1.00	156,455	144,129	0.921
		B	0.250	1.00	150,437	138,720	0.922
		C	0.250	1.00	141,894	133,167	0.939
I-5	12" wide crack at a central hole	A	0.150	0.35	25,464	27,887[1]	1.095
		B	0.150	0.45	38,000	38,583[1]	1.015
		C	0.150	0.35	24,169	26,896[1]	1.113
II-22	12" wide crack at a central hole	A	0.230	0.45	26,000	26,896[1]	1.034
		B	0.162	0.45	37,123	38,109[1]	1.027
		C	0.150	0.35	28,419	20,341[1]	1.068
I-24	6" wide crack at a central hole	A	0.150	0.35	31,518	31,480	0.999
		B	0.150	0.35	28,570	31,115	1.089

[1] 12-inch width assumed effective in resisting bending.

TABLE 2. COMPARISON OF ACTUAL AND PREDICTED LIFE CYCLES (continued)

PANEL	CRACK GEOMETRY	CRACK	a_o (inches)	a_f (inches)	ACTUAL CYCLES N_A	PREDICTED CYCLES N_P	N_P/N_A
I-15	12" wide crack at an eccentric hole	A	0.150	0.35	29,026	31,375	1.082
		B	0.150	0.35	29,899	31,554	1.055
		C	0.200	0.35	19,500	21,734	1.114
II-12	12" wide crack at an eccentric hole	A	0.150	0.35	27,525	29,958	1.088
		B	0.110	0.35	27,618	29,936	1.084
		C	0.150	0.45	43,858	44,514	1.015
II-25	4" wide center crack R = -1.0	A	0.206	0.75	31,055	33,404	1.075
		B	0.211	0.75	31,253	33,473	1.071
II-26	4" wide center crack R =-1.0	A	0.203	0.65	28,250	30,136	1.067
		B	0.213	0.75	30,216	32,563	1.078

NOTES:

1. σ_{max} = 15,500 psi ---- R = 0.1 --- except as noted

2. The theoretical life predictions for cracks A, B, and C, are different, as they are made for each crack (individually) at actual crack lengths, as measured in the experiments, and linear interpolations is used by the computer to obtain the stress intensity factors at these crack lengths.

will be higher, resulting in larger stress intensity factors and lower predicted life. To illustrate the effect of width in the 12-inch wide, center-cracked panels, the stress intensity factors were corrected for the influence of bending by using a six-inch effective width. The actual life cycles and predicted life, based on these new stress intensity factors, are shown in Table 3. It is seen that the agreement between actual and predicted life is improved.

The actual life and predicted life for the panels tested at R = -1.0 (σ_{max} = 15.5 ksi and σ_{min} = -15.5 ksi), are also shown in Table 2. The ΔK for the theoretical life prediction is based on σ_{min} = 0 for these panels. In predicting theoretical life, the constant C, in the Paris equation was modified to account for R = -1.0. The studies of Reference 21 show that the fatigue life for 7075-T6 aluminum at R = -1.0, was about 13 percent lower than that at R = 0.0. Similar effects were observed for 2024-T3 aluminum in Reference 22. The constant C, in the Paris equation, obtained for basic data on 7075-T73 at R = 0.1, was increased by just 13 percent to give the value of the constant C for R = -1.0. This modified value of C was used in theoretical life predictions.

4.4 INFLUENCE OF ADHEREND AND ADHESIVE SIZES AND PROPERTIES ON ACTUAL CRACK GROWTH LIFE

The test program was structured so that the influence on the crack growth life of the adherend and adhesive thickness, material properties, and finite boundary effects could be experimentally studied. In the following paragraphs, measured effects of these influences are discussed. All crack length versus cycles curves presented in this section describe the central tendency of the data collected in the experimental program.

4.4.1 Influence of Strap Thickness and Strap Material on Crack Growth Life in a Cracked Sheet with a Bonded Strap

The actual number of cycles required to propagate the crack from a half-crack length of 0.25 inch to 0.8 inch in a sheet with an adhesively bonded strap are shown in Figure 11. The results shown are for 7075-T73 aluminum straps 0.125-inch thick, and a 2024-T3 aluminum strap 0.125-inch

TABLE 3. COMPARISON OF ACTUAL AND PREDICTED LIFE FOR A 12-INCH WIDE CENTER CRACKED SPECIMEN

PANEL	CRACK GEOMETRY	CRACK	a_o (inches)	a_f (inches)	ACTUAL CYCLES N_A	PREDICTED CYCLES N_P	N_P/N_A
I-1	12" wide center crack	A	0.25	1.0	61,779	65,163	1.055
		B	0.25	1.0	66,278	67,145	1.013
		C	0.25	1.0	62,605	65,416	1.045
II-2	12" wide center crack	A	0.25	1.0	63,897	68,863	1.076
		B	0.25	1.0	71,800	71,872	1.001
		C	0.25	1.0	65,854	69,570	1.056
II-16	12" wide center crack	A	0.25	1.0	32,052	31,341	0.978
	P_{max} = 20 ksi	B	0.25	1.0	34,526	31,346	0.980
		C	0.25	1.0	30,563	30,647	1.003

NOTE: Six-inch width assumed effective in resisting bending.

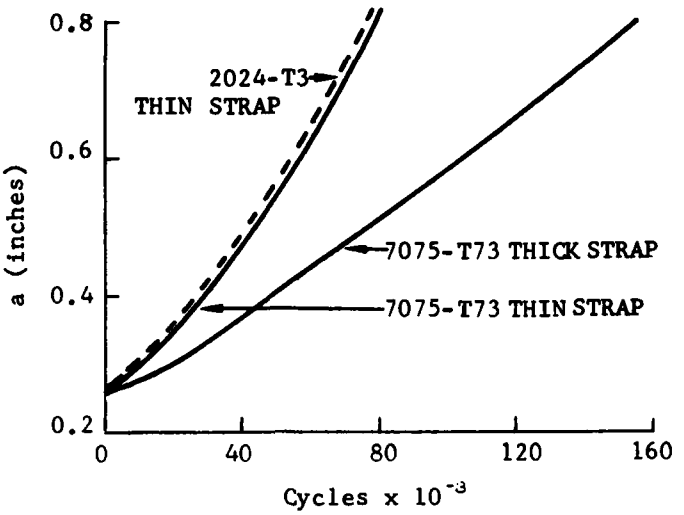

Figure 11. Influence of Strap Thickness and Material on Crack Growth Life

thick. It is seen that approximately the same number of cycles are required for the 7075-T73 and 2024-T3 aluminum straps 0.125-inch thick, as expected from analytical considerations. The difference is within the experimental data scatter. In the analysis, the only distinction between materials (within the elastic range) is in the value of the tensile modulus used, and 2024-T3 and 7075-T73 aluminum have an almost identical modulus. Hence, the stress intensity factors and crack growth life will be the same. The crack growth life for a strap 0.25-inch thick is almost double that of one that is 0.125-inch thick. The presence of the thicker strap increases the load transfer to the sound layer (strap), resulting in reduced stress intensity factors, as well as reduced bending effect in the structure, thus considerable increase in life is obtained.

4.4.2 Influence of Adhesive Type on Crack Growth Life in a Cracked Sheet with a Bonded Stringer

Figure 12 shows the influence of adhesive type on crack growth in a sheet with a bonded stringer in a plot of crack length versus the number of cycles. It is seen that the crack growth life for the FM-400 adhesive is slightly smaller than that for the FM-73 adhesive. The elastic modulus

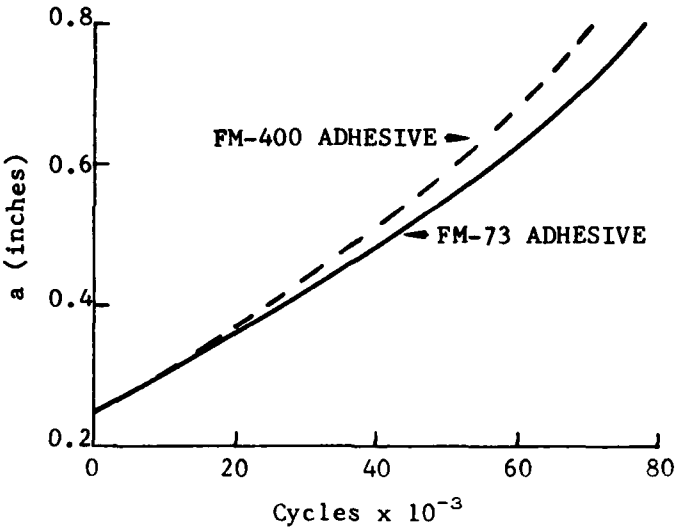

Figure 12. Influence of Adhesive Type on Crack Growth Life

the FM-400 adhesive is much higher than the elastic modulus for the FM-73 adhesive, which gives a lower value of thickness to the modulus ratio, hence lower values of stress intensity (Section 2). However, the cricical failure strain of the FM-400 adhesive is about one-half that of the FM-73 adhesive, so the debond size for the FM-400 adhesive will be much larger than that for the FM-73 (Section 3). A larger debond size will cause a smaller load transfer to the sound layer and a larger value of stress intensity. Hence, the net difference in life due to different adhesive types, is less than might be expected. The net effect of using less ductile adhesive on stress intensity factors will depend on the type of structure and the adhesive thickness.

4.4.3 Influence of Adhesive Thickness on Fatigue Crack Growth Life

The influence of adhesive thickness on fatigue crack gorwth life for a cracked sheet with a bonded stringer is shown in Figure 13. The fatigue life for a thick adhesive is lower than that for a thin adhesive. This is due to the fact that a thick adhesive causes less load transfer to the sound layer resulting in higher values of stress intensity factors.

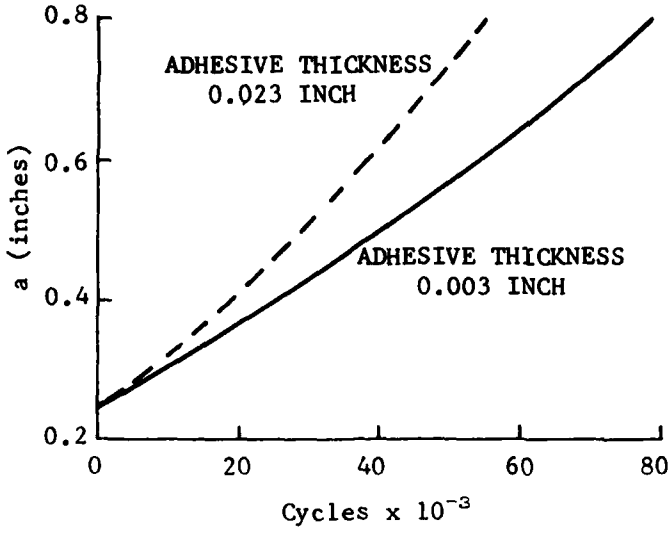

Figure 13. Influence of Adhesive Thickness on Crack Growth Life

4.4.4 Influence of Uncracked Layer Width on Crack Growth Life

Figure 14 shows the plot of crack length versus the number of fatigue cycles for a 12-inch wide and 6-inch wide center-cracked specimen, and a 12-inch wide, center-cracked specimen with a bonded strap. It is seen that the crack growth life for the bonded strap is much longer than that for the 12-inch and 6-inch wide specimen due to the fact that the sound layer in the bonded strap is thicker than in the 12-inch or 6-inch wide panels. The surprising result is lower crack growth life for the 12-inch wide panel. Perhaps this is due to the influence of localized bending in the panels because of the presence of a crack in only one layer. The entire 6-inch wide panel is able to resist bending because of the smaller width, while for wider panels, only a small, localized width on either side of the crack resists bending. This will produce larger bending stresses in a 12-inch wide panel. This figure also shows that the crack growth life of a single-ply, 12-inch wide panel is about one-half of that for a two-ply, bonded panel.

4.4.5 Influence of Crack Location on Crack Growth Life

The crack growth life for an edge crack in a 6-inch wide panel, and center cracks in 6-inch and 12-inch wide panels, is shown in Figure 15.

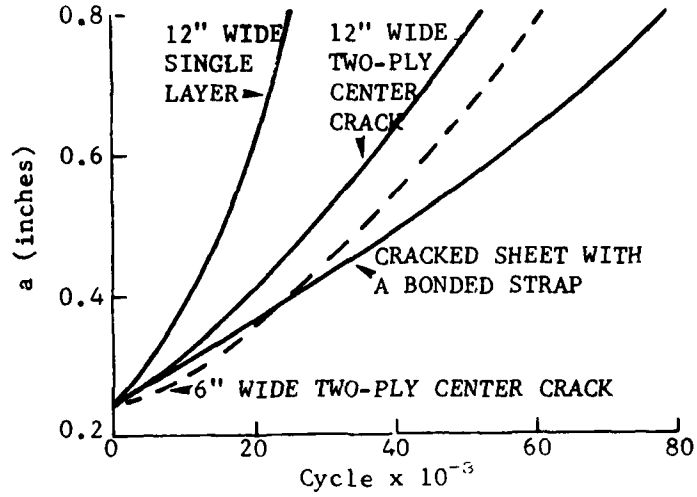

Figure 14. Influence of Uncracked Layer Width on Crack Growth Life

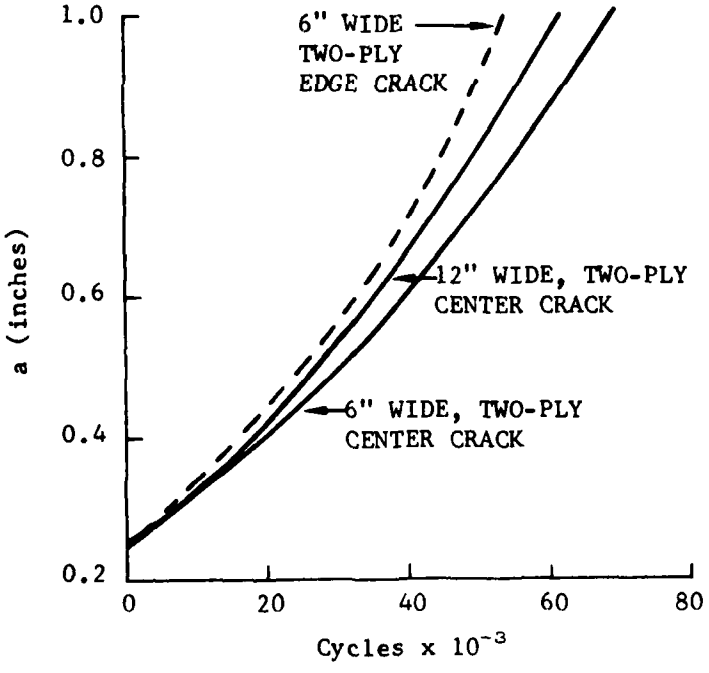

Figure 15 Influence of Crack Location on Crack Growth Life

The crack growth life for an edge crack is shorter than that for a center crack, due to higher stress intensity factors for an edge-cracked panel.

4.4.6 Influence of Sound Layer Material on Crack Growth Life

Figure 16 shows the plot of crack length versus fatigue cycles for two-ply (aluminum-to-aluminum) and three-ply (aluminum-titanium-aluminum) panels. It is seen that the three-ply panel has a much longer life. This is due to the stiffer titanium inner ply and two uncracked plies in the three-ply panel. The influence of having a stiffer titanium ply (a higher modulus than the cracked layer) is to cause more load transfer to it, hence reduce the stress intensity factors. This will result in increased fatigue life.

4.4.7 Influence of Panel Width on Crack Growth Life for a Two-Ply Bonded Panel with a Crack at a Hole

The crack growth life for two-ply, bonded panels with a crack at a central hole, and widths of 6 inches and 12 inches, respectively, is shown in Figure 17. The crack growth life is shown from a length of 0.15 inch

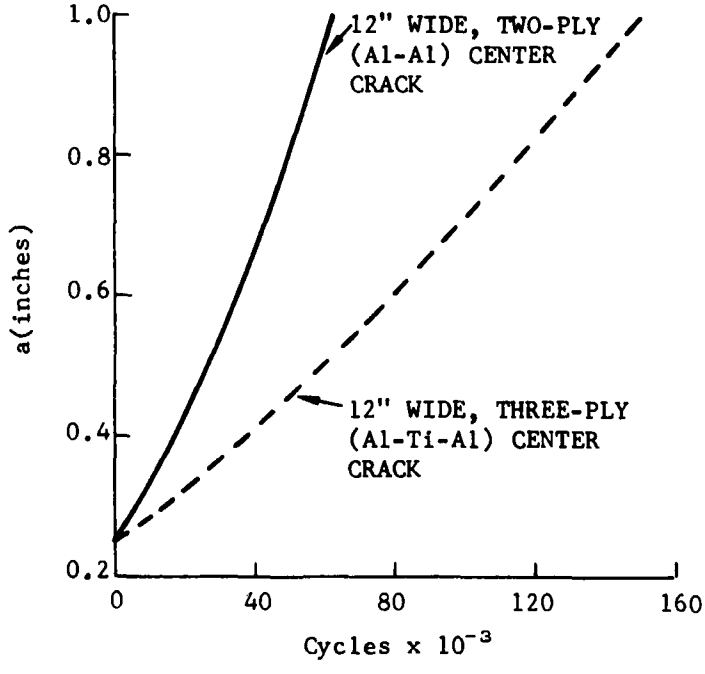

Figure 16. Influence of Sound Layer Material on Crack Growth Life

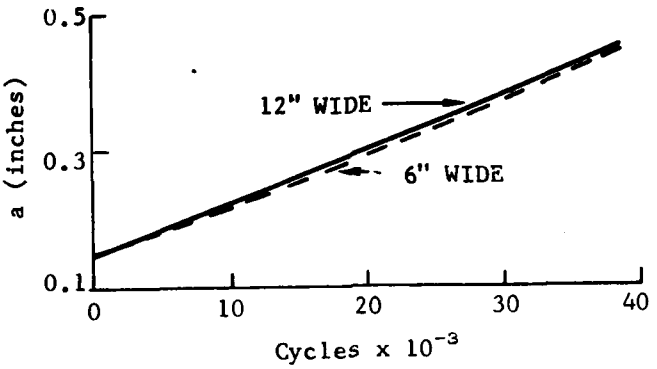

Figure 17. Influence of Panel Width on Crack Growth Life for Crack at a Central Hole

to 0.45 inch, since the crack in the sound layer has initiated at that point. The crack growth life for a 12-inch wide panel is only slightly longer than that of a 6-inch wide panel. A similar effect was observed in a center-cracked panel. For the small crack lengths considered here, the finite width effects will be negligible. However, this difference in life predictions is within experimental data scatter.

4.4.8 Influence of Crack Location on Crack Growth Life of a Crack at a Hole

There are two 12-inch wide panel geometries considered here, one with a crack at a 3/16-inch central hole, and the other with a crack at an eccentric 3/16-inch hole (three inches from one edge). The crack growth life for these two panels is shown in Figure 18. While the crack at an eccentric hole panel has a slightly shorter life than the crack at a central hole, this difference is within the experimental data scatter. The finite width effects for the crack lengths considered, are negligible.

4.4.9 Influence of Stress Ratio on Crack Growth Life

The influence of the stress ratio (R) on the crack growth life of a 4-inch wide panel (R = -1.0) and a 6-inch wide panel (R = 0.1) is shown in Figure 19. The fatigue crack growth life for a 4-inch wide panel is much shorter than that for a 6-inch wide panel. This is due to the finite width of the panel, as well as the influence of R.

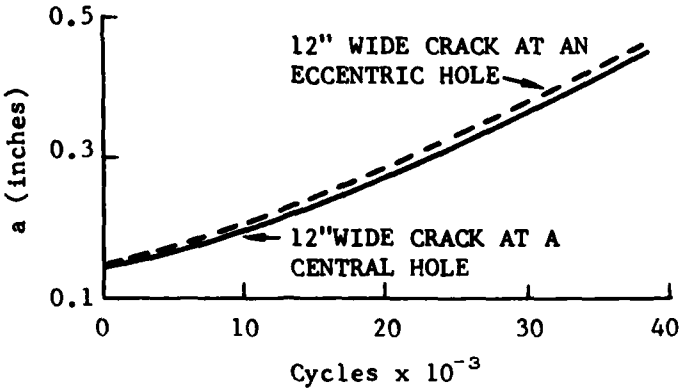

Figure 18. Influence of Hole Location on Crack Growth Life

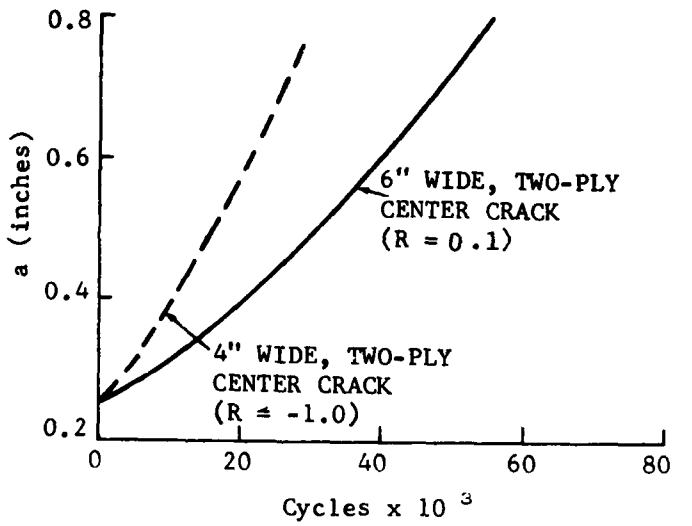

Figure 19. Influence of Stress Ratio (R) on Crack Growth Life

4.5 COMPARISON OF ANALYTICAL AND EXPERIMENTAL DEBOND SIZES

The debond produced in the adhesive during fatigue crack growth in a metallic layer was predicted analytically for a variety of crack geometries, as discussed in Section 3. These analytical predictions were compared with the debond sizes observed in the test verification program. During the course

of fatigue cycling the test panels, nondestructive inspection (NDI) was used to determine the debond size. The results obtained by this technique were inconsistent, and are discussed in Appendix C. Therefore, after obtaining the crack growth data, the panels are peeled apart in such a way that the debond area is marked by charring the debonded or loose adhesive. This is accomplished by heating the specimen at 375F for three hours, then removing it from the oven and driving in a wedge from an edge. The wedge is driven away from the area where the crack is located.

The analytical predictions were made for certain crack lengths. After peeling the test specimen, the crack lengths, corresponding to debond shape and size, were found to be slightly different from those at which predictions were made.

Table 4 shows the comparison of predicted debond sizes and actual debond sizes measured in the experiments. The experimental debond shape and size measured in Panel II-16 (Crack B), is shown in Figure 20. The debond is elliptical, with a minor-to-major axis ratio equal to about 0.12. The crack length at which this debond shape was observed is 1.8 inches. This compares favorably with the predicted shape shown in Table 4.

The experimental debond in a cracked sheet with a bonded stiffener (Panel I-7) is shown in Figure 21. In this case, the crack is within the stiffener. The correlation between the predicted and actual shape is good, as shown in Table 4.

In cracked sheet with a bonded stiffener panels, the debond is elliptical if the crack length is smaller than the width of the stiffener. As the crack propagates beyond the edge of the stiffener, the debond changes shape as predicted in Section 3. The debond shapes for Cracks A and C, in Panel I-21 are shown in Figure 22. For Crack A, the half-crack length at Point R, was 3.0 inches, and at Point Q, was 2.2 inches. The shape and size of the debond at P and Q agrees well with that predicted for a half-crack length of 2.0 inches, as shwon in Table 4. For crack B, the half-crack length on Side U is 1.4 inches, and on Side S is 2.2 inches.

TABLE 4. COMPARISON OF ACTUAL AND PREDICTED DEBOND SHAPES AND SIZES

PANEL	DEBOND PREDICTION AT a =	DEBOND MEASURED AT a =	PREDICTED AND ACTUAL DEBOND SHAPES AND SIZES
II-16 - 12-inch wide center crack h_a = 0.008 inch	1.00 inch	0.90 inch	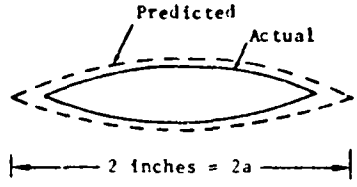
I-7 - Bonded stiffener h_a = 0.003 inch	0.75 inch	0.90 inch	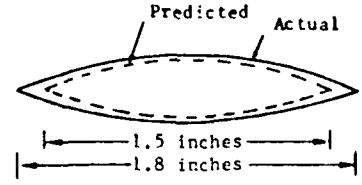
I-21 - Bonded stiffener h_a = 0.006 inch	2.00 inches	2.20 inches	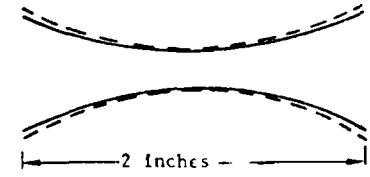
II-6 - Bonded stiffener h_a = 0.023 inch	0.75 inch	0.75 inch	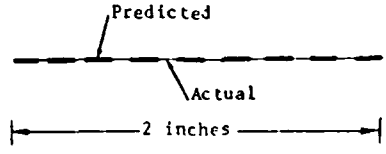
II-20 - Bonded stiffener h_a = 0.010 inch	0.75 inch	0.85 inch	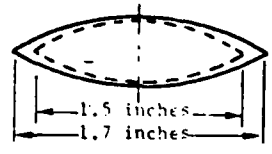
II-22 - Crack at a hole h_a = 0.007 inch	0.41 inch	0.32 inch	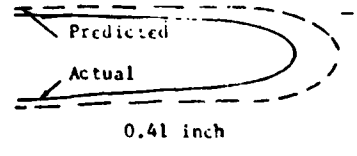

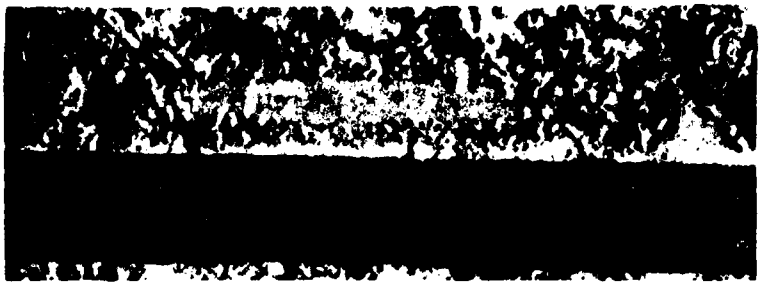

(a) Initially sound panel - inside

(b) Initially cracked panel - inside (glue line)

Figure 20. Debonding in Panel II-16

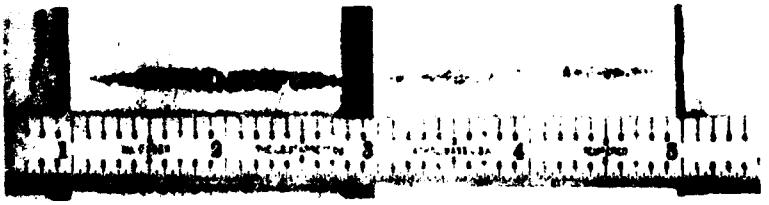

(a) Initially cracked panel - inside (glue line)

(b) Initally sound panel - inside

Figure 21. Debonding at Crack A in Panel I-7

The shape on Side S and at T, compares with the predicted shape, as shown in Table 4. The debond at U is still undergoing the transition from elliptical (observed at a = 1.0) to the shape of a parabola (observed for a = 2.0 inches).

Figure 23 shows the debond shape observed for a panel with a thick bondline (0.023 inch). The observed size agrees well with the predicted size of the zero debond, as shown in Table 4.

Crack A (total crack length = 5.2 inches)

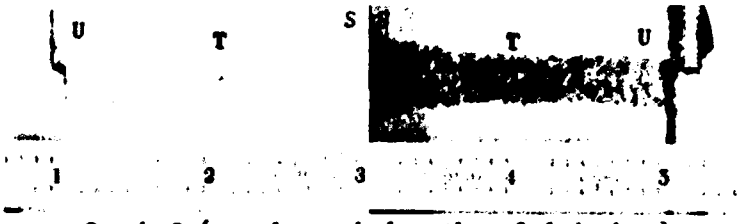

Crack C (total crack length = 3.6 inches)

Figure 22. Debond Shape in a Cracked Plate with a Bonded Stringer for Large Crack Lengths

Cracked layer Sound layer

Figure 23. Debond Shape in Panel II-6 with a Thick Bondline

The predicted shape of the debond in the FM-400 adhesive is elliptical with b/a = 0.30 at a half-crack length of 0.75 inch. The actual debond size for Panel II-20 (FM-400 adhesive) is shown in Figure 24. It is seen that the debond is much larger than that observed for the FM-73 adhesive, with a b/a ratio of about 0.26.

The debond shapes observed for other panels are discussed in Appendix C.

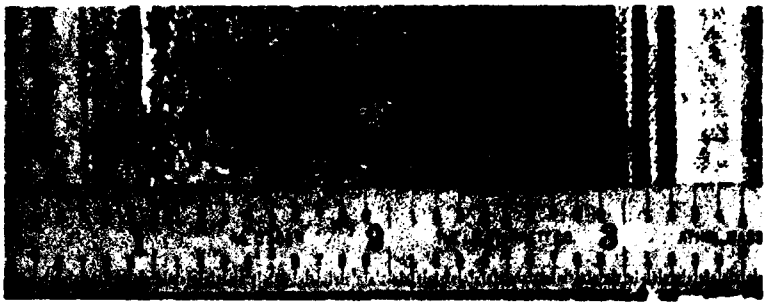

Cracked layer

Figure 24. Debond Shape in Panel II-20 with FM-400 Adhesive

4.6 COMPARISON OF ACTUAL AND PREDICTED CRACK LENGTHS FOR THE CRACKING OF A SOUND LAYER

A criterion for the cracking of a sound layer has been developed based on the critical load transferred to the sound layer. The crack lengths at which the sound layer in a two-ply bonded panel cracked are shown in Table 5. The table also shows the critical load transfer factor M_c and the values of K_{max} (stress intensity factor) in the cracked layer when the sound layer cracked. It is seen that the values of M_c are fairly uniform and well within the experimental data scatter. The average value of M_c is 0.645. The stress intensity factors in a cracked layer at the cracking of the sound layer, as shown in Table 5, show a large variation.

The cracking of a sound layer in two-ply, bonded panels with a crack emanating from a hole, was predicted based on the critical load transfer factor $M_c = 0.645$ (Table 5). The values of predicted crack lengths and actual crack lengths at which the sound layer cracked are shown in Table 6. It is seen that the predicted crack lengths agree very well with the experimental results. The table also shows the values of K_{max} at the cracking of the sound layer. These values differ significantly from those given in Table 5 for center-cracked panels. This indicates that the criterion for the cracking of a sound layer could not be based on the critical stress intensity factor in the cracked layer.

TABLE 5. CRITICAL LOAD TRANFER FACTORS FOR THE CRACKING OF A SOUND LAYER

SPECIMEN AND TYPE OF FLAW	SECOND PLY CRACKING AT a = AND LOCATION ( )	CRITICAL LOAD TRANSFER FACTOR M_C	K_{max}**
Center crack			
I-1			
12" wide	1.363 (A)	0.640	15.870
h_a = 0.0125"	1.433 (B)	0.645	16.220
	1.339 (C)	0.635	15.730
II-2			
12" wide	1.357 (A)	0.645	15.620
h_a = 0.0125"	1.295 (B)	0.631	15.230
II-16			
12" wide	1.114 (A)	0.605	19.480
h_a = 0.008"	1.270 (C)	0.630	20.560
II-10			
6" wide	1.353 (B)	0.657	15.480
h_a = 0.015"			
I-11			
6" wide	1.382 (A)	0.680	15.890
h_a = 0.015"	1.460 (C)	0.685	16.180

**Stress intensity in the cracked layer at the cracking of the sound layer.

Average M_C = 0.645

TABLE 6. PREDICTED CRACK LENGTHS FOR THE CRACKING OF A SOUND LAYER

SPECIMEN AND TYPE OF FLAW	SECOND PLY CRACKING AT a = AND LOCATION ( ) (inches)	PREDICTED 'a' FOR SECOND PLY CRACKING (inches)	K_{max} ksi $\sqrt{inches}$
Cracked at a central hole			
I-5			
12" wide	0.370 (A)	0.415	9.924
h_a = 0.007"	0.395 (B)	0.415	9.900
	0.360 (C)	0.415	9.957
II-22			
12" wide	0.528 (A)	0.415	9.198
h_a = 0.007"	0.420 (B)	0.415	9.935
	0.403 (C)	0.415	9.910
I-24			
6" wide	0.495 (A)	0.415	10.488
h_a = 0.01"	0.395 (B)	0.415	10.070
	0.423 (C)	0.415	10.280
Average	0.421	0.415	9.962
Cracked at an eccentric hole			
II-12			
12" wide	0.364 (A)	0.385	9.843
h_a = 0.009"	0.328 (B)	0.385	9.827
	0.384 (C)	0.385	9.868
Average	0.359	0.385	9.868

SECTION 5

SENSITIVITY STUDIES

The analysis of a cracked, adhesively bonded structure was discussed in Section 2. In the analysis, the thickness and properties of the adhesive and adherends are used in computing the stress intensity factors. Any change in the adhesive or adherend thickness or properties will influence the stress intensity factors, and subsequently, the life of the structure. The stress intensity factors were obtained in previous sections based on the linear elastic behavior of the adhesive. A study was carried out to investigate the influence of nonlinear behavior of the adhesive on the stress intensity factors. Also a parametric study was undertaken to investigate the influence of various factors on stress intensity factors in the following three categories:

1. a two-layer, adhesively bonded structure with a crack in one layer,
2. a cracked sheet with a bonded stringer,
3. a cracked sheet with two bonded stringers symmetrically located about the centerline.

The results of this parametric study on cracked sheets with one and two bonded stringers are given in Appendix D. The influence of nonlinear behavior and results of the parametric study for a two-ply, adhesively bonded structure with a crack in one layer (Figure 1a, W = infinity) are discussed in the following paragraphs.

5.1 INFLUENCE OF NONLINEAR BEHAVIOR ON STRESS INTENSITY FACTORS

In a cracked, adhesively bonded structure, the adhesive around the crack is subjected to high shear stresses, and the load transfer to the sound layer takes place in this region. The value of the shear stress will depend on the properties and thickness of the adhesives and adherends, crack length, and applied load. Adhesives exhibit nonlinear behavior at small stresses, and

BLANK

the shear stress-strain curve for adhesives is linear in only a small, initial region and exhibits large nonlinearity at higher stresses. Hence, in a cracked, adhesively bonded structure, the stresses in the adhesive near the crack may be in the nonlinear region of the stress-strain curve. If the shear stresses in the adhesive are in the nonlinear region, the adhesive will undergo more deformation than for elastic behavior, thus allowing larger crack openings and less load transfer to the sound layer. This will result in higher values of stress intensity factors. To investigate this problem, the shear stresses in the adhesive for the bonded panel geometry shown in Figure 1a, were plotted as shown in Figure 25. The normalized adhesive shear stresses at two locations ($x = 0$ and $x = 0.5$) are plotted as a function of the distance from the crack plane for various crack lengths. During the test verification program, the mean cyclic applied stress on the panels was approximately 8,500 psi, with a maximum cyclic stress of 15,500 psi. The shear stresses in the adhesive corresponding to these applied stresses, from Figure 25, are about 1,440 psi and 2,650 psi. The shear stress-strain curve of the FM-73, exhibits only a slight nonlinearity at the stress of 2,650 psi as seen from the stress strain curve of the FM-73 adhesive shown in Figure 26 (Reference 23).

To study the effect of nonlinearity, the adhesive properties in the finite element model were varied. In this analysis, the elliptical shaded area above the debond shown in Figure 27, was assumed to have an elastic shear modulus of 20,000 psi, or about one-third of the shear modulus for the linear portion of the stress-strain curve. With this variation in the adhesive properties, the stress intensity factor increased only nine percent for a half-crack length of one inch.

This reduction in the adhesive modulus considered here will correspond to the adhesive shear stress of about 4,500 psi (Figure 26), or a maximum applied stress of about 26,500 psi in the panel.

In an aircraft structure, the limit design stress of aluminum will be about 30 ksi, and at this design stress, the stresses in the adhesive will exhibit nonlinear behavior, which will increase stress intensity

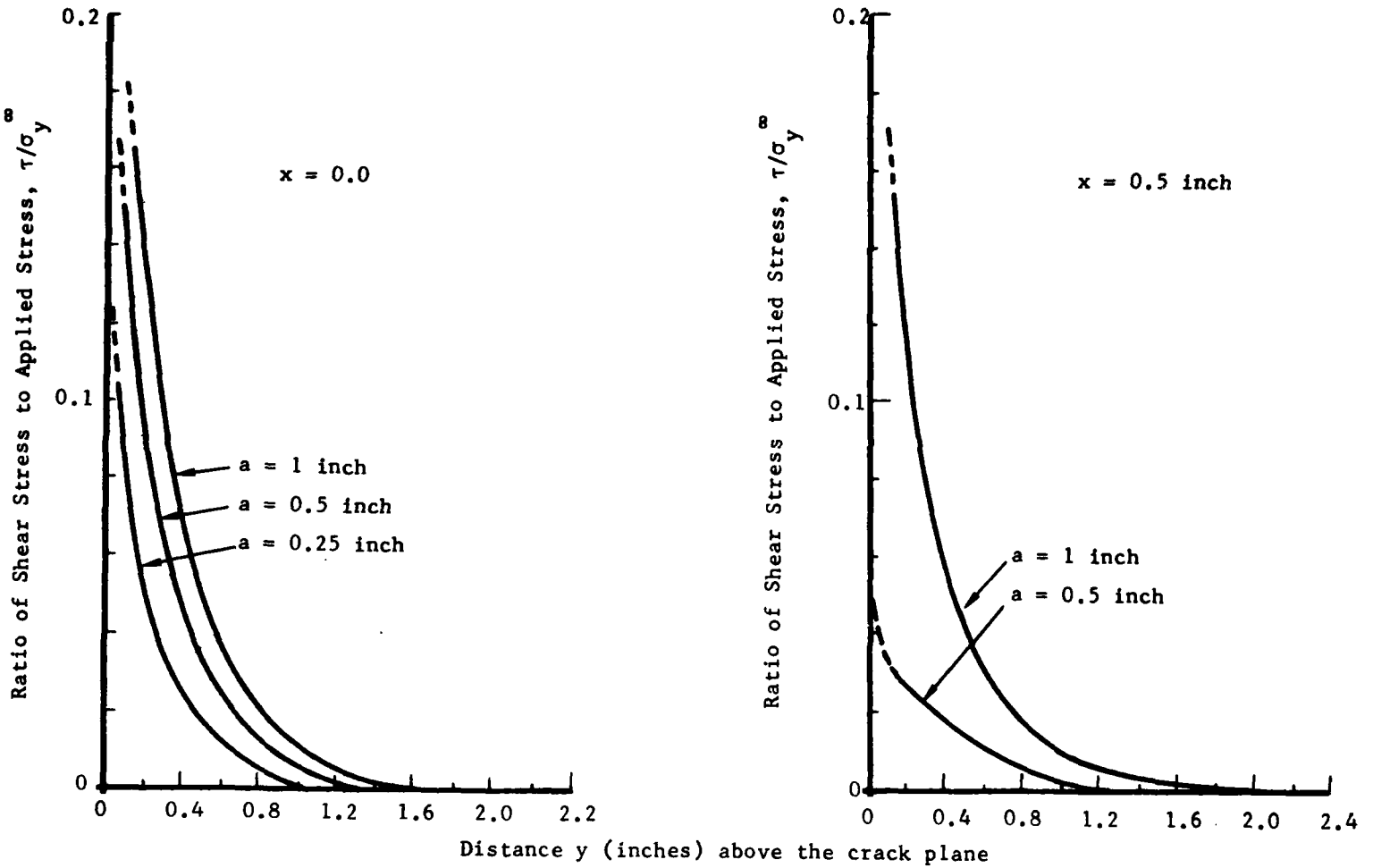

Figure 25. Shear Stress Distribution as a Function of the Distance from the Crack Plane for a Cracked, Adhesively Bonded Panel

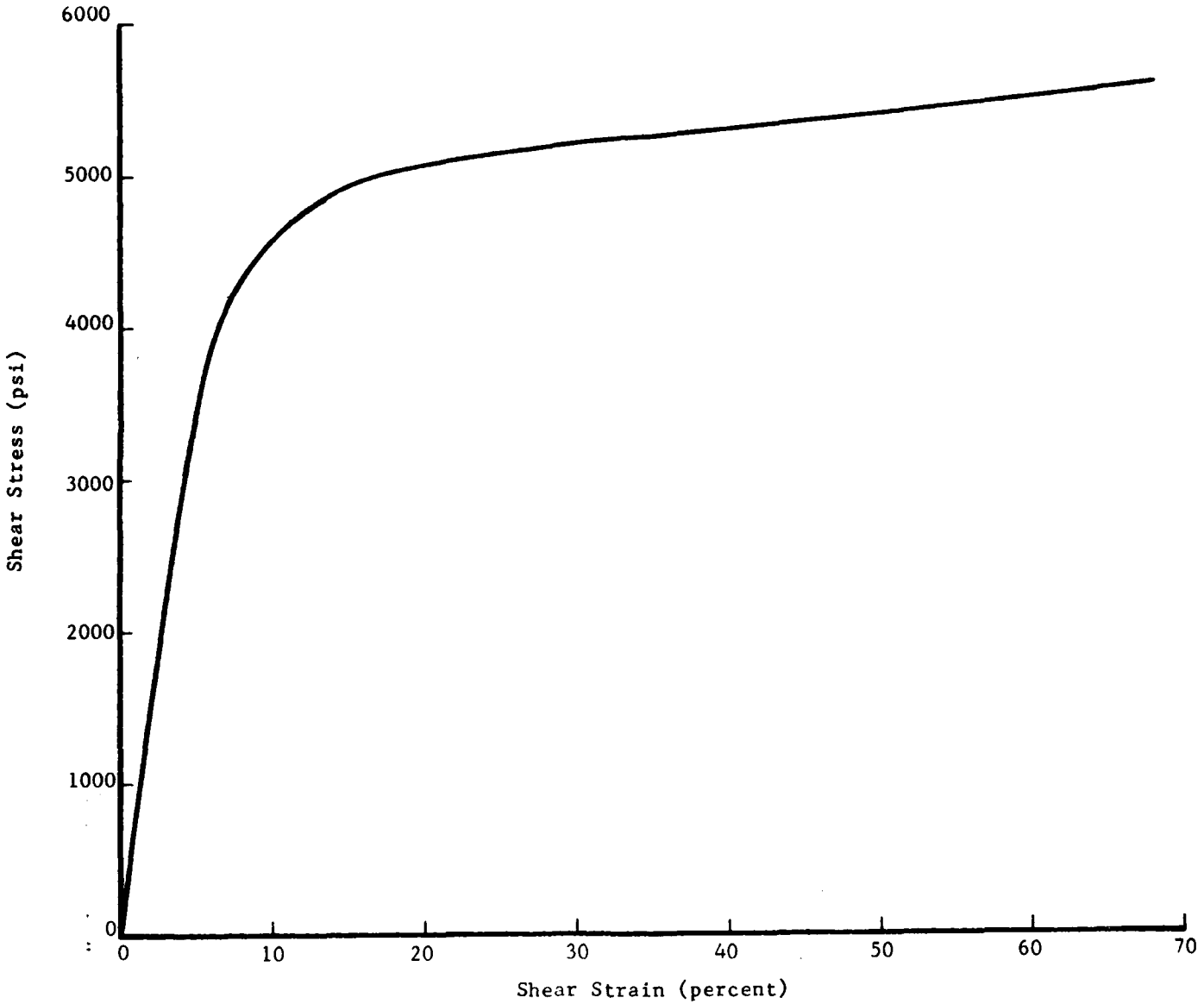

Figure 26. Shear Test, 0.00451-inch Bondline, 74F

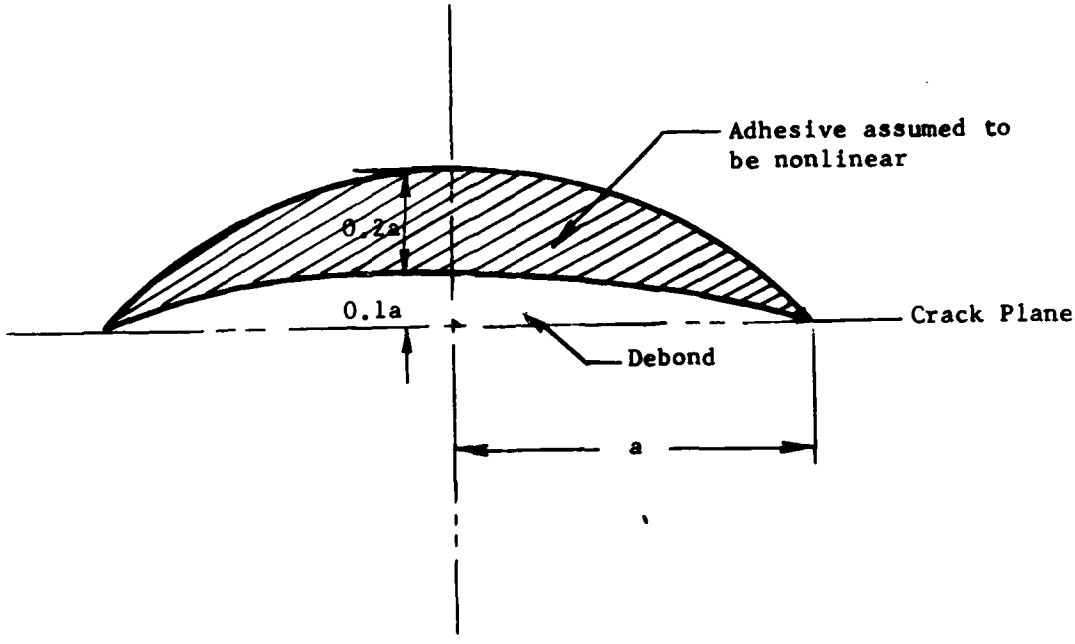

Figure 27. Model of Debond and Assumed Nonlinear Behavior in Analysis

factors or reduce crack growth life. Thus, the influence of nonlinear behavior in adhesives such as FM-73 should be considered at limit design stresses. However, at normal operating stresses of 10 ksi to 15 ksi, the influence of nonlinearity is negligible and can be ignored.

5.2 A PARAMETRIC STUDY FOR A TWO-LAYER, ADHESIVELY BONDED STRUCTURE WITH A CENTER-CRACK IN ONE LAYER

The mathematical method of analysis was used in this parametric study. The associated computer programs developed in this research contract (detailed in the appendices of Volume II of this report) have been used to compute the stress intensity factors. The integral equation formulation discussed in Section 2, has shown that the influence of adhesives on stress intensity factors can be studied by the parameter h_a/μ_a (ratio of adhesive thickness to shear modulus). Similarly, the influence of the cracked and sound layer parameters can be studied by the parameter hE (where h is the thickness and E is the modulus of the given sheet). In the studies, Poisson's ratio was assumed to be 0.33 for metallic layers.

The structure shown in Figure 1a is considered here. Two layers are assumed to have an infinite width. The following notations are used in the parametric study:

a = half-crack length
h_1 = thickness of the cracked layer
E_1 = modulus of the cracked layer
h_2 = thickness of the sound layer
E_2 = modulus of the sound layer
h_a = thickness of the adhesive layer
μ_a = shear modulus of the adhesive

The influence of debond size on the stress intensity factors for various crack lengths is shown in Figure 28. These stress intensity factors have been obtained for no debond, and an elliptical debond. The end of the major axis of the debond is assumed to coincide with the leading edge of the crack. It is seen that an increase in debond size increases the stress intensity factors, due to less load transfer to the sound layer.

The variation of the stress intensity factor with half-crack length a, for various values of the adhesive parameter h_a/μ_a, is shown in Figure 29. An increase in the adhesive thickness, or a decrease in the shear modulus, causes an increase in the stress intensity factors.

Figure 30 shows the variation of stress intensity factors with half-crack length a, for various values of cracked layer parameter $h_1 E_1$. An increase in $h_1 E_1$ causes an increase in the stress intensity factors due to the reduced stiffening influence of the sound layer.

The influence of the sound layer parameter on the stress intensity factors is shown in Figure 31. An increase in $h_2 E_2$ causes a reduction in the stress intensity factors due to an increased stiffening effect. The reduction in stress intensity factors is dependent on the crack length.

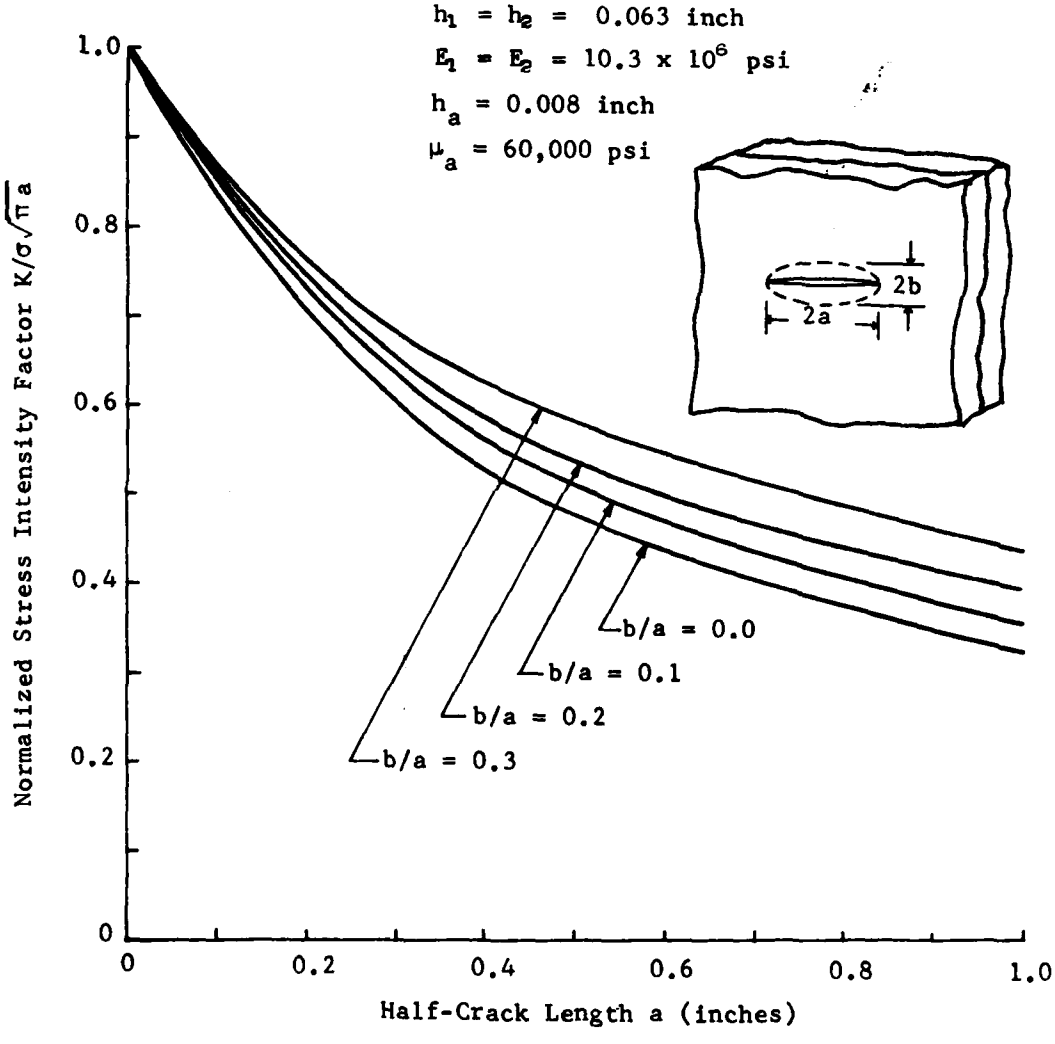

Figure 28. Influence of Debond Size on Stress Intensity Factors in a Two-Layer Bonded Structure

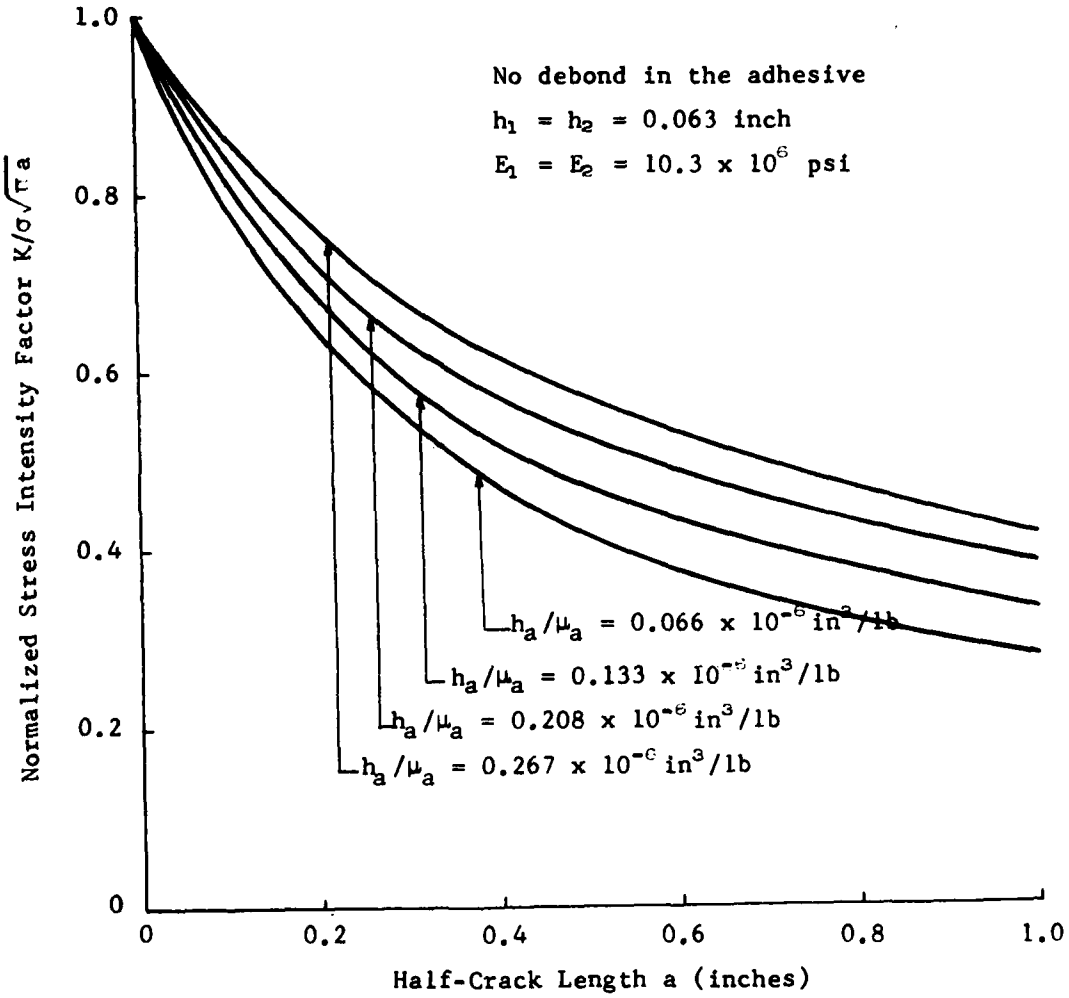

Figure 29. Influence of Adhesive Parameter h_a/μ_a on Stress Intensity Factors in a Two-Layer Bonded Structure

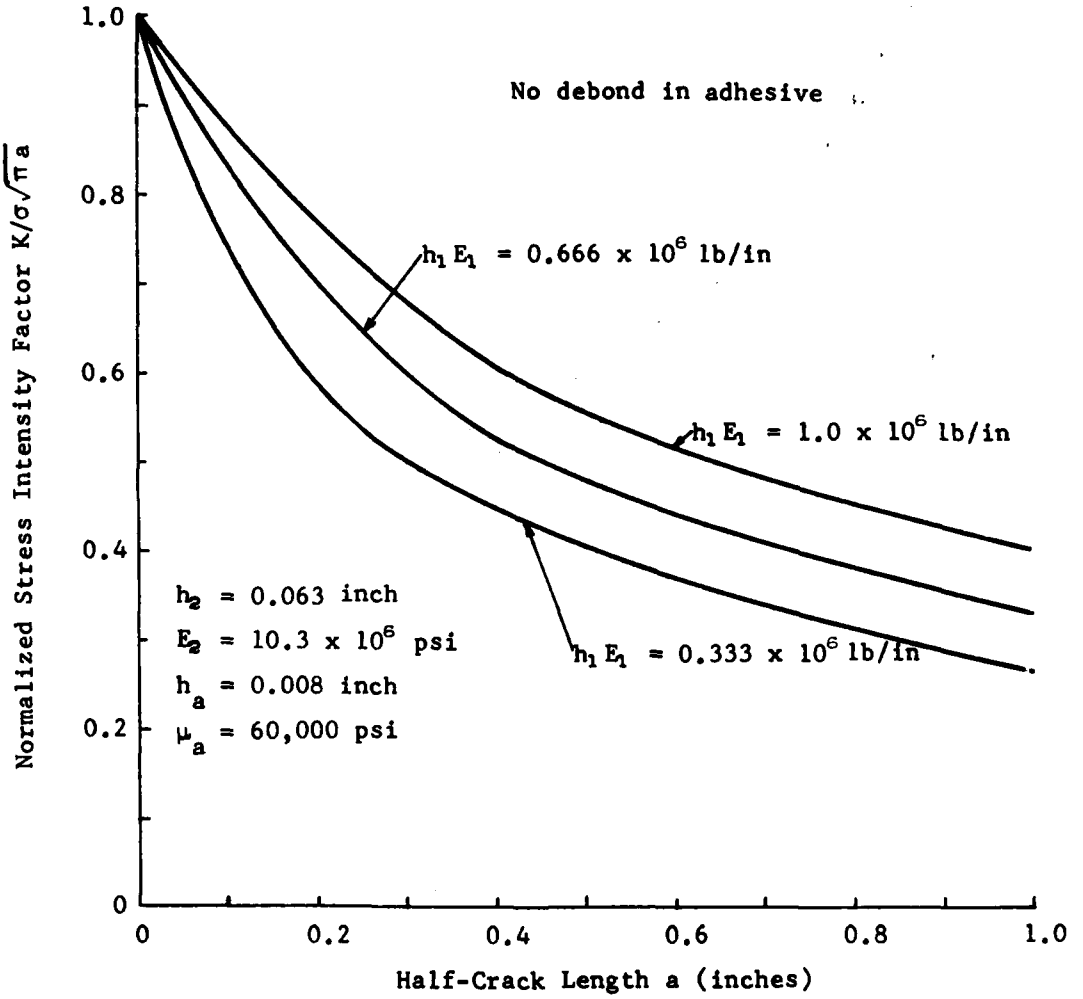

Figure 30. Influence of Cracked Layer Parameter $h_1 E_1$ on Stress Intensity Factors in a Two-Layer Bonded Structure

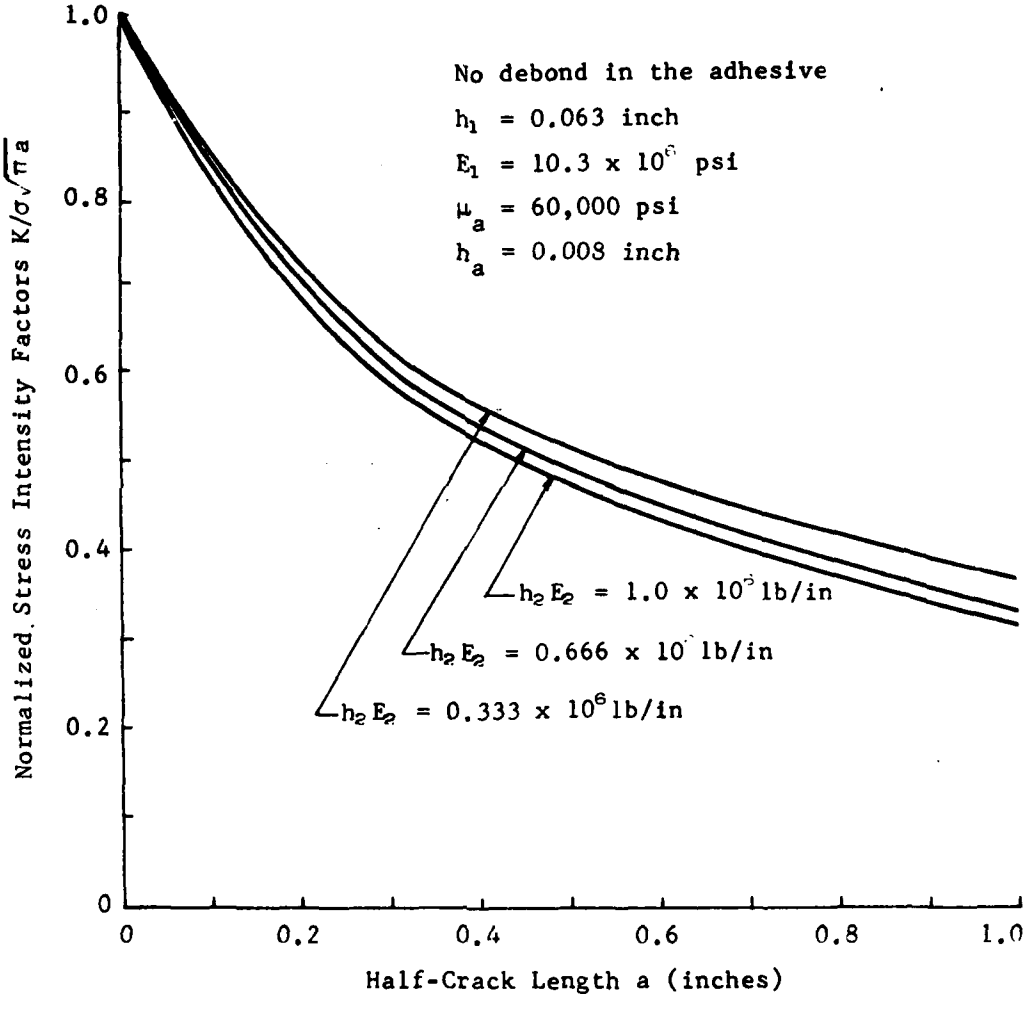

Figure 31. Influence of Sound Layer Parameter $h_2 E_2$ on Stress Intensity Factors in a Two-Layer Bonded Structure

SECTION 6

Limitations of Analytical Methods

The methods of analyzing cracked, adhesively bonded structures were based on certain assumptions, as discussed in Section 2 and Section 3. The analytical results obtained will be accurate only if the assumptions made are satisfied. For instance, in the analysis it was assumed that the material properties to be used in the analysis are readily available. However, some of these data may not be readily available and may have to be generated. The various factors that restrict the application of the analysis are discussed in the following paragraphs.

6.1 ADHESIVE CHARACTERIZATION

In the analysis of cracked, adhesively bonded structures, elastic modulus is used (corresponding to the initial linear portion of the stress-strain curve). The modulus has considerable influence on the stress intensity factors, hence an accurate determination of the modulus is necessary. Tests on an adhesive have sometimes shown a very wide variation in data on the stress-strain curve, resulting in a very wide variation in the moduli values.

The criterion for the propagation of the debond in the adhesive was based on ϵ_R, which was defined as the resistance of the adhesive to facture. This was taken as the failure strain of the adhesive in the tensile test. The value of failure strain will influence the predicted debond size in the adhesive, hence the stress intensity factors. Thus, a proper characterization of adhesive properties is essential for a successful life prediction of adhesively bonded structures.

6.2 MAXIMUM STRESS AND STRESS RATIO INFLUENCE

The influence of the R ratio, and maximum stress in a single-layer, metallic structure, has been investigated extensively. Similar observations will apply for crack growth in the metallic layer of an adhesively bonded

structure. The stress intensity factors computed for adhesively bonded structures can be used to study these effects.

The debond propagation criterion developed in Section 3, was dependent on the applied maximum stress, and was independent of the R ratio. Two of the tests under this program were conducted at R = -1.0, all others at R = 0.1. The results of these tests did not show dependence of debond size and shape on the R ratio. This is consistent with the criterion developed here. Thus, the debond size will be dependent on the maximum applied stress and will not depend significantly on the stress ratio.

6.3 INFLUENCE OF ADHEREND PROPERTIES

The elastic properties of the adherends are used in computing the stress intensity factors in a cracked, adhesively bonded structure. These metallic material properties are well established in literature, and are easily obtainable in the laboratory.

The criterion for cracking of a sound layer, based on the critical load transfer developed in this research program, is a new concept. The load transfer factor, M, depends on the thicknesses and properties of the adhesives and adherends and stress concentrations. The influence of stress concentrations (e.g., cracks at holes) was taken into consideration in the computation of the critical load transfer factor M_c. The value of the critical load transfer factor M_c, at which a crack will initiate in a sound layer, will depend on the thickness and the material of the sound layer. The critical load transfer factor M_c was found to be 0.65, for 7075-T6 aluminum with a thickness of 0.063 inch. The value of M_c may be different for other thicknesses and materials, e.g., it may be higher for tougher materials, as titanium. The critical values of M_c have not been established for other thicknesses and materials.

The analysis techniques developed, were for plane stress conditions, and it was assumed that the thickness of the adhesive was small compared to the thickness of the plates. If the bonded plates are thick, the plane stress conditions will not be satisfied, and the stress intensity factors computed will be in error.

6.4 ENVIRONMENTAL EFFECTS

In the analysis of a cracked, adhesively bonded structure, no environmental effects were taken into consideration. The crack growth rates are affected by the environments (e.g., moisture increases crack growth rate), however their influence can be easily accounted for by varying the constants in the crack growth equations; the analytical methods developed will still apply.

The environment also has an influence on the adhesive properties (e.g., the stress-strain curve and failure strain of an adhesive will change if moisture is present). This change in the adhesive properties will influence the effectiveness of the adhesive in load-shedding from the cracked layer to the sound layer, and the debond size will change as a result of the change in the failure strain of the adhesive. The influence of these factors can be taken into account by the use of a modified modulus in the computation of the stress intensity factors and debond size.

SECTION 7

SUMMARY AND CONCLUSIONS

7.1 SUMMARY

Finite element and mathematical techniques for the analysis of cracked, bonded structures have been developed. These analytical techniques, experimentally verified for adhesive bonding, are also considered to be applicable to weldbonded, and brazed structures. Good agreement was obtained between the results of the finite element and the mathematical approaches. Stress intensity factors have been obtained (through the use of these analytical techniques) for the geometries of a cracked sheet with an adhesively bonded stringer, and a two-layer, adhesively bonded panel with a center-crack, an edge-crack, and a crack-at-a-hole. The influence of bending, debond size, and finite width, on the stress intensity factors has been studied.

A criterion for the cracking of an initially sound layer has been developed, based on the critical load transfer to the sound layer, and has been examined for a variety of crack geometries in aluminum.

A criterion has also been developed (using a new concept) for the propagation of a debond in an adhesively bonded structure. This criterion predicts the shape and size of a debond in an adhesive, as the crack in the metallic layer grows. A good agreement in shape and size was found between the predicted and actual debond size.

A test program was developed to verify the analytical techniques. The crack growth life predictions, based on analytical stress intensity factors, were found to agree within ten percent of those determined from the experiments. The influence of the adhesive thickness, type of adhesive, and the material of the sound layer, on crack growth life was examined experimentally.

A parametric study was conducted to investigate the influence of adhesive and adherend properties on stress intensity factors. The studies were

PRECEDING PAGE NOT FILMED
BLANK

conducted for a cracked sheet with a bonded stringer, a cracked sheet with two bonded stringers, and a two-layer, bonded structure with a crack in a single layer.

The various locations, and the size of the cracks likely to occur during the manufacturing process of the adhesively bonded structures, have been examined. The metallic flaws in an adhesively bonded structure will have the same size and location, as in any other metallic structure, however at certain locations, these flaws will be associated with debonding, or flaws in the adhesive. The crack growth rate of metallic flaws, will be influenced by the presence of a debond in the adhesive. An initial debond around the crack in a metallic layer, will cause less load transfer to the sound layer, or an increase in the stress intensity factors. This will reduce the crack growth life in comparison with no debond. Hence, the analysis of adhesively bonded structures should account for initial bondline flaws around the assumed metallic flaws.

The good agreement between analytical and experimental life predictions for constant amplitude loading can be attributed to the accuracy in computing the stress intensity factors for bonded structures. To achieve these accurate computations, the following factors must be taken into consideration.

1. Proper boundary conditions and modeling of the structure
2. Correct size of debond
3. Correct adhesive and adherend thicknesses and properties.
4. Cracking of an initially sound layer.
5. Influence of bending.

In actual aircraft structures, the panel boundaries and stiffener geometries will generally be more complex than investigated here. Also the loading will usually be of variable amplitude. However, the methodology developed here is still applicable if the factors discussed above are properly accounted for in the analysis. Special consideration has to be given to the modeling of stiffeners and applying bending corrections. A bending correction, based on load transferred to the sound layer is still necessary, however, the area resisting bending has to be carefully computed. The analysis approach developed here is considered applicable to life predictions under spectrum loading, provided this analysis is based on stress intensity factors computed for adhesively bonded structures.

7.2 GUIDELINES FOR APPLYING METHODOLOGY

The basic steps to be followed in the analysis of adhesively bonded structures with known or unknown bondline flaws are:

1. Choose the method of analysis to be used. Mathematical methods are recommended for parametric studies (computer programs are given in the Appendices). The finite element analysis is recommended for crack growth analysis.

2. Analysis of the structure is carried out assuming no debond (if debond size is not known) or known debond.

3. Using the displacements in cracked and sound layers and the failure strain of the adhesive, the size of the debond is determined by the procedure outlined in Section 6 of Volume II.

4. The analysis of the bonded structure is carried out again (assuming the debond size determined in Step 3). If the debond size obtained in Step 3 is small (say elliptical with a minor-to-major axis ratio of less than about 0.1), the debond size need not be recomputed. If the debond size obtained in Step 3 is large (or significantly larger than the known debond size), the debond size is recomputed with the analysis procedure in this step. The bonded structure is then analyzed again with the new debond size.

5. Compute the stress intensity factors using the analysis of Step 4.

6. Apply bending correction to the stress intensity factors using the method outlined in Section 4 of Volume II.

7. Using the method described in Section 5 of Volume II, determine the load transfer factor or local load transfer (for cracks at stress concentration). If the load transfer factor is less than M_c (the critical load transfer factor of the sound layer material), the sound backup layer has not cracked. The stress intensity factors obtained in Step 6 are correct.

8. The stress intensity factors are determined for various crack lengths using the procedures outlined in Steps 1 through 7.

9. Obtain the crack growth data on a single layer. Using these data and a crack growth equation (e.g., $da/dN = C\Delta K^n$, the constants C and n are obtained.

10. Using the stress intensity factors of Step 8 and the crack growth rate equation constants C and n, the crack growth life of a bonded structure is obtained.

11. The crack growth life in Step 10 is predicted only up to crack length a_c, at which the sound layer cracks. For crack lengths beyond sound layer cracking, the analysis can be carried out by assuming crack length a_c in the initially cracked layer, and a crack in the initially sound layer.

7.3 CONCLUSIONS

The studies undertaken in this program have resulted in the following conclusions:

1. The analytical techniques (finite element and mathematical) can be used to reliably predict crack growth life in multilayered, bonded structures.

2. The two-dimensional finite element model gives stress intensity factors that are close to those obtained experimentally.

3. The results of analytical stress intensity factors obtained by finite element and mathematical methods for adhesively bonded structures will be the same, if proper boundary conditions are incorporated.

4. The shape and size of the debond in the adhesive can be predicted through the use of analytical techniques and a failure criterion for the adhesive.

5. The cracking of a sound layer can be based on the critical load transfer to the sound layer. The sound layer will crack, when the load transfer factor reaches a critical value, which can be analytically predicted.

6. A crack in one layer of a multilayered structure may cause significant bending, which will increase the stress intensity factors ahead of the crack tip. The influence of bending must be considered in crack growth life predictions.

7. A debond in the adhesive will cause less load transfer to the sound layer, hence an increase in stress intensity factors.

8. An increase in adhesive thickness, causes less load transfer to the sound layer, resulting in an increase in the stress intensity factors. However, an increased thickness, will produce a smaller debond size, which will reduce the stress intensity factors. The net influence of the increase in adhesive thickness will depend on the type of structure and the thickness and properties of the adhesive and adherend.

9. A small elastic modulus of the adhesive will give more flexibility to the adhesive and allow larger crack openings in the cracked layer. This will result in higher stress intensity factors.

10. The influence of adhesive properties on stress intensity factors can be studied by one parameter - the ratio of adhesive thickness to the adhesive elastic modulus.

11. The influence of a sound or cracked layer on the stress intensity factors can be studied by two parameters - Poisson's ratio, and the product of the modulus and thickness.

12. There was no significant difference between the crack growth life of a cracked sheet with a 7075-T6 and 2024-T3 aluminum bonded stiffener, due to the fact that the two materials have almost the same values of elastic modulus.

13. The extent of debond propagation depends on the type of adhesive used (brittle adhesives give larger debond sizes).

14. The stress in the adhesive near the design limit loads, are such that the nonlinear behavior of the adhesive could have a significant effect on the stress intensity factors in a metallic layer.

15. There may be no debonding in a very thick adhesive (depending on its failure strain).

16. The initial flaw assumptions for damage tolerant analysis of single-layer structures, is applicable to bonded structures, however, appropriate bondline flaws must be assumed around these initial flaws.

6. A crack in one layer of a multilayered structure may cause significant bending, which will increase the stress intensity factors ahead of the crack tip. The influence of bending must be considered in crack growth life predictions.

7. A debond in the adhesive will cause less load transfer to the sound layer, hence an increase in stress intensity factors.

8. An increase in adhesive thickness, causes less load transfer to the sound layer, resulting in an increase in the stress intensity factors. However, an increased thickness, will produce a smaller debond size, which will reduce the stress intensity factors. The net influence of the increase in adhesive thickness will depend on the type of structure and the thickness and properties of the adhesive and adherend.

9. A small elastic modulus of the adhesive will give more flexibility to the adhesive and allow larger crack openings in the cracked layer. This will result in higher stress intensity factors.

10. The influence of adhesive properties on stress intensity factors can be studied by one parameter - the ratio of adhesive thickness to the adhesive elastic modulus.

11. The influence of a sound or cracked layer on the stress intensity factors can be studied by two parameters - Poisson's ratio, and the product of the modulus and thickness.

12. There was no significant difference between the crack growth life of a cracked sheet with a 7075-T6 and 2024-T3 aluminum bonded stiffener, due to the fact that the two materials have almost the same values of elastic modulus.

13. The extent of debond propagation depends on the type of adhesive used (brittle adhesives give larger debond sizes).

14. The stress in the adhesive near the design limit loads, are such that the nonlinear behavior of the adhesive could have a significant effect on the stress intensity factors in a metallic layer.

15. There may be no debonding in a very thick adhesive (depending on its failure strain).

16. The initial flaw assumptions for damage tolerant analysis of single-layer structures, is applicable to bonded structures, however, appropriate bondline flaws must be assumed around these initial flaws.

REFERENCES

1. Kaufman, J.G., "Fracture Toughness of 7075-T6 and T651 Sheet Plate, Multilayered Adhesive Bonded Panels," Transactions of ASME, Journal of Basic Engineering, Volume 89, September 1967, pp. 503-307.

2. Alic, J.A., and Archange, H., "Comparison of Fracture and Fatigue Properties of Clad 7075-T6 Aluminum in Monolithic and Laminated Forms," Society of Automotive Engineers Business Aircraft meeting, Wichita, Kansas, April 8 - 11, 1975, SAE paper No. 750511.

3. Kula, E.B., Anctil, A.A., and Johnson, H.H., "Fatigue Crack Growth in Dual-Hardness Steel Armor," Army Materials and Mechanics Research Center Report AMMRC TR 74-6.

4. Smith, S.H., Porter, T.R., and Engstrom, W.L., "Fatigue Crack Propagation Behavior and Residual Strength of Bonded Strap Reinforcement, Laminated and Sandwich Panels," AFFDLTR-70-144, pp. 611-634, 1969.

5. Alic, J.A., "The Influence of Layer Thickness on Fatigue of Adhesively Bonded Laminates," ICM-II Conference, Boston, August 1976, pp 958-962.

6. Johnson, W.S. and Stratton, J.M., "Effect of Remote Stresses and Stress Intensity Factors for an Adhesive Bonded Multi-Ply Laminate," Submitted for publication in the Journal of Engineering Fracture Mechanics, June 1976.

7. Anderson, J.M., Hsu, T.M., and McGee, W.M., "Characterization of Crack Growth in Bonded Structures," proceedings of 12th Annual meeting of the Society of Engineering Science, University of Texas, at Austin, 1975, pp. 1283-1292.

8. Roderick, G.L., Everett, R.A., and Crews, J.H., "Cyclic Debonding of Unidirectional Composite Bonded to Aluminum Sheet for Constant-Amplitude Loading," NASA TN-D-8126.

9. McHenry, H.I., and Key, R.E., "Brazed Titanium Fail-Safe Structures," Welding Journal, Volume 53, No. 10, October 1974, pp. 432-S to 439-S.

10. Erdogan, F., and Arin, K., "A Sandwich Plate with a Part-Through and a Debonding Crack," Engineering Fracture Mechanics, Volume 4, 1972, pp. 449-458.

11. Arin, K., "A Plate with a Crack, Stiffened by a Partially Debonded Stringer," Engineering Fracture Mechanics, Volume 6, 1974, pp. 133-140.

12. Arin, K., "A Note on the Effect of Lateral Bending Stiffness of Stringers Attached to a Plate with a Crack," Engineering Fracture Mechanics, Volume 7, 1975, pp. 173-179.

13. Keer, L.M., Liu, C.T., and Mura, T., "Fracture Analysis of Adhesively Bonded Sheets," Presented at the Winter Annual Meeting of the American Society of Mechanical Engineers, December 1976, Paper No. 76-WA/APM-12.

14. Ratwani, M.M., and Wilhem, D.P., "Development and Evaluation of Methods of Plane Stress Fracture Analysis - A Technique for Predicting Residual Strength of Structures," AFFDL-TR-73-3, Part II, Volumne I, April 1975.

15. Sih, G.C., "Handbook of Stress - Intensity Factors," Institute of Fracture and Solid Mechanics, Lehigh University, Bethlehem, Pa.

16. Tada, H., Paris, P., and Irwin, G., "The Stress Analysis of Cracks Handbook," Del Research Corporation, Hellertown, Pa., 1973.

17. Erdogan, F., and Ratwani, M.M., "Stress Distribution in Bonded Joints," Journal of Composite Materials, July 1971, pp. 378-393.

18. Tong, P., Pian, T.H.H., and Lasry, S.J., "A Hybrid Element Approach to Crack Problems in Plane Elasticity," International Journal of Numerical Methods in Engineering, Volume 7, 1973, pp. 297-308.

19. Wilhem, D.P., "Fatigue Crack Growth in a Three-Ply, Adhesively Bonded Structure," Northrop Report NOR-76-117.

20. James, L.A., and Anderson, W.E., "A Simple Experimental Procedure for Stress Intensity Factor Calibration," in Compendium to Engineering Fracture Mechanics, Volume 1, 1969, pp. 565-568.

21. Stephens, R.K., McBurney, B.W., and Oliphant, L.J., "Fatigue Crack Growth with Negative R Ratio Following Tensile Overloads," International Journal of Fracture, Volume 10, 1974, pp. 587-589.

22. Hudson, C.M., "Effect of Stress Ratio on Fatigue Crack Growth in 7075-T6 2024-T3 Aluminum Alloy Specimens," NASA TND-5390, August 1969.

23. Hughes, E.J., and Rutherford, J.L., "Selection of Adhesives for Fuselage Bonding," Final Report No. KD-75-37, The Singer Company Kearfott Division, Little Falls, New Jersey.

APPENDIX A

METALLIC FLAWS IN BONDED STRUCTURES

To satisfy the damage tolerant requirements as given in MIL-A-83444 and to establish design stress levels for limiting the amount of slow crack growth, certain assumptions regarding the location and size of the flaws must be made by the analyst during design. These assumptions will depend on the type of strcture under consideration, thus it is necessary to examine the structure during fabrication and service to arrive at the flaw sizes and locations.

To characterize initial flaw types and sizes for the bonded structures considered in this program, Northrop's quality control experience with bonded structures was surveyed together with available literature and other industry experience. To satisfy the requirements of this program, special attention was given to the identification of initial flaw types and sizes in metallic elements that are generic to bonded primary aircraft structure.

Metallic flaws in bonded structures are introduced into the adherend material, primarily during the fabrication process. The presence of debond areas may be introduced during the bonding process, and in many cases, through the fabrication procedure as well. The occurrence of the debond tends to accentuate the severity of the metallic flaw problem. Specific examples of the types of flaw that can occur during the bonding/fabrication process are given herein. Emphasis has been placed on the metallic (ply) flaw situation, and where applicable, those debond situations associated with the induced metallic flaw. The initial metallic flaw assumptions in primarily adhesively bonded structures (PABST Program) at Douglas Aircraft Company Long Beach, California (Reference A1), have been based on those given in MIL-A-83444.

FLAWS IN ADHESIVELY BONDED STRUCTURES

The flaws in adhesively bonded structures will be different from other bonded structures in certain situations. Typical metallic flaws in adhesively bonded structures (References A2 through A4) are discussed in the following paragraphs.

PRECEDING PAGE NOT FILMED BLANK

1. Flaws at Edges

When an exposed free edge occurs, there is always the possibility of nicks, which under cyclic loading, can be developed into fatigue cracks. An example of the type of flaws that fall in this category, is shown at A, B, and C in Figure A1, with A and B more prevalent. The structure of Figure A1 could represent a tear strap bonded to a panel, a reinforcing doubler, or a bonded stiffener flange. These flaws may be caused by knife blades during the trimming of the adhesive or they may occur as the result of using trimming tools with a dull edge during detail fabriaction and final bonded assembly trim operations.

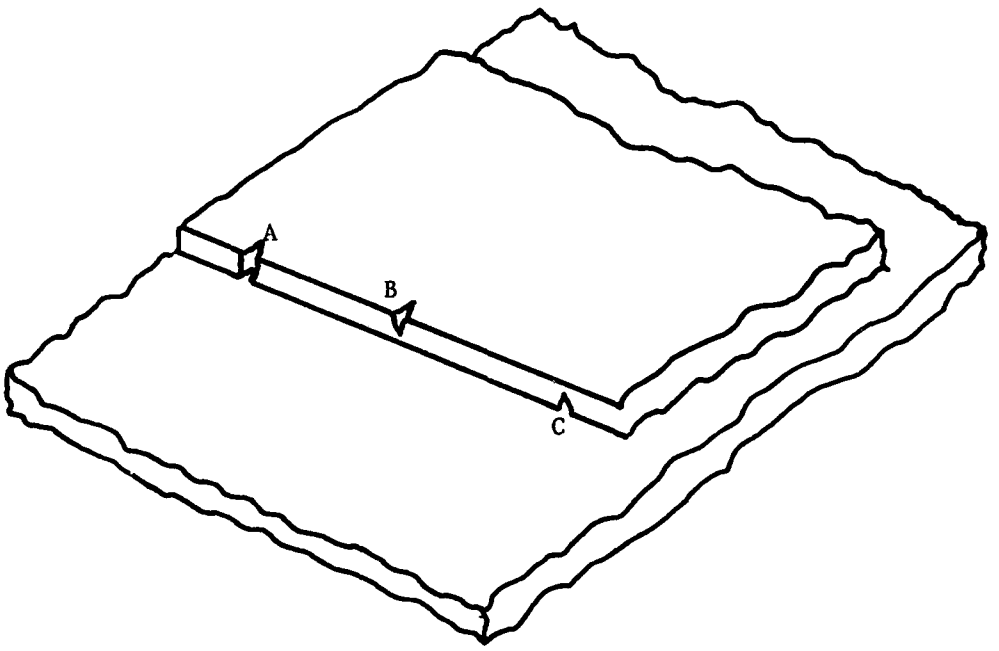

Figure A1. Edge Flaws in Adhesively Bonded Structures

Nicks along the edges of detail parts are usually covered by adhesive "squeeze-out" fillets. Nicks in the edge of "trimmed-on-assembly" bonded joints are usually covered by joint/seam

filler or sealant. Such edge nicks usually are from 0.001 inch to 0.008 inch deep (Reference A2).

2. Surface Flaws

Surface scratches, dents, cuts, etc., are normally caused by improper handling. These may also be caused by scribe marks.

Scribe marks in the form of scratches are generally made by a sharp, pointed instrument and are usually found on a skin at the edge of detail parts overlaying the skin to temporarily locate the detail part. Such marks are generally covered by subsequent adhesive "squeeze-out" at the edge of the bond joint.

Cuts into skin surfaces may occur due to the cutting of adhesive film to the size of detail part and are subsequently covered by the adhesive "squeeze-out."

Scribe marks and cuts are normally from 0.001 to 0.004 inches deep (Reference A2).

Thin skins and detail parts (0.02 inch thick or less) are frequently burnt at the clamp contact points during anodize surface treatment. This generally occurs when a clamp is not completely secured to the part surface. The burns normally occur within one inch of the outer periphery and may be up to one-quarter square inch in area. The depth of the burnt pit in thin parts (less than 0.02 inch) can be as much as one-half the part thickness (Reference A2).

3. Flaws at Holes

The normal metallic flaw is caused by a nick, drill chatter, or other mechanical means that produce flaw types A and B (Figure A2a). In this case, the flaw will grow as a part-through-the-thickness crack and will eventually reach the adhesive layer, at which time debonding will occur with increased fatigue crack growth. The size of these flaws will be the same as in any metallic structure (Reference A1).

The drilling of a hole may cause delamination around the holes. A dull drill can cause excessive, local heating of the metallic plies. This can lead to burnout of the adhesive in a donut shape debond between the plies as noted at C in Figure A2b. The adhesive failure at the periphery of the hole ranges from 0.005 inch to 0.02 inch in width (References A3 and A4).

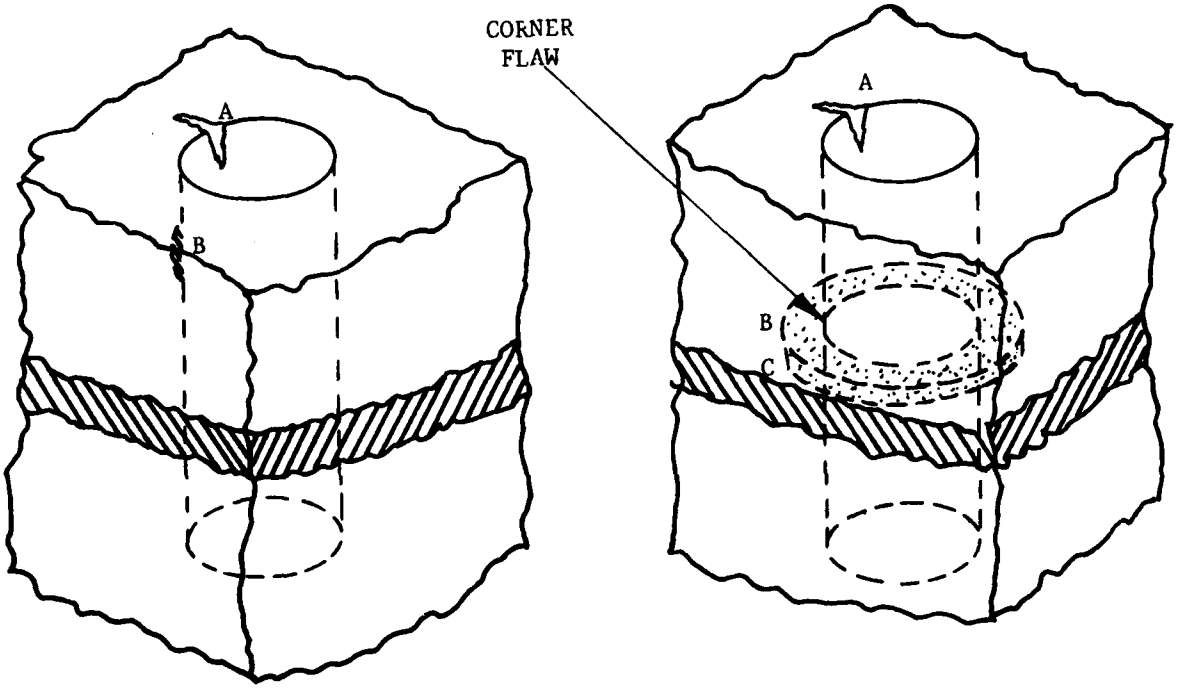

(a) Flaws at holes (b) Delamination at holes

Figure A2. Flaws at a Hole in Adhesively Bonded Structures

FLAWS IN WELDBONDED STRUCTURES

The flaws locations, and sizes discussed for adhesively bonded situations will be applicable to weldbonded structures. In addition, weldbonded structures will have flaws associated with weldbonding. The flaws in weldbonded structures are discussed below.

1. Cracks in a Nugget

Weld nuggets formed during the welding process may develop cracks due to either inappropriate welding parameters or surface preparation. The larger the size of the nugget, the more the possibility

of cracks. The size of the cracks is governed by the parameters used in the welding process. Even under controlled automatic conditions a machine malfunction may introduce cracks. The size of such cracks may be as large as one-quarter the size of the nugget (References A5 and A6). During welding, the molten metal will fill any base metal flaws in the faying surface. Hence, no initial surface flaws in welded parts need be assumed in the nugget region.

2. Expulsion

Excessive welding current or inadequate electro-force causes expulsion, which in turn may cause a debond in the adhesive in this area. The expulsion may be as large as twice the size of the nugget.

3. Porosity in the Weld

The weldbonding process may cause some porosity in the weld, which may affect the fatigue strength of the joint. However, the effect of a porous weld on fatigue strength will not be as severe as a crack in the nugget (Reference A5)

FLAWS IN WELD-BRAZED STRUCTURES

Metallic flaws in weld-brazed structures will be similar to the flaws in any other metallic structure. For weld-brazed titanium structures, filler-metal voids may occur at the edge of the lap joint or at the joint interface. A void at the edge of a lap joint may grow in size during fatigue loading, depending on the size of the void, the maximum stress and the number of fatigue cycles.

Experience at Northrop has indicated the voids to be less than 15 percent of the interface area. A void in the filler metal up to 15 percent of the interface area does not reduce the fatigue strength of the joint at a maximum applied stress of 50 ksi (Reference A7). The interface voids in the filler metal is less detrimental to the fatigue strength than voids at the edge of the lap joint since the maximum stress concentration occurs at the edge of the overlap rather than at the central area of the overlap.

It was concluded from this survey of bonded structure defects, that the initial flaw sizes and types currently specified in MIL-A-83444, are appropriate for at least one ply of the adherend material in a bonded metallic laminate. However, these initial flaw requirements should include initial debond sizes adjacent to the adherend flaw. The size of the debond will depend on the location of the flaw.

REFERENCES

A1 Swift T., Douglas Aircraft Company, Long Beach, California,
A private communication, April 1977.

A2 Hsu, T. M., The Lockheed Georgia Company,
A Private communication, April 1977.

A3 Hart Smith, J., Douglas Aircraft Company, Long Beach, California,
A private communication, April 1977.

A4 Preliminary Design Report, PABST Program, Douglas Aircraft Comapny,
Long Beach, California, 1977.

A5 Wu, K. C., Northrop Corporation, Hawthorne, California,
A private communication, April 1977.

A6 Chanani, G. R., Northrop Corporation, Hawthorne, California,
A private communication, April 1977.

A7 Hocker, R. G., Northrop Corporation, Hawthorne, California,
A private communication, April 1977.

APPENDIX B

STRESS INTENSITY FACTORS

The stress intensity factors obtained for various panel geometries by the finite element method are discussed in the following pages.

[illegible] BLANK

TWO-PLY (ALUMINUM-TO-ALUMINUM) ADHESIVELY BONDED STRUCTURE WITH A CENTER CRACK IN ONE PLY (FIGURE 1a, SECTION 2)

The variation of the stress intensity factors for the two panel widths, and the elliptical debond in the adhesive with b/a = 0.1, is shown in Figure B1. The stress intensity factor for a = 1.0 in a six-inch wide panel is about three percent higher than that for the same size crack in a 12-inch wide panel.

The stress intensity factors corrected for the influence of bending are also shown. The influence of bending on the six-inch wide panel is much higher than that for the 12-inch wide panel, as the bending correction is dependent on the width of the panel (Section 3, Volume II).

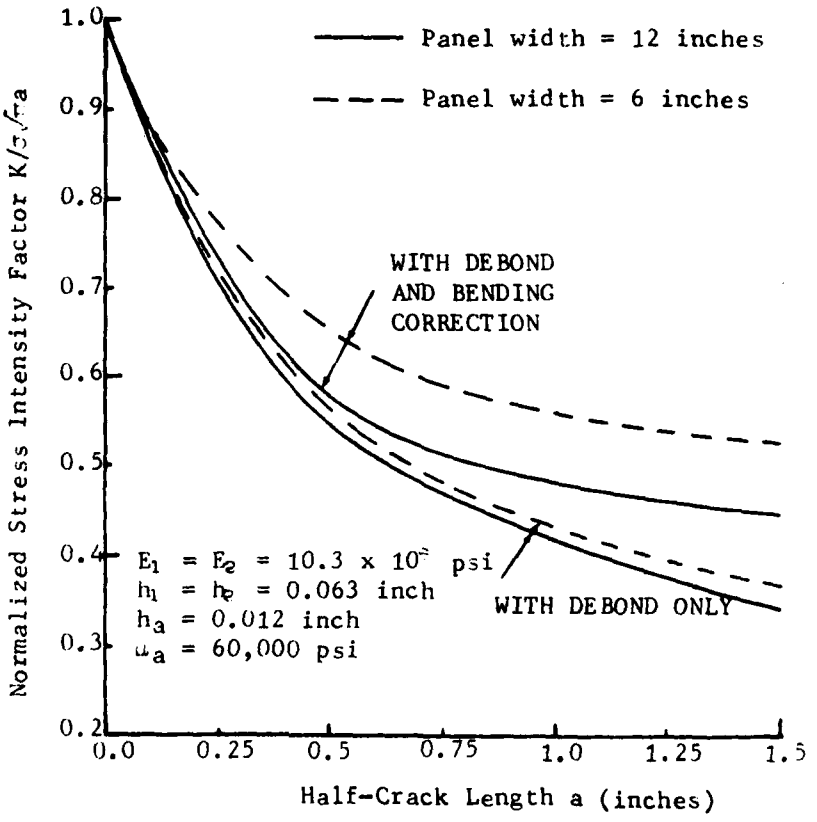

Figure B1. Variation of Stress Intensity Factors with a Half-Crack Length for a Two-Ply, Bonded Structure with a Center Crack

A CRACKED PLATE WITH AN ADHESIVELY BONDED STRINGER (FIGURE 1b, SECTION 2)

The variation of the stress intensity factors for the two stiffener thicknesses and the elliptical debond in the adesive with minor-to-major axis ratio of 0.1 is shown in Figure B2. It is seen that doubling the thickness of the stiffener from 0.125 inch to 0.25 inch has only a slight influence on the stress intensity factors. The stress intensity factor reduces by only 5.5 percent for a half-crack length of one inch (crack at the edge of the stiffener).

The stress intensity factors corrected for the influence of bending are also shown in Figure B2. It is seen that the influence of the bending correction, in this case, is smaller than that for the two-ply bonded structure, due to the fact that the sound layer (stiffener) is much thicker than the sound layer in a two-ply, bonded structure (Paragraph 2.4.1).

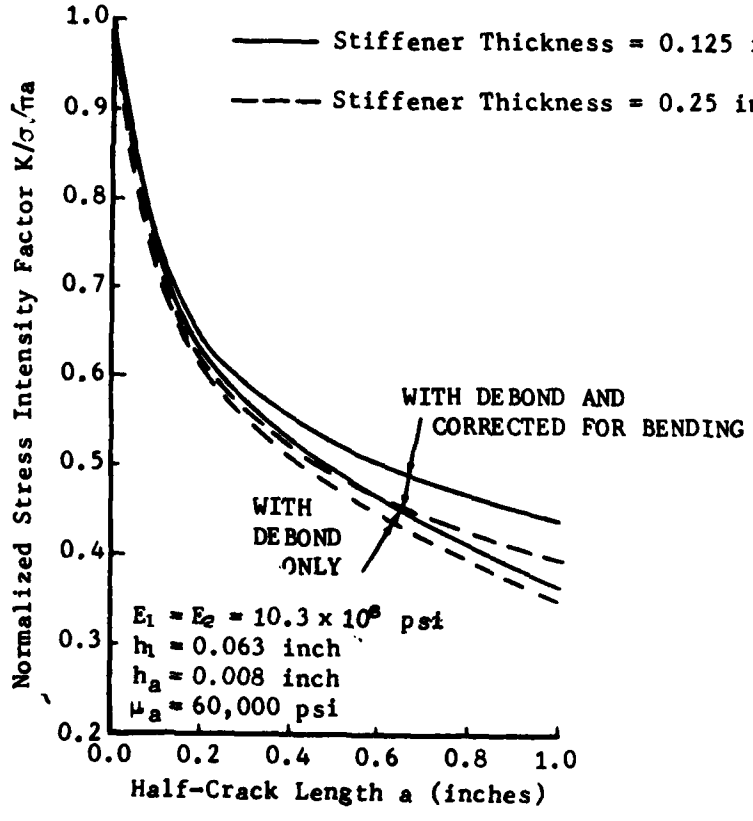

Figure B2. Variation of Stress Intensity Factors with a Half-Crack Length for a Cracked Plate with a Bonded Stringer

TWO-PLY ADHESIVELY BONDED STRUCTURE WITH AN EDGE CRACK IN ONE PLY (FIGURE 1c, SECTION 2)

The variation of the stress intensity factors as a function of crack length for the cases of no debond in the adhesive, and elliptical debond with minor-to-major axis ratio of 0.1, is shown in Figure B3. The stress intensity factors corrected for the influence of bending are also shown. In calculating the bending correction, only 3 inches of the layer width is considered effective, since for the small crack lengths, the influence of bending will be localized, and the entire width of the plate will not resist bending.

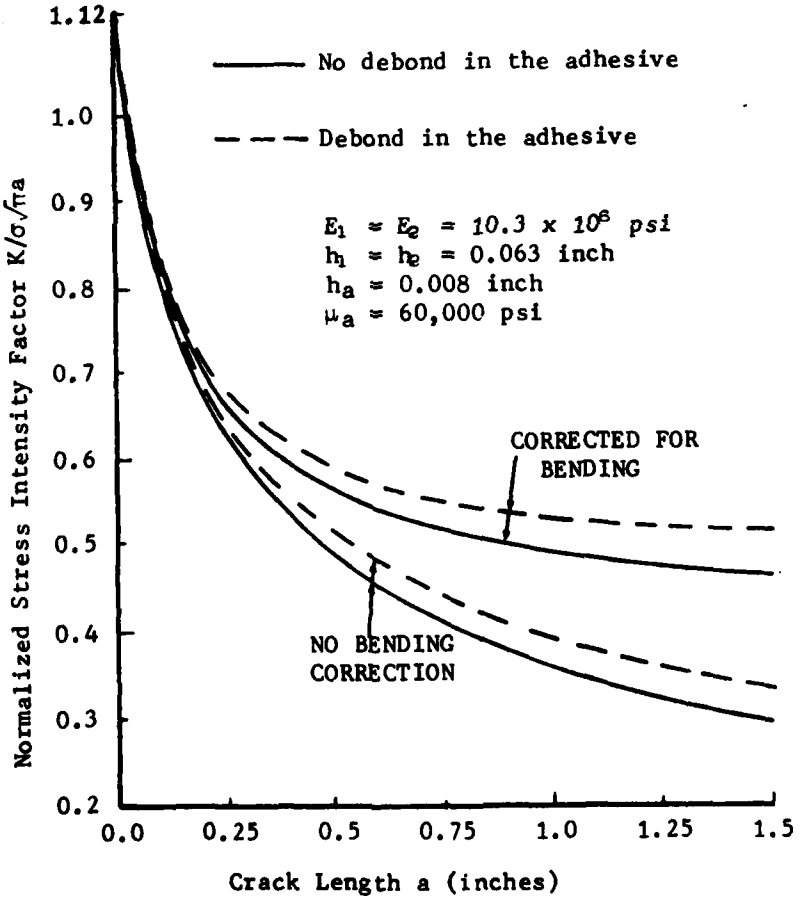

Figure B3. Variation of Stress Intensity Factors with Crack Length a for a Two-Ply, Bonded Structure with an Edge Crack

TWO-LAYER ADHESIVELY BONDED STRUCTURE WITH A CRACK EMANATING FROM A CENTRAL HOLE (FIGURE 1d, SECTION 2)

The variation of stress intensity factors as a function of half-crack length a for the case of no debond in the adhesive, is shown in Figure B4. It is seen that for the 6-inch and 12-inch wide panels, the stress intensity factors are identical. The stress intensity factors corrected for the influence of bending are also shown in this figure. The influence of bending is higher for the 6-inch wide panel than for the one 12 inches wide. In applying the bending correction, the influence of stress concentration on load transfer due to the presence of the hole, was taken into consideration (Section 3, Volume II).

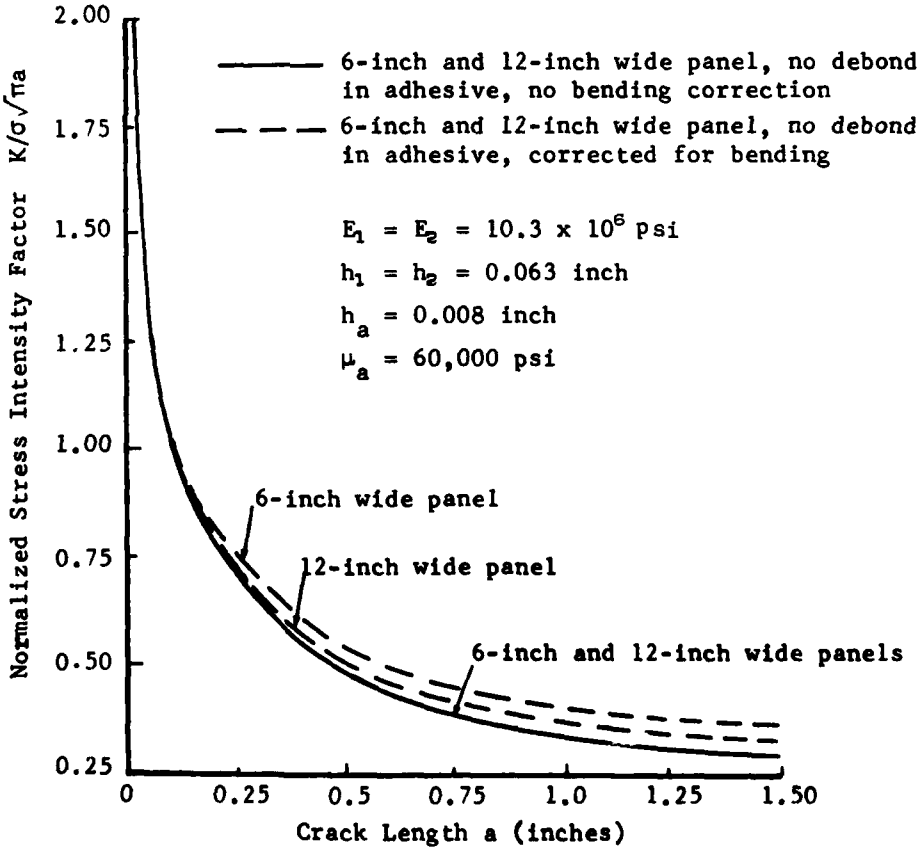

Figure B4. Variation of Stress Intensity Factors with Crack Length a for a Two-Ply, Adhesively Bonded Structure with a Crack Emanating from a Hole

TWO-LAYER, ADHESIVELY BONDED STRUCTURE WITH A CRACK EMANATING FROM AN ECCENTRIC HOLE (FIGURE 1e, SECTION 2)

The plot of stress intensity factors as a function of a half-crack length is shown in Figure B5. These stress intensity factors differ only slightly from those obtained for a crack at a central hole in Figure B4. The stress intensity factors corrected for bending are also shown in Figure B5. In applying bending correction, only the 6-inch width (twice the distance of the center of the hole from the nearest free edge of the plate) was taken into consideration.

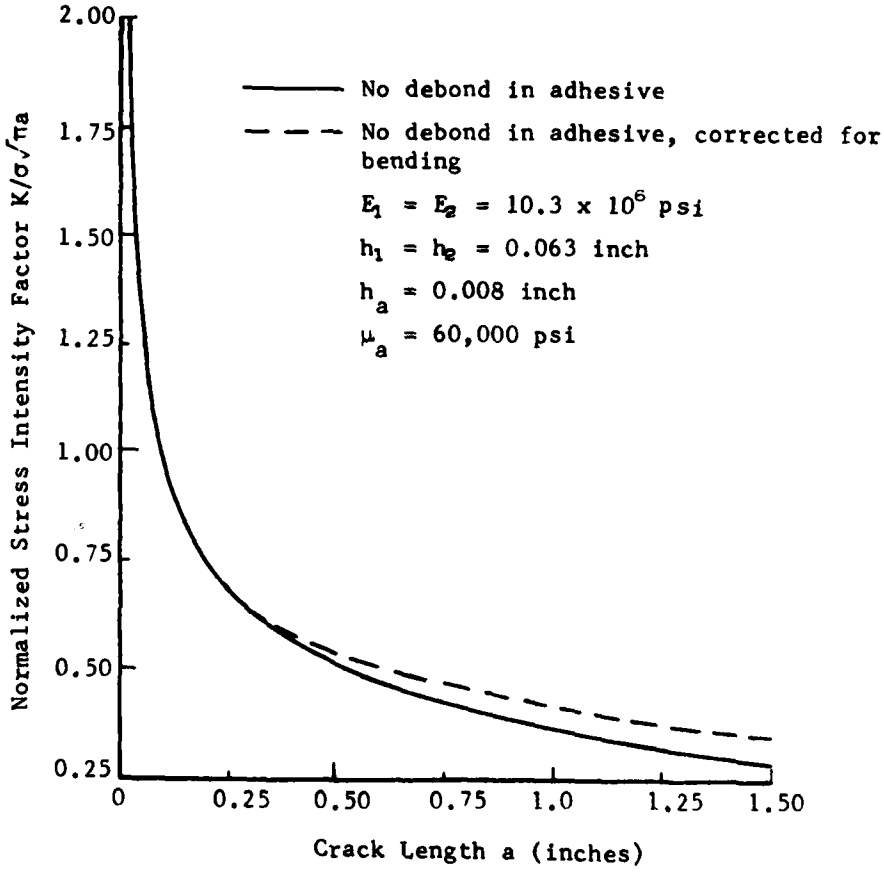

Figure B5. Variation of Stress Intensity Factors with Crack Length a for a Two-Ply, Bonded Structure with a Crack Emanating from an Eccentric Hole

THREE-PLY ADHESIVELY BONDED STRUCTURE (ALUMINUM-TITANIUM-ALUMINUM) WITH A CENTER CRACK IN THE OUTER ALUMINUM LAYERS (FIGURE 1f, SECTION 2)

The variation of stress intensity factors with half-crack length a, for an elliptical debond with a minor-to-major axis ratio of 0.1, is shown in Figure B6. The figure also shows the stress intensity factors corrected for bending. It is seen that in this case, the influence of bending is small compared to the two-ply bonded structure, due to the presence of two sound layers.

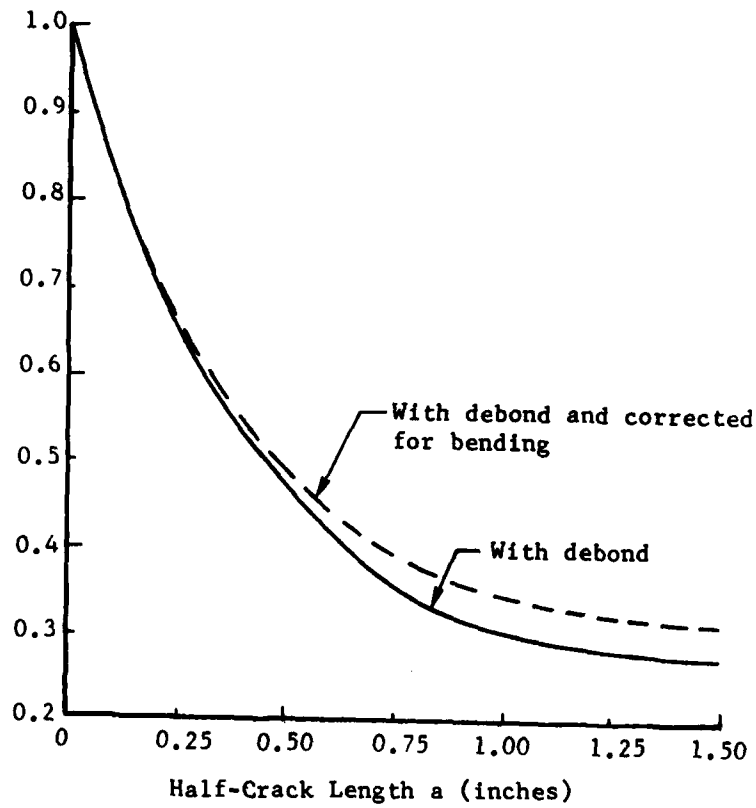

Figure B6. Variation of Stress Intensity Factors with Half-Crack Length a for a Three-Ply, Bonded Structure

APPENDIX C

EXPERIMENTAL DEBOND SHAPES

The nondestructive inspection (NDI) technique was used to determine the debond size. The results of NDI, and the comparison of the debond sizes and shapes are discussed in the following paragraphs.

NONDESTRUCTIVE INSPECTION TO ASSESS DEBONDING

For the 12-inch wide CCT panels, an extensive NDI was accomplished during the fatigue crack growth periods using the following methods.

Harmonic Bond Tests

A Branson 301 harmonic bond tester and a 0.187-inch, 10 mHz quartz crystal was used for these tests, and the results are summarized in Table C1. The panel was scanned at various crack lengths, using a bonded standard with a known defect (a precured adhesive of elliptical shape with a length of approximately 0.125 inch), and indications of the size (length and width) of the debond were noted. In all cases, the debond could not be located without putting at least a mean load on the specimen. It will also be noted from Table C1, that this method of NDI for debond detection produces inconsistent results. For example, the debond length for Specimen I-1 (Crack A) at 150,380 cycles, is longer than at 167,980 cycles. This inconsistency could be due to operator error.

Ultrasonic "C" Scan

The results of the immersion "C" scans will be reported by panel number. Care was exercised to place tape over the cracks so that moisture would not enter the crack during the immersion process. The ultrasonic test unit employed was an Erdman 412 or a Branson 301, with frequencies in the 20 mHz to 25 mHz range.

PANEL I-1

With the longest crack at approximately one inch (114,780 cycles), the "C" scans indicated no delamination in the crack area. At 167,890 cycles, the "C" scan readings were taken with the panel placed

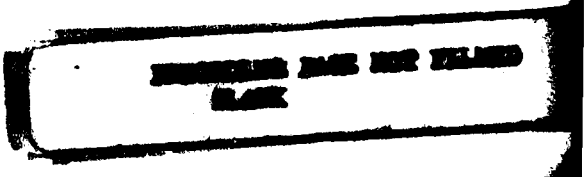

TABLE C1. HARMONIC BOND TES. FOR DEBONDING SIZE

SPECIMEN NUMBER	CYCLES APPLIED	VOID SIZES AT			CRACK SIZES AT		
		A (inches)	B (inches)	C (inches)	A 2a (inches)	B 2a (inches)	C 2a (inches)
I-1	114,780	*	*	*	1.148	1.078	0.983
	150,380	2.70 x 0.10	2.50 x 0.10	2.40 x 0.10	2.216	1.965	1.931
	167,980	2.25 x 0.25	2.25 x 0.25	2.25 x 0.25	2.949	2.534	2.552
II-2	144,960	*	*	*	2.047	1.824	1.773
	168,910	2.00 x 0.20	1.90 x 0.20	1.70 x 0.25	3.064	2.587	2.610

*No voids detected

in slight bending while under water. The bending was applied by supporting the panel on each end and placing weights on either side of the crack(s) (with the cracked surface away from the transducer). This procedure assists in opening the crack and creating a larger air void between the cracked material and the debond. Figures C1, C2, and C3 show the results recorded on a Taktronix 611 storage unit for the debond of Cracks A, B, and C. In Figures C1 and C3, the debonds at Cracks A and C are noted. The cracks are nearer the ends, hence sufficient deflection of the panel was not possible to indicate the full width of the debond (in the vertical direction). However, the lengths correspond quite well with those noted using the harmonic bond tester. In Figure C2, the elliptical debond is well defined for the middle crack (B), and matched the dimensions determined from the harmonic bond test in both width and length. The debond shape is probably well defined due to the bending caused over the 36-inch panel length at Crack B, versus a 12-inch to 15-inch length for Cracks A and C.

PANEL II-2

At crack lengths of A = 1.065 inches, B = 1.008 inches, and C = 0.906 inch (at 110,660 cycles), this panel was "C" scanned using a loaded condition in the immersion tank. In this case, the panel was supported in the middle (crack face toward transducer), and deflected approximately one inch on each end. Using a 20 mHz quartz crystal, debonds were noted for Cracks A, B, and C (Figures C4, C5, and C6). An elliptical debond is evident in all cases. The crack was then propagated and a second "C" scan at 159,660 cycles (A = 2.592 inches, B = 2.272 inches, and C = 2.267 inches) under the same applied bending load, indicated no debonds at any crack. In an attempt to explain this anomaly, the panel was tested at all focal lengths and frequencies, and still no debonds were indicated. Finally, a loss-of-back-signal test was conducted. In this test, the pulse is transmitted throught the panel and

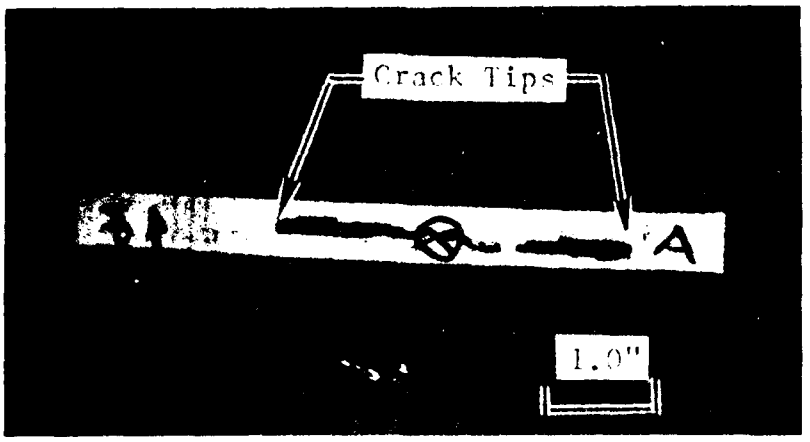

Figure C1. Ultrasonic "C" Scan of Debonded Area, Panel I-1, Crack A

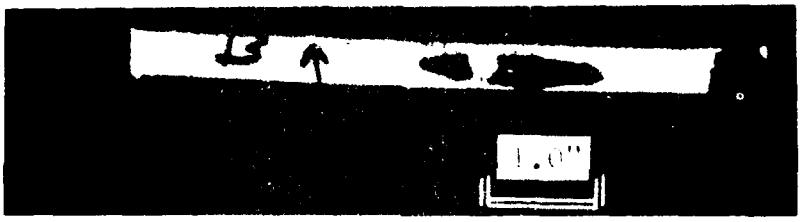

Figure C2. Ultrasonic "C" Scan of Debonded Area, Panel I-1, Crack B

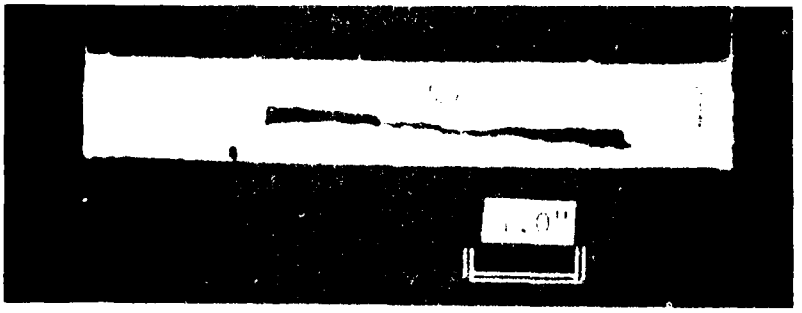

Figure C3. Ultrasonic "C" Scan of Debonded Area, Panel I-1, Crack C

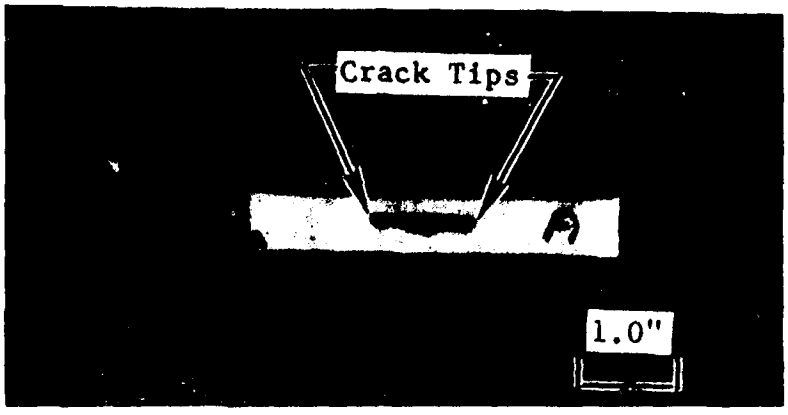

Figure C4. Ultrasonic "C" Scan of Debond Area, Panel II-2, Crack A

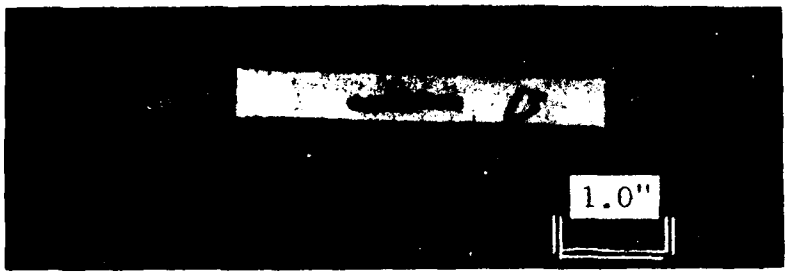

Figure C5. Ultrasonic "C" Scan of Debond Area, Panel II-2, Crack B

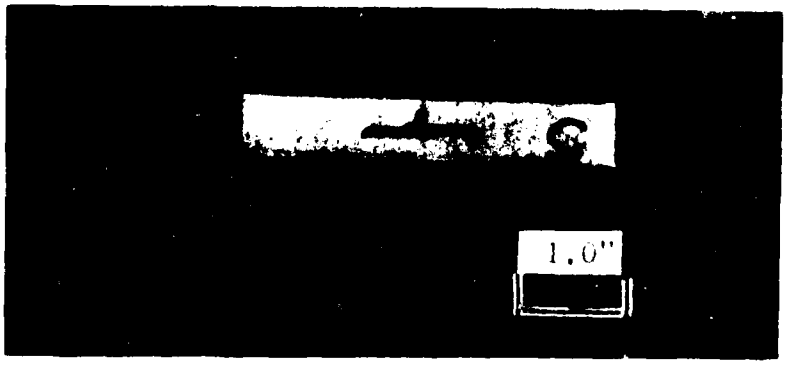

Figure C6. Ultrasonic "C" Scan of Debond Area, Panel II-2, Crack C

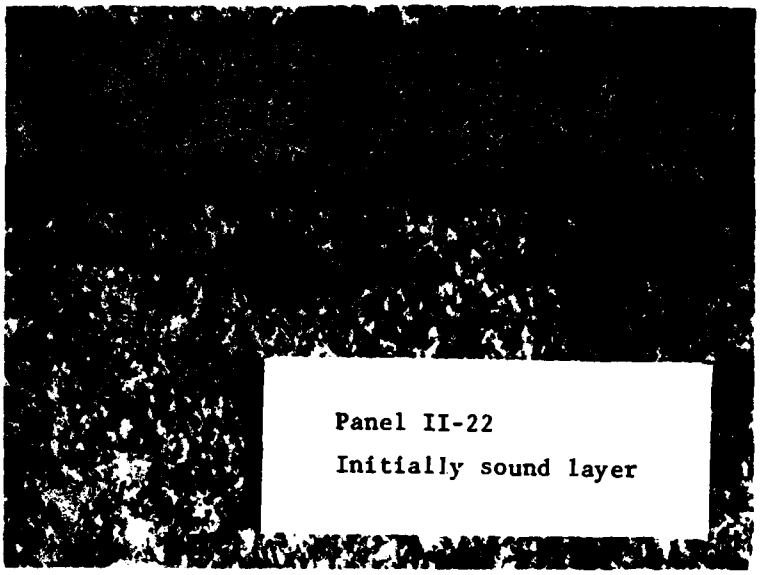

Figure C7. Debond in a Crack at a Central Hole

its reflection from the face, displayed on a Cathode Ray Tube (CRT). If a debond is present in any position between the front and back faces, the sonic pulse does not reach the back face, hence no pulse will occur on the CRT display. The results of this test indicated no delaminations at any crack position. Since the delamination was known to exist in this panel, as evident from Figures C4, C5, and C6, it is believed that either a couplant from prior harmonic bond tests, and/or moisture had entered the cracks and caused the appearance of a sound bond.

As a result of an apparent contradiction in these NDI studies and the degree of care required to provide reproducibility, it was decided to disregard the results of NDI and separate the panels after the test to examine the debond size and shape.

OBSERVED DEBOND SHAPES

After the crack growth data was obtained, the test panels were peeled apart in such a way that the shapes and sizes remained intact. Debond shapes observed for various test geometries are discussed in the following paragraphs.

Debond Size in a Panel with a Crack at a Hole

In a panel with a crack at a hole, the sound layer develops cracks at relatively small crack lengths due to large load transfer. In most panels, the sound layer cracked at about a = 0.4. Once the sound layer has cracked, there is small load transfer to it, hence no debond propagation. Therefore, the shape and size of the debond will essentially correspond to the crack length at which the sound layer has cracked. The shape of the debond at about a = 0.4 was predicted for a panel with a crack at a hole in Section 3, and was approximately in the form of a strip as shown by Curve D in Figure 6 of that section. The tests on all panels with cracks at holes exhibited similar behavior. One typical geometry is shown in Figure C7. On Side A, the sound layer had already cracked, and the crack length was about 0.7 inch. As predicted, the debond was in the form of a strip. On Side B, the sound layer had not cracked, and the crack length was about 0.32 inch. The shape of the debond compares well with that predicted for a = 0.406. The width of the debond found in the experimental panel, was 0.06 inch at a = 0.32, as compared to a predicted width of 0.1 inch for a = 0.406.

Debond in a Panel with an Edge Crack

The analytical debond predictions for panels with edge cracks were not made. However, from predictions of center-cracked panels, it is obvious that the debond will have an elliptical shape. A typical debond observed in the experiments, is shown in Figure C8. In this panel, the sound layer cracked to a length of about 1.1 inches. It is seen that the debond has an elliptical shape up to a crack length of about one inch, and beyond this, the debond is in the form of a strip. With the cracking of the sound layer, the debond will propagate a small amount at the center, as well as at the ends until the cracks join. The width of the debond at A is about 0.2 inch.

Debond Under Tension-Compression Loading

The criterion for debond propagation developed in Section 3 also applies to tension-compression loading, since the size of the debond in this case, will be governed by the maximum tensile load. Hence, the predictions made

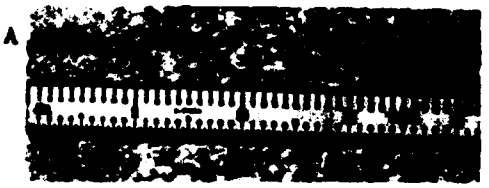

Panel I-13, cracked layer

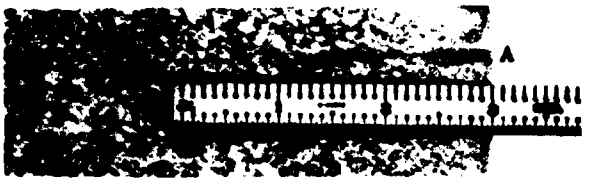

Panel I-13, sound layer

Figure C8. Debond in a Panel with an Edge Crack

in Section 3 for a two-ply, center-cracked panel, will be applicable to tension-compression loading as well. The debond obtained in a four-inch wide, center-cracked panel, tested at ±15,500 psi cyclic loading (R = -1.0), is shown in Figure C9. The debond is elliptical, as predicted. At a crack length of 1.25 inches, the minor axis is 0.14 inch, thus the experimental minor-to-major axis ratio for the debond is 0.11, matching that of the analysis.

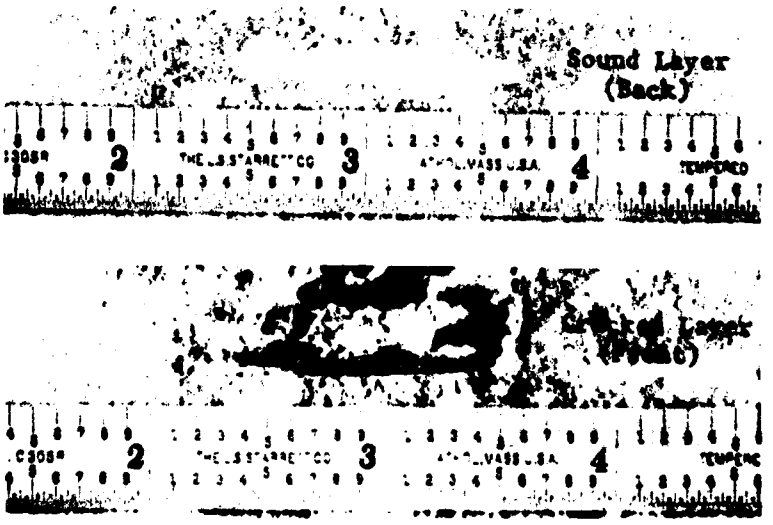

Figure C9. Debond Shape in Panels Tested Under Tension-Compression Loads

APPENDIX D

PARAMETRIC STUDY RESULTS

A parametric study was carried out to study the influence of the cracked and sound layers and adhesive parameters on stress intensity factors for the case of a cracked plate with one bonded stiffener, and a cracked plate with two bonded stiffeners symmetrically located. The results of this parametric study are discussed in the following paragraphs.

A CRACKED PLATE WITH AN ADHESIVELY BONDED STIFFENER

The parametric studies were carried out for a cracked sheet with an adhesively bonded stiffener, as shown in Figure 1b, in Section 2 of this report. The stiffener is located along the centerline of the crack. In the parametric study, the following notations are used:

a = half-crack length
d_s = the width of the stiffener
A_s = the area of the stiffener
E_s = Young's modulus of the stiffener material
E_p = Young's modulus of a cracked plate
h_p = thickness of the cracked plate
h_a = thickness of the adhesive
μ_a = shear modulus of the adhesive material
b = length of the debond

The influence of debond sizes on the stress intensity factors for various crack lengths is shown in Figure D1. It is seen that an increase in debond size increases the stress intensity factors. This is expected, as an increase in debond size will cause a reduction in the load transfer to the sound layer, hence the stress intensity factors will be increased.

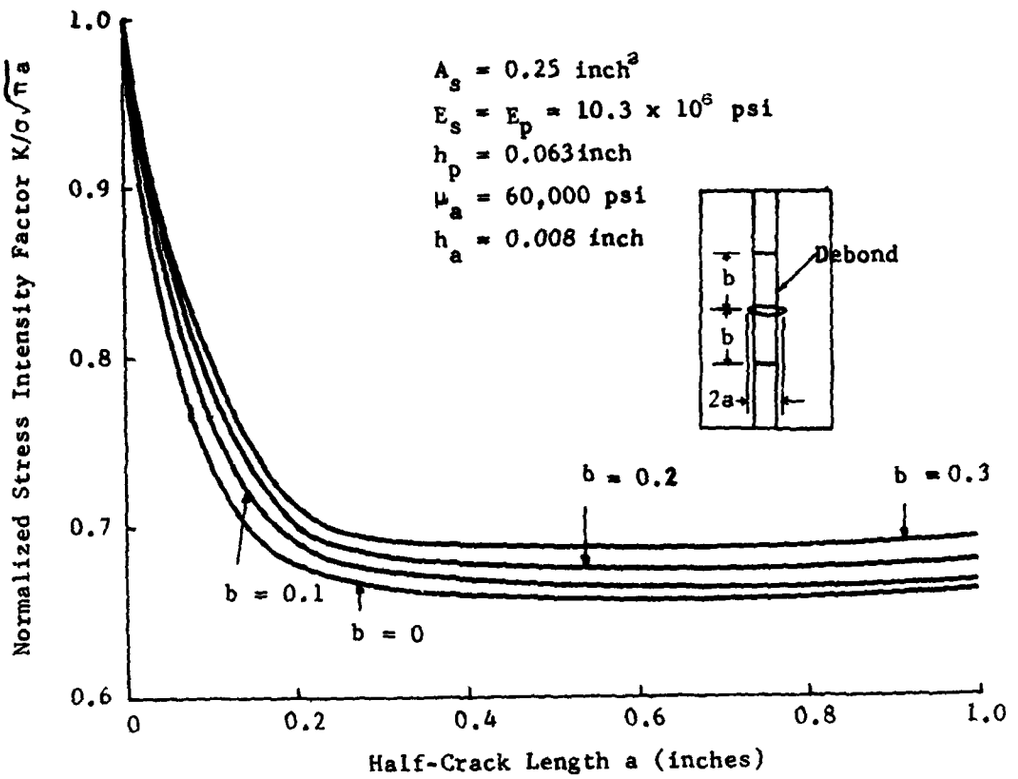

Figure D1. Influence of Debond Size on Stress Intensity Factors for a Cracked Sheet with a Bonded Stringer

The plots of normalized stress intensity factors versus half-crack length a for various values of h_a/μ_a, are shown in Figure D2. It is seen that increasing the value of h_a/μ_a increases the stress intensity factors, thus an increase in the adhesive thickness or a reduction in the shear modulus of the adhesive will increase the stress intensity factors, and vice versa.

The influence of stiffener parameter A_sE_s on the stress intensity factors, is shown in Figure D3. An increase in stiffener parameter A_sE_s causes a reduction in the stress intensity factors as it increases the stiffening effect of the sound layer.

The variation of stress intensity factors with half-crack length a, for various values of cracked layer parameter h_pE_p, is shown in Figure D4. It is seen that an increase in the value of h_pE_p causes an increase in stress intensity factors. An increase in the value of h_pE_p reduces the stiffening effect of the sound layer, resulting in less load transfer to the sound layer.

As discussed in Section 2, the results of this study are applicable for small crack lengths and for cases where the stiffener width is smaller than the crack length.

A CRACKED SHEET WITH TWO BONDED STIFFENERS SYMMETRICALLY LOCATED ABOUT THE CENTERLINE

The structure shown in Figure D5 is considered for parametric studies in which the centerline of each stringer is assumed at each crack tip, i.e., d = a.

The influence of the various parameters on the stress intensity factors is shown in Figures D6 through D9. It is seen that the influence of these parameters is similar to that for a single stiffener bonded to the plate. However, in this case, the influence of the various parameters is more predominant, due to the location of the stiffeners at the crack tip.

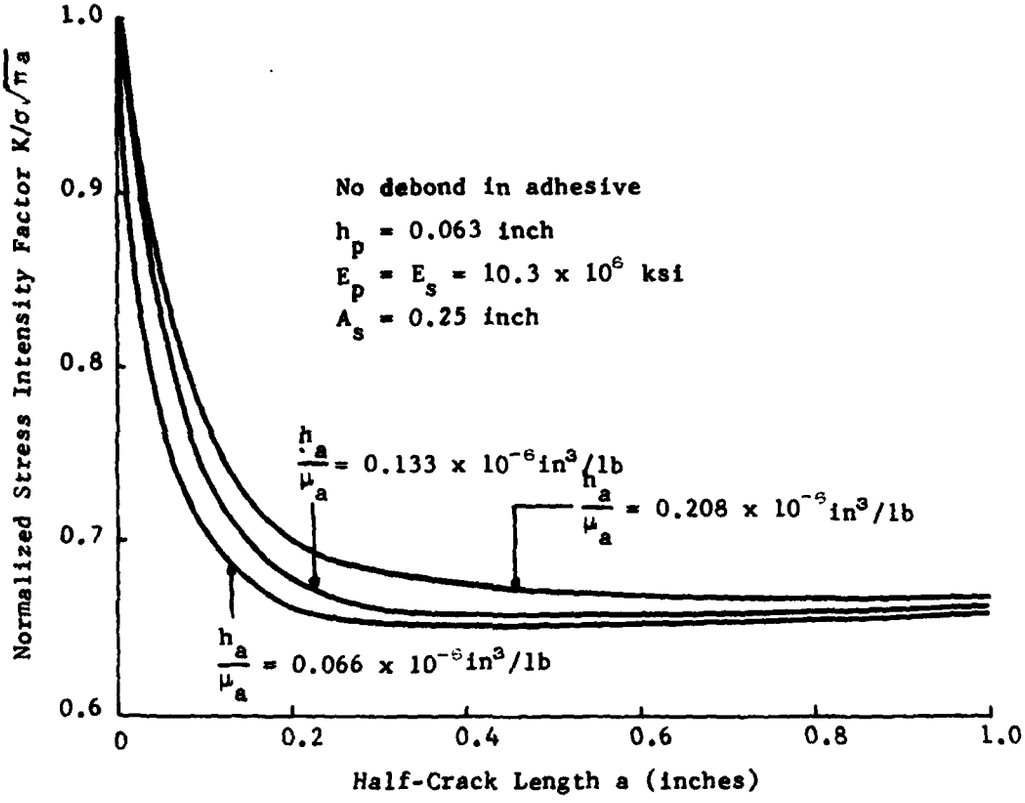

Figure D2. Influence of Adhesive Parameter h_a/μ_a on Stress Intensity Factors for a Cracked Sheet with a Bonded Stringer

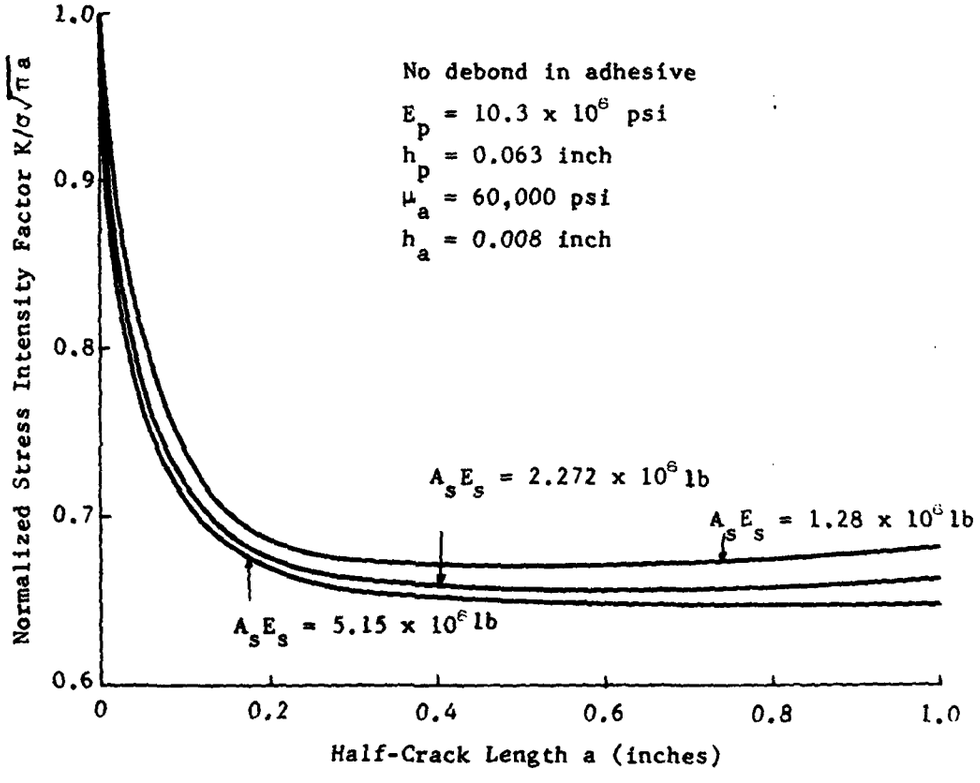

Figure D3. Influence of Stiffener Parameter A_sE_s on Stress Intensity Factors for a Cracked Sheet with a Bonded Stiffener

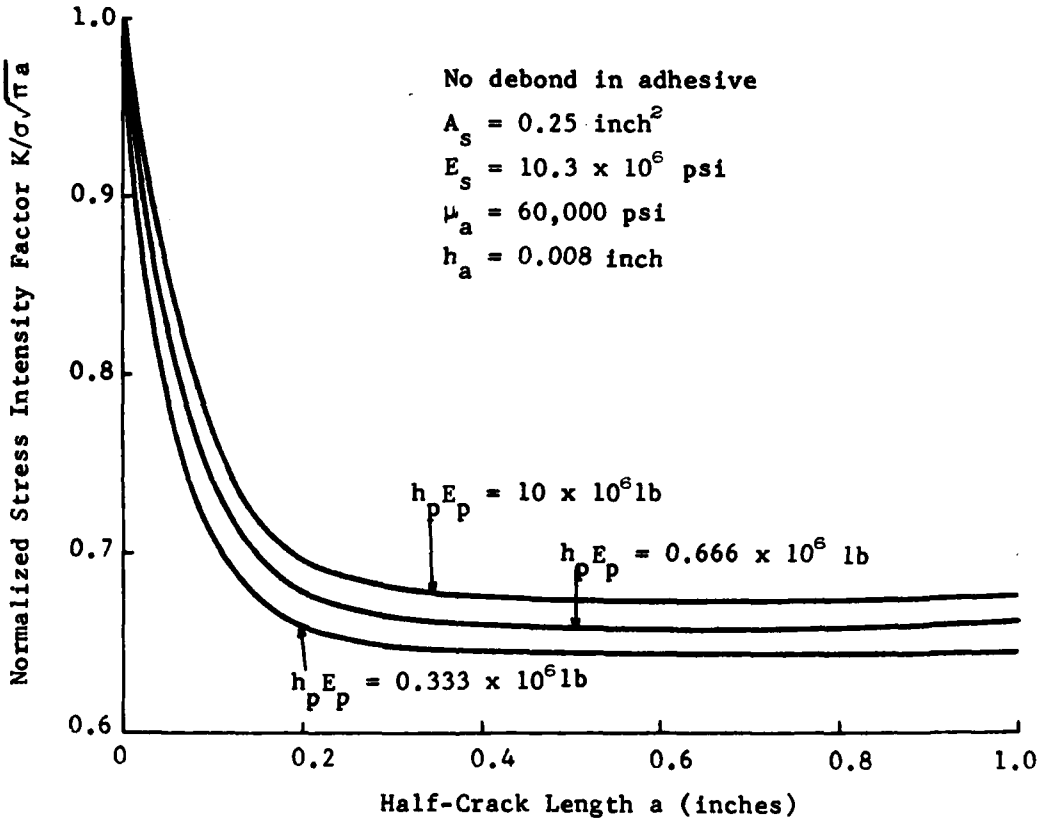

Figure D4. Influence of Cracked Layer Parameter $h_p E_p$ on Stress Intensity Factors for a Cracked Sheet with a Bonded Stringer

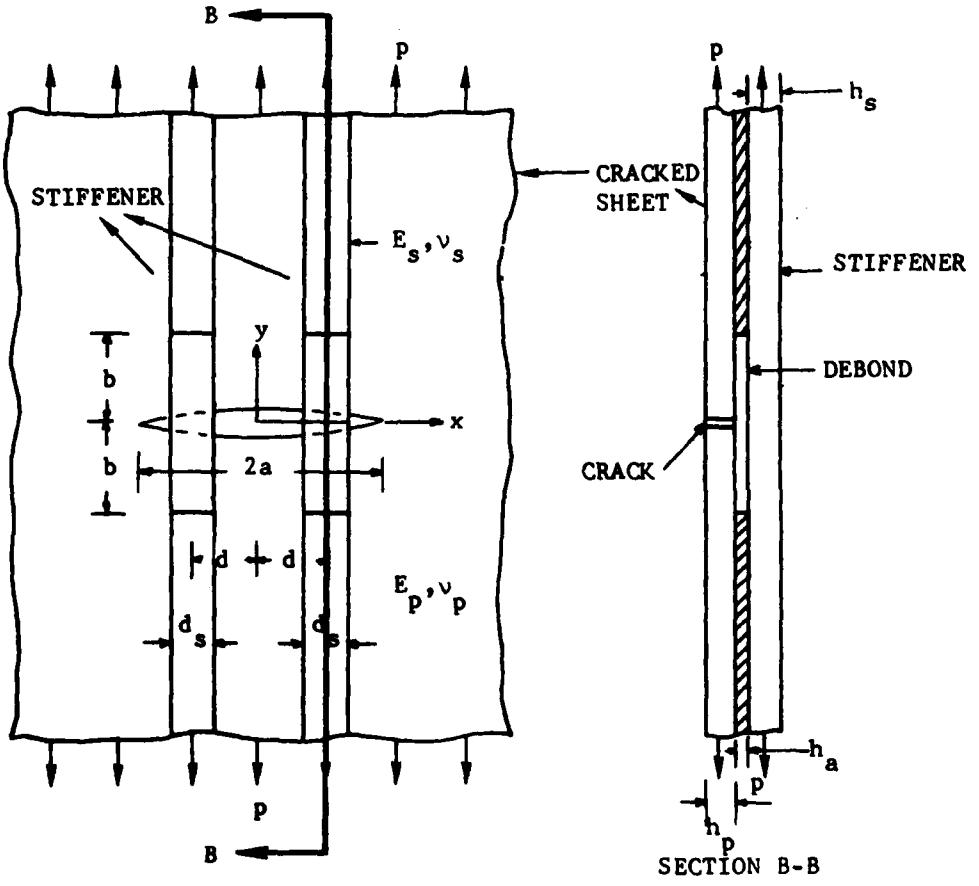

Figure D5. Cracked Plate Stiffened by Two Bonded Stringers

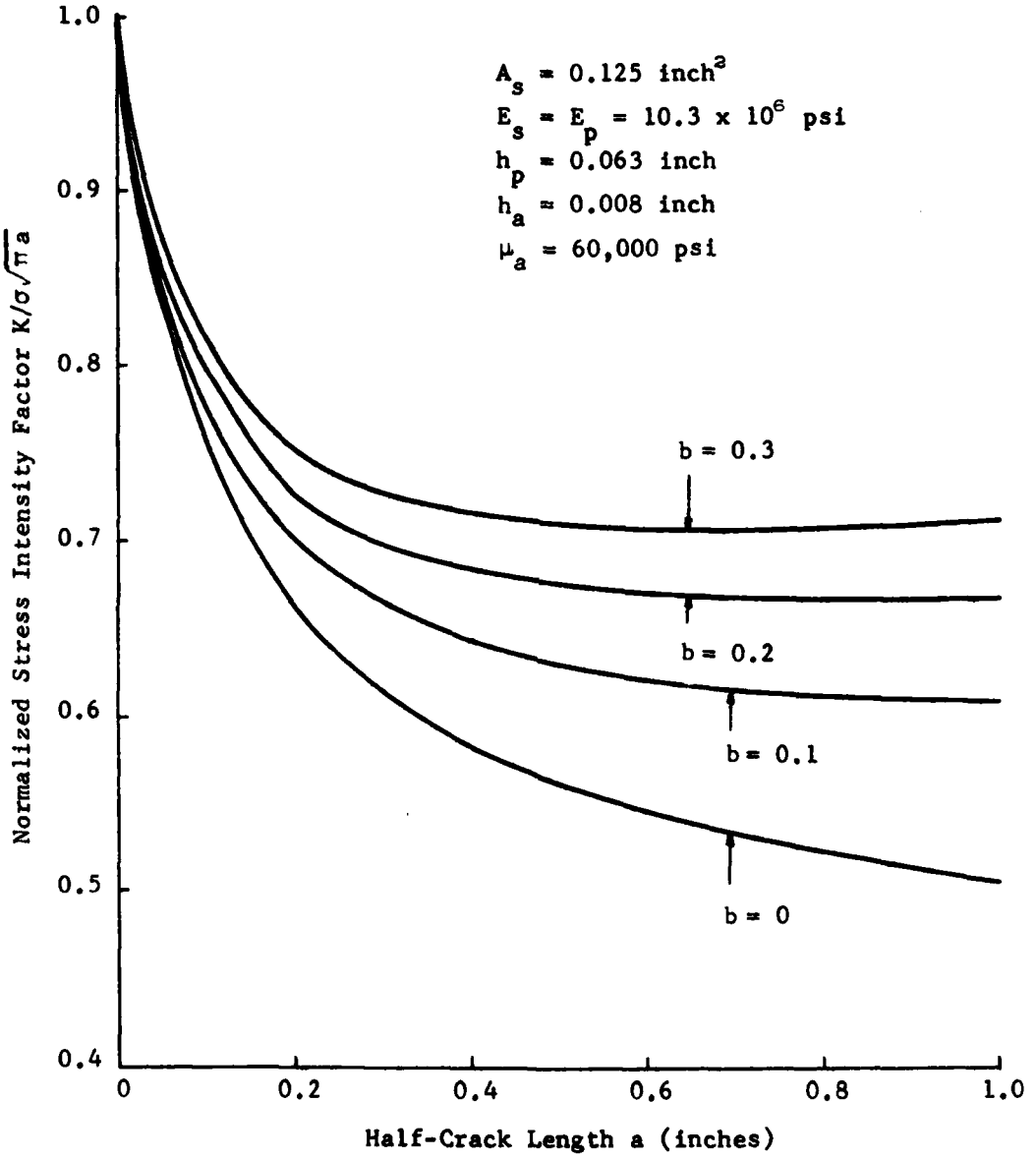

Figure D6. Influence of Debond Size on Stress Intensity Factors in a Cracked Sheet with Two Bonded Stiffeners

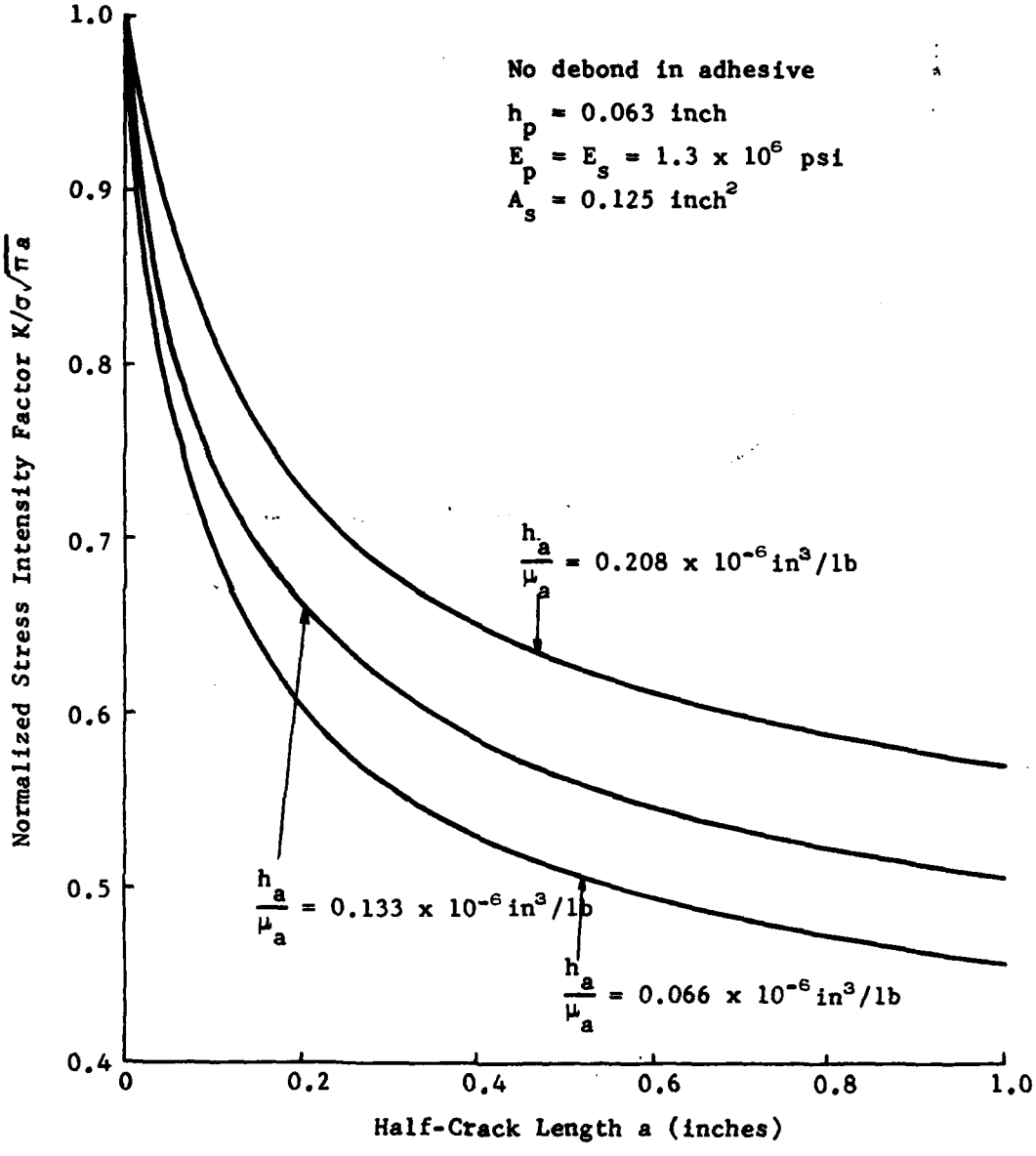

Figure D7. Influence of Adhesive Parameter h_a/μ_a on Stress Intensity Factors for a Cracked Sheet with Two Bonded Stringers

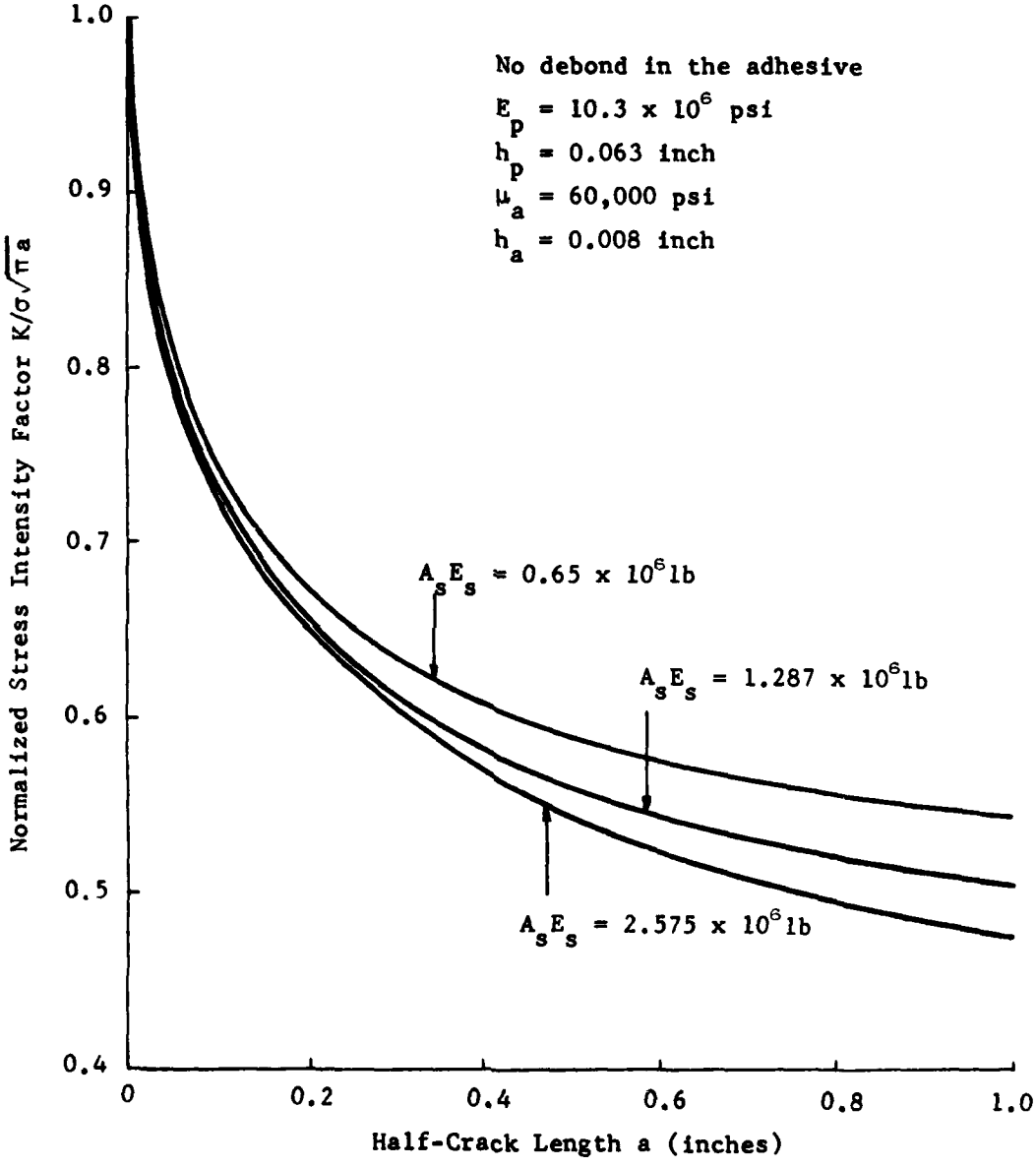

Figure D8. Influence of Stiffener Parameter A_sE_s on Stress Intensity Factors in a Cracked Sheet with Two Bonded Stiffeners

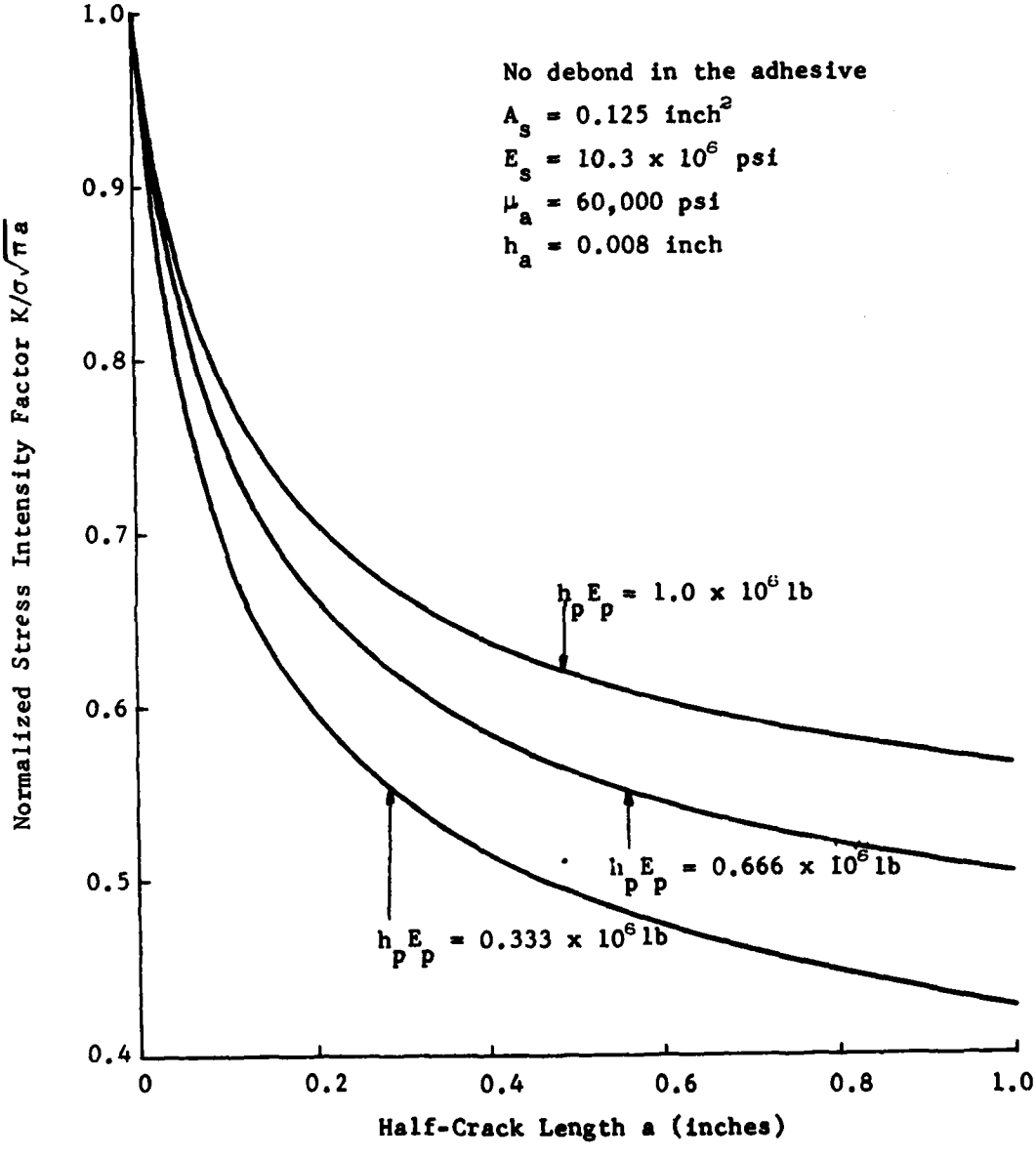

Figure D9. Influence of Cracked Layer Parameter h_pE_p on Stress Intensity Factors in a Cracked Sheet with Two Bonded Stiffeners

*U.S.Government Printing Office: 1977 — 757-001/119